

WCAP-2858

REACTIVITY COEFFICIENTS IN  
WESTINGHOUSE PRESSURIZED  
WATER REACTORS

by

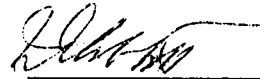
R. J. French

J. S. Moore

R. A. Wiesemann

October 1965

APPROVED BY:



W. E. Abbott, Manager  
Reactor Development



T. Stern, Manager  
Plant Projects

Prepared under DGR-7701

8110240429 651206  
PDR ADDCK 05000247  
B PDR

TABLE OF CONTENTS

	<u>Page</u>
1. INTRODUCTION AND SUMMARY	1
2. PHYSICS ASPECTS	6
2.1 Reactivity Coefficients of the PWR Core	6
2.2 Effect of Non-Uniform Moderator Temperatures on PWR Cores	21
2.3 Spatial Stability	39
2.4 Basis for Confidence in Analysis	52
3. CONTROL AND PROTECTION ASPECTS	74
3.1 Routine Transient	74
3.2 Abnormal Transients	88
3.3 Basis for Confidence in Analog Studies	93
4. CONCLUSIONS	95

LIST OF FIGURES

<u>FIGURE NO.</u>	<u>TITLE</u>	<u>PAGE</u>
2.1-1	Doppler Coefficient versus Effective Fuel Temperature	7
2.1-2	Fuel Temperatures for a Typical PWR Core	8
2.1-3	Power Coefficient versus per cent Power	9
2.1-4	Moderator Temperature Coefficient versus Moderating Ratio	12
2.1-5	Effective Multiplication Factor versus Time	12
2.1-6	Moderator Temperature Coefficient versus Moderator Temperature for Different Boron Concentrations	14
2.1-7	Moderator Density Coefficient versus Density for Different Boron Concentrations	16
2.1-8	Spectral Temperature Coefficient versus Moderator Temperature - 2500 ppm Boron	17
2.1-9	Spectral Temperature Coefficient versus Moderator Temperature - 1500 ppm Boron	18
2.1-10	Spectral Temperature Coefficient versus Moderator Temperature - No Boron	19
2.1-11	Temperature Coefficient of Water Density versus Temperature	20
2.2-1	Maximum Reactivity Insertion versus Boron Concentration	24
2.2-2	Region Boundaries for Area with Decreased Water Density	26
2.2-3	Effective Neutron Multiplication Factor versus per cent of the Core Volume with Moderator Temperature of 640°F	27

<u>FIGURE NO.</u>	<u>TITLE</u>	<u>PAGE</u>
2.2-4	Effective Multiplication Factor versus Moderator Density for Density Changes in 25% of the Core	29
2.2-5	Radial Nuclear Hot Channel Factor versus per cent of the Core with a Moderator Temperature of 640°F	30
2.2-6	Movement of the Hot Channel Factor with Increasing Fractions of the Core Moderator at Saturation Temperature	31
2.2-7	Radial Plot from a Two Dimensional Calculation of Relative Power versus Core Radius - 5% of the Core at Saturation Temperature	32
2.2-8	Typical Control Rod Pattern with Stuck Center Rod	34
2.2-9	Effective Neutron Multiplication Factor versus per cent of the Core Volume with a Moderator Temperature of 640°F Rod Pattern of Figure 2.2-8	35
2.2-10	Effective Neutron Multiplication Factor versus Moderator Density or Density Changes in 25% of the Core - Rod Pattern	36
2.2-11	Maximum Radial Nuclear Hot Channel Factor versus Percentage of the Core Volume with a Moderator Temperature of 640°F - Rod Pattern of Figure 2.2-8	37
2.3-1	Temperature versus per cent Power	48
2.4-1	Plutonium/Uranium Mass Ratio as a Function of Uranium - 235 Depletion	54
2.4-2	Fraction of Plutonium - 239 in Plutonium as a Function of Uranium - 235 Depletion	55
2.4-3	Composition of Plutonium as a Function of Uranium - 235 Depletion	56
2.4-4	SELNI Moderator Temperature Coefficient versus Moderator Temperature at 1600 ppm Boron	58

<u>FIGURE NO.</u>	<u>TITLE</u>	<u>PAGE</u>
2.4-5	Selni Moderator Temperature Coefficient versus Boron Concentration	59
2.4-6	Comparison of Calculated and Measured Moderator Temperature Coefficient versus Burnup	61
2.4-7	Calculated and Measured Power Distribution through a voided Region of a Critical Lattice - Unborated	63
2.4-8	Calculated and Measured Power Distribution through a Voided Region of a Critical Lattice - 1046 PPM Boron	64
2.4-9	Comparison of Metal-Oxide Resonance Integral Correlation with Hellstrand's Correlation for Isolated Rods	69
2.4-10	Effective Fuel Temperature Change per KW/FT versus Core Average KW/FT	70
2.4-11	$\alpha$ versus Pellet Surface Heat Flux	71
2.4-12	Difference in $T_{eff}$ Between Measured and Calculated Value versus Pellet Surface Heat Flux	72
3.1-1	Transient Responses for a 10% Step Load Increase from 20% Power - Nuclear Power, Pressurizer Pressure, Rod Speed	76
3.1-2	Transient Responses for a 10% Step Load Increase from 20% Power - Steam Flow, Steam Temperature, Average Temperature	77
3.1-3	Transient Responses for a 10% Load Decrease from Full Power - Power, Pressurizer Pressure, Rod Speed	78
3.1-4	Transient Responses for a 10% Load Decrease from Full Power - Steam Flow, Steam Temperature, Average Temperature	79
3.1-5	Transient Responses for a 10% Load Decrease from Full Power - Nuclear Power, Pressurizer Pressure, Rod Speed	80

<u>FIGURE NO.</u>	<u>TITLE</u>	<u>PAGE</u>
3.1-6	Transient Responses for a 10% Load Decrease from Full Power - Steam Flow, Steam Temperature, Average Temperature	81
3.1-7	Transient Responses for a 10% Step Load Increase from 90% Power - Nuclear Power, Pressurizer Pressure, Rod Speed	83
3.1-8	Transient Responses for a 10% Step Load Increase from 90% Power - Steam Flow, Steam Temperature, Average Temperature	84
3.1-9	Low Power Operation, 10% Step Load Decrease, Manual Control No Operation Action for 1 Minute, Incremental Rod Worth = $3 \times 10^{-4} \delta k/in$	85
3.1-10	Low Power Operation, 10% Step Load Decrease, Manual Control No Operator Action for 2 Minutes Incremental Rod Worth = $3 \times 10^{-4} \delta k/inch$	86
3.1-11	Low Power Operation, 10% Step Load Decrease, Manual Control No Operator Action for 2 Min., Incremental Rod Worth = $6 \times 10^{-4} \delta k/^{\circ}F$	87
3.2-1	Transient Response to a Complete Loss of Load from Full Power Without an Immediate Reactor Trip (Temperatures)	90
3.2-2	Transient Response to a Complete Loss of Load from Full Power Without an Immediate Reactor Trip (Pressure, Volume Surge, Core Power)	91
3.3-1	Comparison of Transient Behavior, Predicted versus Actual for the SELNI Plant Rapid Load Decrease from 185 to 140 MWe	94

1.0

INTRODUCTION AND SUMMARY

The introduction of chemical shim as a means of reactivity control provides a number of significant improvements in the operating characteristics of the core which are reflected in an increase in the safety of the system. These include:

1. Improved Prediction of Power Distribution
2. Improved Spatial Stability through Reduction of the Infinite Multiplication Factor and
3. Reduced Reactivity Subject to Rapid Change

First is the increase in the predictability of the core power distribution with chemical shim. This is to be contrasted with the situation where movable neutron absorbers (control rods) are used to compensate for the reactivity loss due to depletion. Both critical experiments and measurements performed in operating reactors with in-core instrumentation have demonstrated good agreement between design prediction and power distribution for chemical shim configurations (i.e. in unrodded core regions). However, in cores where reactivity control is achieved by movable control rods, local differences between experiment and prediction of 15% are not uncommon. It is axiomatic that predictability and safety are directly correlated.

Second, the uniformity of neutron poison distribution in a chemical shim core contributes to the spatial stability of the power distribution in contrast to shim by control rods since it operates to reduce  $k_{\infty}$  rather than chop the core into small, independent regions of high  $k_{\infty}$ . This effect has been demonstrated in the Shippingport reactor, where the core was subject to azimuthal xenon oscillations at the beginning of life when control rods were inserted, but was stable near the end of life when these rods were removed.

The third characteristic of chemical shim operation which enhances the safety of the core is the fact that large rapid changes in core reactivity are not possible when the reactor is operating at full power. In this case 15 to 20 partially inserted mechanical rods are used to control the small reactivity increment (0.15 to 1.0%) required for load variation

flexibility. It is physically impossible to achieve rapid reactivity changes through boron dilution. The probability of any of the rods being suddenly removed from either a chemical shim or rod controlled reactor is very small. However, the potential for rapid loss of reactivity control and the upper limit of reactivity which could be inserted is considerably higher in a rod controlled core.

The use of chemical shim in the present generation of high-burnup reactors introduces a change in the moderator temperature coefficient rendering it slightly positive at the beginning of the first cycle, at power and with no xenon or samarium poisoning. The presence of a dissolved neutron absorber in the coolant creates a positive contribution to the coefficient since water expansion with an increase in temperature results in a decreasing core poison content. Control rod worth on the other hand increases as temperature rises primarily because of an increase in the neutron migration length which increases the core volume "seen" by the control rods. As opposed to boron control, the presence of control rods, therefore, constitutes a negative contribution to the moderator temperature coefficient.

Careful evaluation has been made of the effects of chemical shim on the reactivity feedback mechanisms in large power reactors and their influence on reactor stability, control, and protection. From this work it is apparent that the sign of the moderator temperature coefficient is not a design constraint. The reason for this arises from two effects; first, the prompt negative reactivity coefficient of the fuel which is a result of Doppler broadening of the U-238 neutron absorption resonances; and second, the relatively long thermal time constant for transfer of heat from the  $\text{UO}_2$  fuel rods to the coolant. These characteristics result in the primary reactivity shutdown mechanism being insensitive to the moderator temperature coefficient for all cores fueled by slightly enriched oxide rods. This has been demonstrated by transient experiments with low enrichment fuel in the SPERT series of tests <sup>(1)</sup> at the NRTS in Idaho.

In general, the desirable value of the moderator coefficient in a water moderated reactor is neither strongly negative nor strongly positive.

It is the purpose of this report to present a quantitative discussion of the relative significance of the fuel and moderator coefficients, and to justify the position that operation with a positive moderator temperature or void coefficient does not prejudice the basic safety and performance characteristics of the pressurized water reactor core.

In Section 2.1 the general reactivity characteristics of the PWR core are presented and discussed with particular emphasis on the effect of boron on the moderator temperature coefficient of reactivity. The negative power coefficient is discussed because it represents the primary terminating mechanism (prompt) for transients in the PWR core. This coefficient, of course, is independent of boron concentration in the moderator and reacts promptly to the variation in power level.

Isothermal moderator temperature coefficients are presented as a function of core temperature and boron concentration for the full power unpoisoned core. A core with 2500 PPM boron (a representative boron concentration for an unpoisoned PWR core) operated at 578°F does have a slightly positive coefficient. However, it is important to observe (Figure 2.1-6) that as the temperature rises the coefficient becomes negative rapidly with a potential insertion of only about 0.1% (the area under the 2500 PPM curve above zero and at core temperatures higher than 578°F). The moderator density coefficient is also presented to demonstrate that the same characteristic exists in terms of void coefficient. The introduction of void (reduction in moderator density) can insert a small amount of positive reactivity (with 2500 PPM boron); but, as with temperature increase, the insertion is limited to only 0.1%. Because the temperature coefficient is largely due to water density change, generally speaking, the temperature and density coefficients are merely two ways of viewing the same effect and they are not additive effects.

In Section 2.2, the effect of non-uniform temperature distributions is considered. The absolute maximum insertion for a non-uniform temperature distribution is 0.25% compared with a maximum insertion of 0.1% for an

isothermal temperature increase. This maximum insertion increases with boron concentration above 2500 PPM at a rate no greater than 0.6% per 1000 PPM of boron. It is clear that there is no danger of an auto catalytic run-away particularly when the long time constant associated with coolant heatup is considered. It is also clear that large changes in core design (boron concentration) are necessary before a problem could possibly arise. Results of this section also demonstrate the fact that power is reduced in the region of a local temperature increase. This is very important with respect to any considerations of temperature-induced transients. It is also demonstrated that the maximum reactivity insertion with maldistributions in power (resulting from stuck or ejected rods) is much smaller (by a factor of 3) than the maximum found for the normal distribution.

In Section 2.3, a stability criterion is developed which shows the effect of moderator coefficient on core distribution spatial stability. It is concluded that under any conceivable circumstance the boron concentration must be increased by almost 1000 PPM before concern for spatial stability arises.

In Section 2.4, a detailed experimental verification of calculational techniques is presented which is pertinent specifically to the prediction of reactivity coefficients in PWR cores. It is demonstrated that the design techniques have a high degree of reliability associated with them and are perfectly adequate to substantiate the conclusions presented herein.

Section 3 shows that the effects of the most positive magnitude of moderator coefficient of reactivity anticipated for large pressurized water reactors with chemical shim are insignificant with respect to control or protection of the core. In Section 3.1 a discussion and results of analog studies of routine plant transients are presented for automatic and manual control. The figures giving the results of the analog studies show that transient behavior with a positive moderator coefficient is very similar to that obtained with a small negative coefficient.

Section 3.2 discusses the effects of positive moderator reactivity coefficients in abnormal plant transients. The fact that reactivity changes due to moderator effects are limited to a small values in both rate and magnitude ensures that sufficient shutdown control can always be provided to terminate safely even the worst abnormal transients.

Section 3.3 presents a brief summary of work that has been done to provide confidence in the validity of analog studies of plant transient behavior.

2.0 PHYSICS ASPECTS

2.1 REACTIVITY COEFFICIENTS OF THE PWR CORE

The factors which can affect the reactivity of the PWR core are:

- 1) power
- 2) moderator temperature
- 3) moderator density

2.1.1 Power Coefficient

The effect of core power on reactivity is primarily the result of temperature variations in the oxide fuel material. Because the PWR core uses slightly enriched uranium oxide, the resonance bearing fertile absorber (U-238) reacts to fuel temperature increases through the Doppler broadening of its resonances to decrease core reactivity rapidly. Figure 2.1-1 illustrates the values of fuel temperature reactivity coefficient (net change in neutron multiplication per degree change in fuel temperature) which are typical of a PWR core. As indicated in this figure, the coefficient is a function of power level primarily due to the non-linear effect of fuel temperature on resonance absorption and, secondarily, through the fact that the moderator temperature changes by 43°F as the power level is increased from zero to full power. The change in moderator density results in a change in resonance absorption which is reflected in the coefficient. In this figure the fuel temperature is indicated as an effective temperature which is taken to be higher than the fuel average temperature to account for non-uniform temperature distribution effects both within a fuel pellet and across the reactor core. Figure 2.1-2 presents these temperatures as a function of power level. Figure 2.1-3, then, combines the information given in Figures 2.1-1 and 2.1-2 to obtain a power coefficient (net change in neutron multiplication per per cent in power). This coefficient also includes the effect

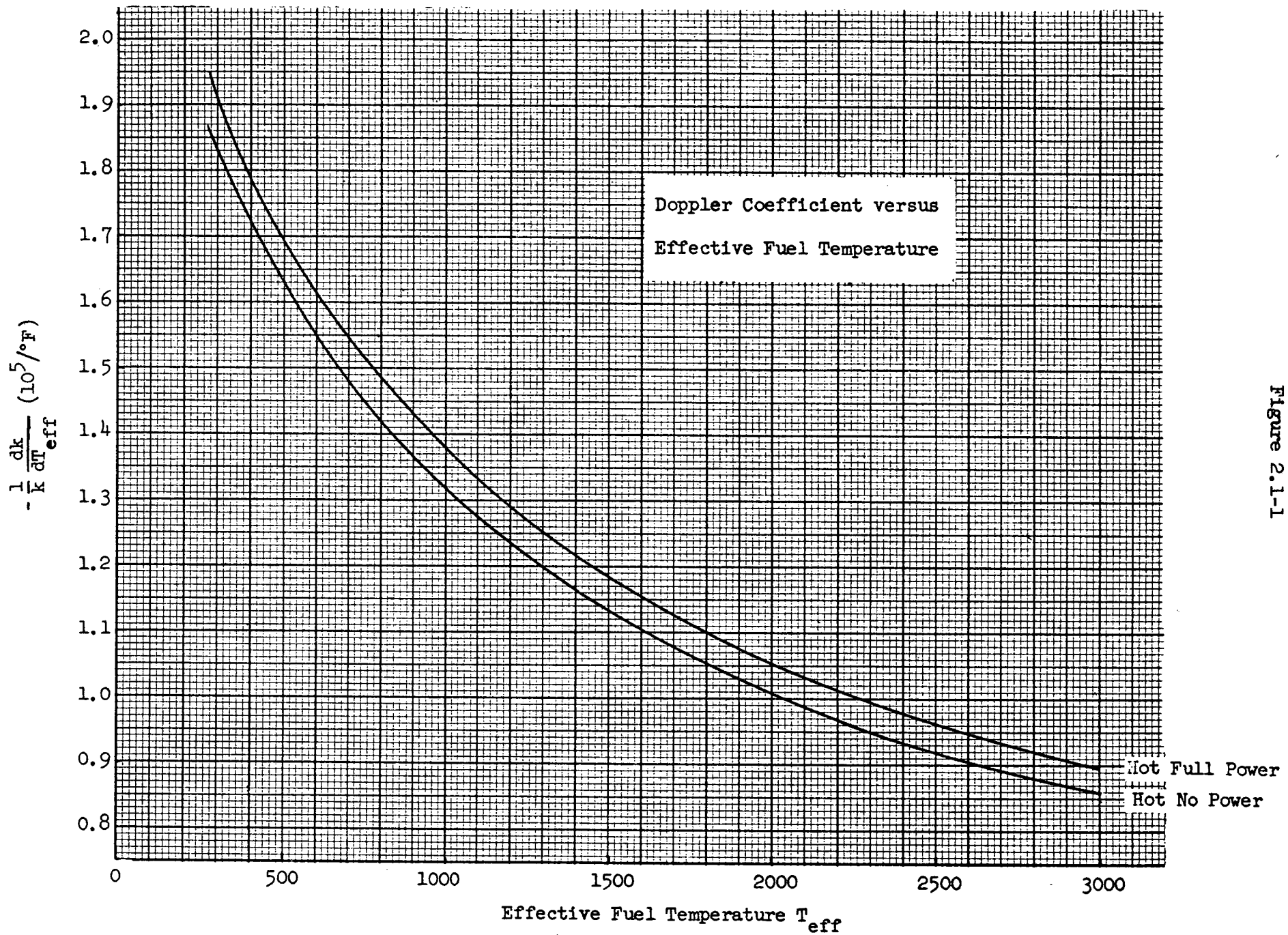


Figure 2.1-1

Figure 2.1-2

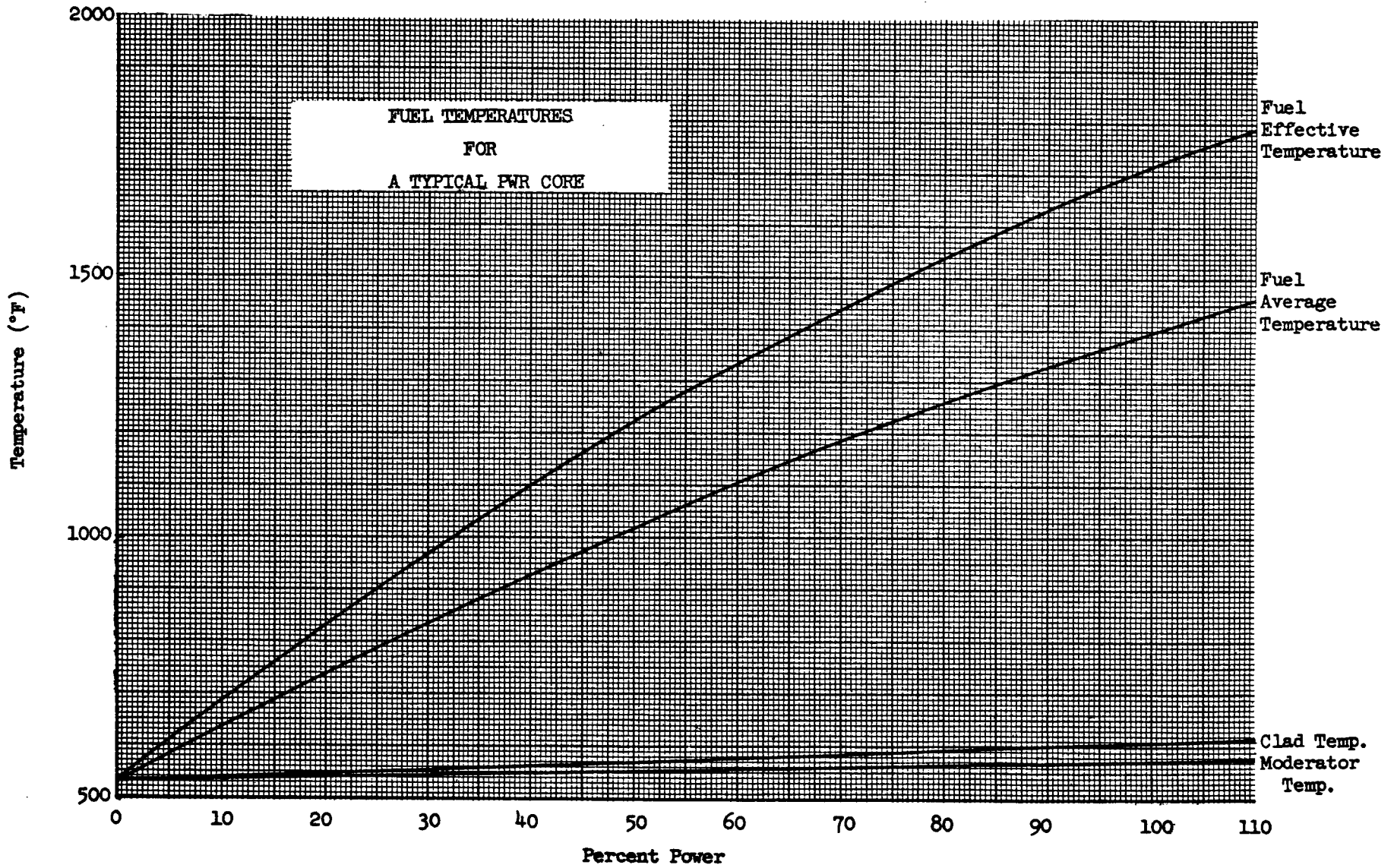
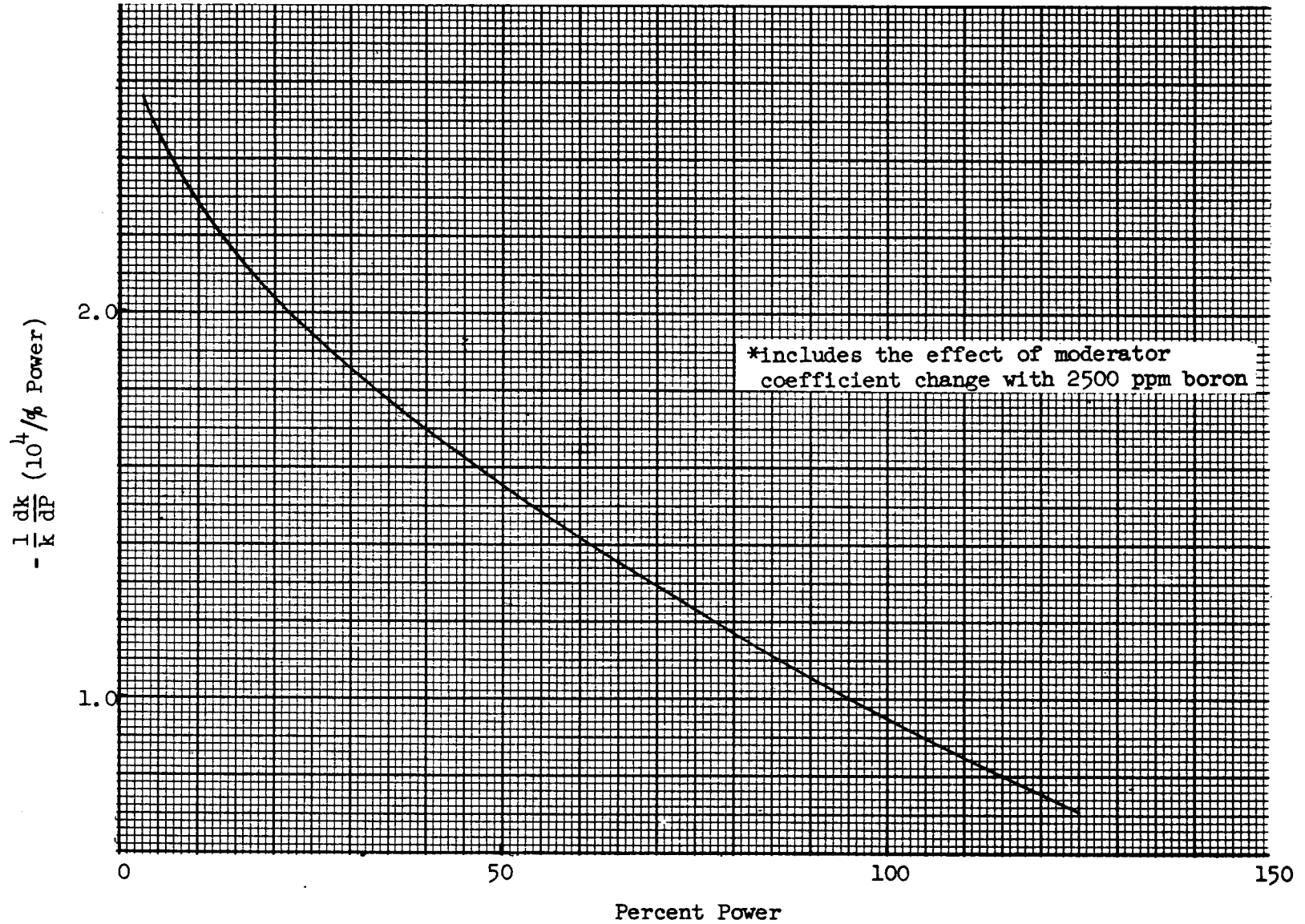


Figure 2.1-3

Power Coefficient\* versus Percent Power



of moderator temperature change with 2500 PPM boron. The temperature variation of the fuel with power shown in Figure 2.1-2 is "quasi static" in that the heat transfer conditions have reached steady state. On rapid power increases, the effective power coefficient is much more negative due to the accumulation of heat energy in the fuel prior to transfer to the moderator.

### 2.1.2 Moderator Temperature Coefficient

The moderator temperature coefficient of reactivity (or net change in neutron multiplication per degree change in moderator temperature) can be broken, roughly speaking, into two additive components. One of these represents the coefficient of the uncontrolled core while the other accounts for the effect of control on the coefficient. Considering the uncontrolled coefficient, it is found that the major factor in establishing the numerical value is the moderating ratio. The other component, the effect of control, varies in sign with the type of control and introduces an additive change which is nearly proportional to the excess reactivity which is controlled.

The moderating ratio of the PWR core is selected to achieve the minimum fuel depletion cost, insofar as this does not compromise power capability or safety. Optimization studies generally result in an undermoderated lattice which exhibits a negative uncontrolled moderator coefficient of the order of  $-2 \times 10^{-4} (\text{°F})^{-1}$ . The reason for the undermoderation is the economic incentive to produce plutonium to be burned as fuel or discharged at end-of-life.

The effect of burnup on the uncontrolled coefficient is to result in a more negative value as burnup progresses for the lattice configurations employed in the PWR core.

If excess reactivity is controlled by movable poison rods, the effect is to introduce an increased leakage component similar to an external boundary. Increased leakage results in a more negative coefficient since the water is the primary deterrent to the leakage. Therefore, control by rods introduces a negative component to the moderator coefficient which is nearly proportional to the amount of reactivity controlled with rods.

When excess reactivity is controlled with dissolved boron, the opposite result takes place. With no boron in the water, an increase in temperature results in a decrease in the water density with water being expelled from the core, yielding the typical negative uncontrolled coefficient. But, with dissolved boron in the water, a portion of the boron is expelled along with the water. It is seen that the chemical poison (boron) must yield a positive increment to the moderator coefficient which again is proportional to the amount of reactivity controlled by boron. Figure 2.1-4 summarizes the preceding comments.

The pressurized water reactor with chemical shim control is designed for cycled or partial core reloading. The cycling technique is specified to achieve the most desirable power distribution, insofar as this does not compromise fuel costs. One of the basic characteristics of this form of cycling is that the first cycle has approximately 50% more excess reactivity than any other. Figure 2.1-5 illustrates this situation.

The conclusion of the foregoing is that with chemical poison control, the moderator coefficient will be least negative at the beginning of the first cycle. In fact, it can be said that the coefficient will never be positive beyond the beginning of the first cycle without a substantial revision to the proposed burnup objectives.

MODERATOR TEMPERATURE COEFFICIENT VERSUS MODERATING RATIO

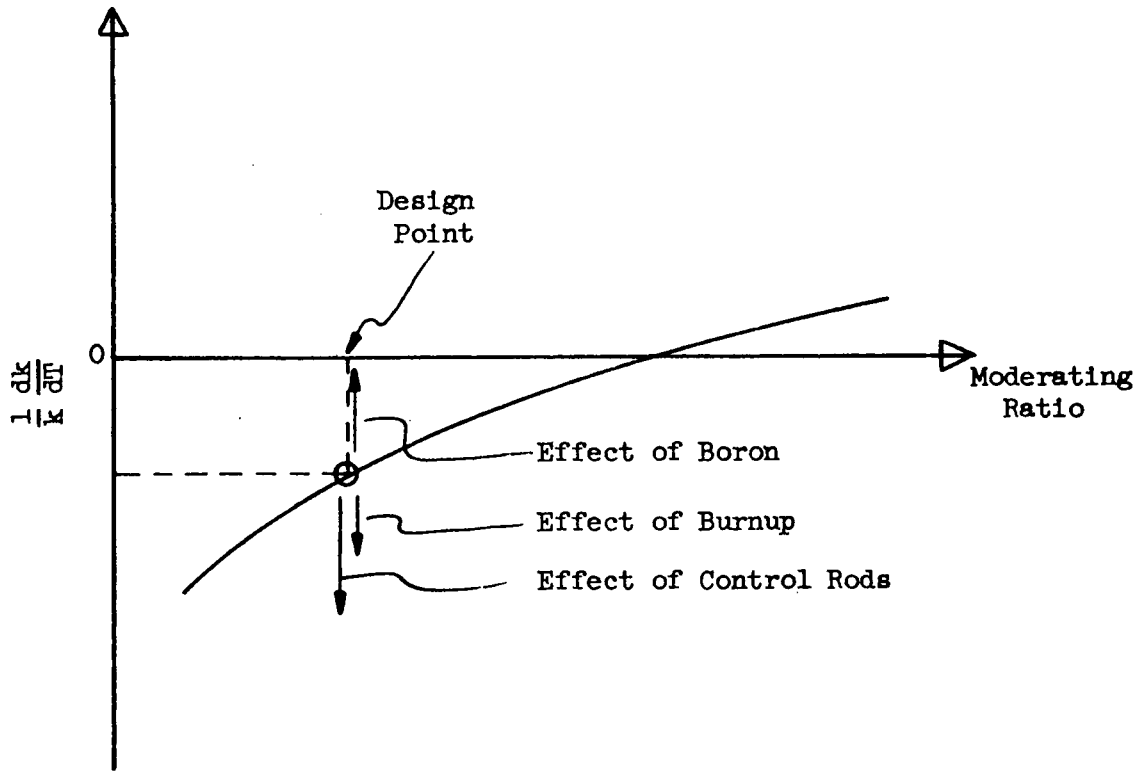


Figure 2.1-4

EFFECTIVE MULTIPLICATION FACTOR VERSUS TIME

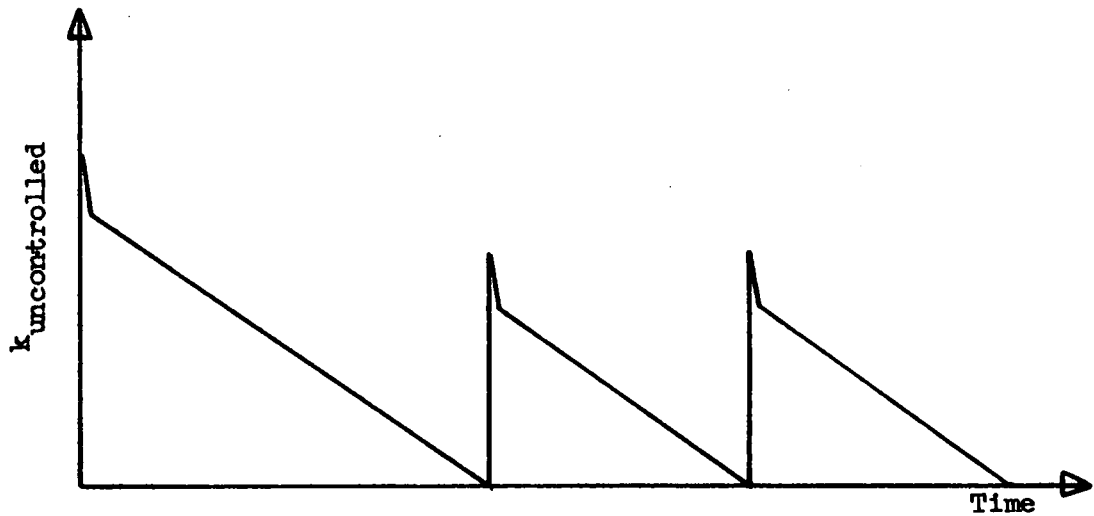


Figure 2.1-5

Note that, following startup, the xenon poisoning results in a rapid reduction in excess neutron multiplication. Thus, one might expect a rapid variation towards a more negative moderator coefficient. The presence of xenon itself, however, yields a positive component in this coefficient which, depending upon moderating ratio, may nearly cancel the anticipated reduction. This positive component results from the cross section energy dependence in the thermal energy range. For the designs under consideration, the net effect is negative although small.

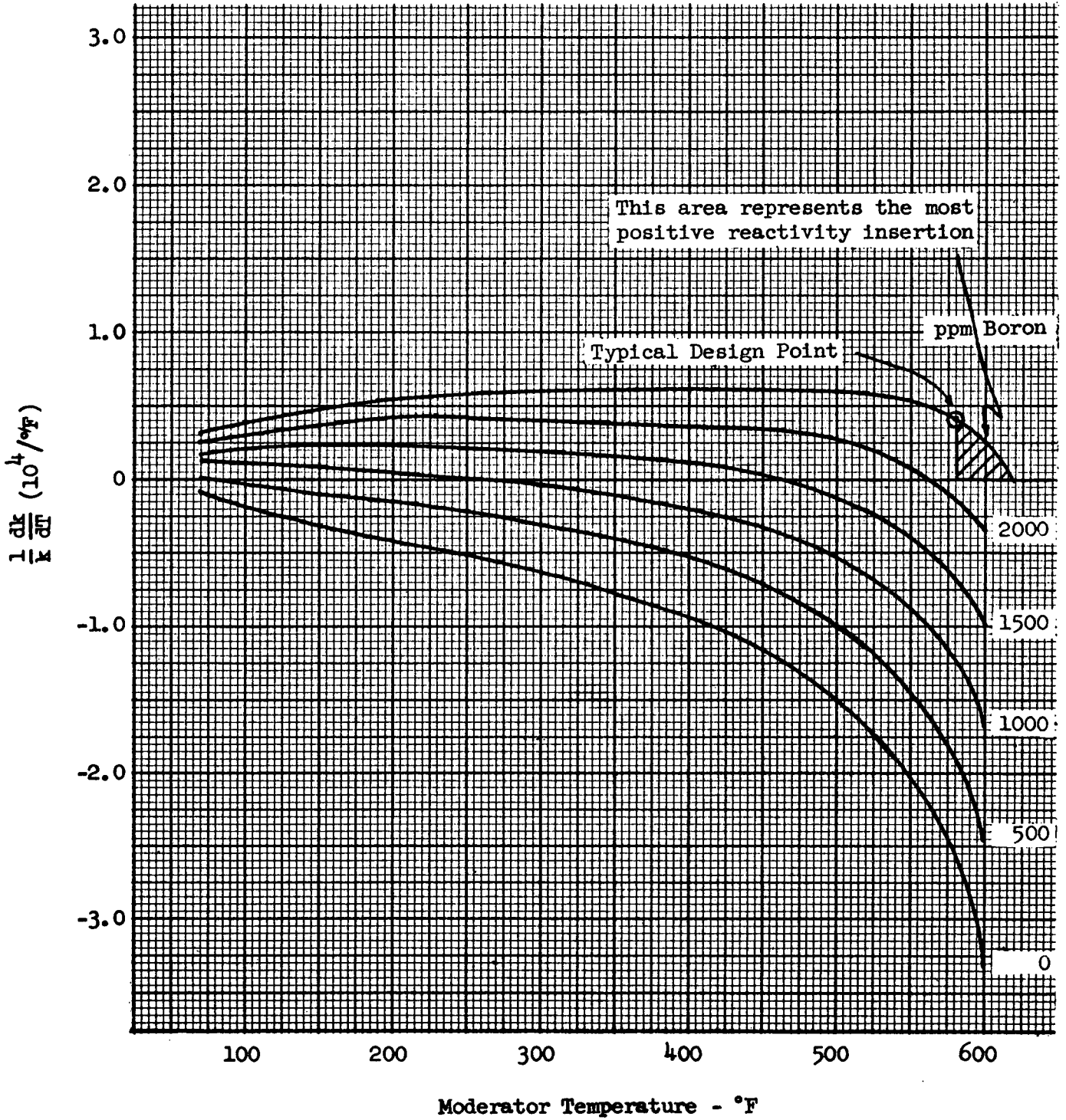
The variation of reactivity due to moderator temperature results:

- 1) through its effect on fuel temperature at constant power
- 2) through its effect on the thermal neutron spectrum,  
(variation in moderator vibrational energy at constant density)
- 3) through its effect on moderator density which, of course, is also a function of the moderator pressure.

Figure 2.1-6 illustrates the variation in the isothermal moderator temperature coefficient in a typical PWR core as a function of moderator temperature and boron concentration. These curves do not include the effect of fuel temperature change, and, therefore, account only for changes in neutron spectrum and water density. Appropriate values (negative) from Figure 2.1-1 must be added to these results to obtain a total moderator coefficient. The moderator is assumed to be at 2065 psia. It is clearly demonstrated that the introduction of a soluble poison results in a positive increment to the moderator coefficient, which is almost directly proportional to the amount of reactivity controlled by the soluble poison. However, the curves of Figure 2.1-6 show clearly that the total reactivity insertion due to temperature rise is limited to small values (approximately 0.1%) for design conditions. This can be seen by considering

Figure 2.1-6

Moderator Temperature Coefficient  
versus Moderator Temperature For  
Different Boron Concentrations



the area indicated in Figure 2.1-6. Figure 2.1-7 illustrates the variation in the water density coefficient of reactivity with water density and boron concentration. The curves of Figure 2.1-7 are based on calculations which are identical to those used to obtain the curves of Figure 2.1-6 except that the thermal neutron spectrum, in this case, is obtained with a constant value of moderator vibrational energy. The effect of the variation in water density on thermal neutron spectrum is included; however, it is assumed as in the previous calculations to be uniformly distributed across the core.

Figure 2.1-8, 2.1-9, and 2.1-10 illustrate the "spectral" coefficient as a function of water density and water temperature for 2500 PPM boron, 1500 PPM boron, and for no boron. By spectral coefficient is meant the theoretical variation in reactivity with the vibrational energy of the moderating lattice but at constant water density. The spectral coefficient is presented for three boron concentrations to illustrate the non-linear effect of boron on the spectral term. The results from Figures 2.1-7, 2.1-8, 2.1-9, and 2.1-10 can be employed along with the variation in water density with temperature to produce the results in Figure 2.1-6.

Figure 2.1-11 presents the temperature coefficient of water density at 2065 psia.

Figure 2.1-7

Moderator Density Coefficient  
versus Density for Different  
Boron Concentrations

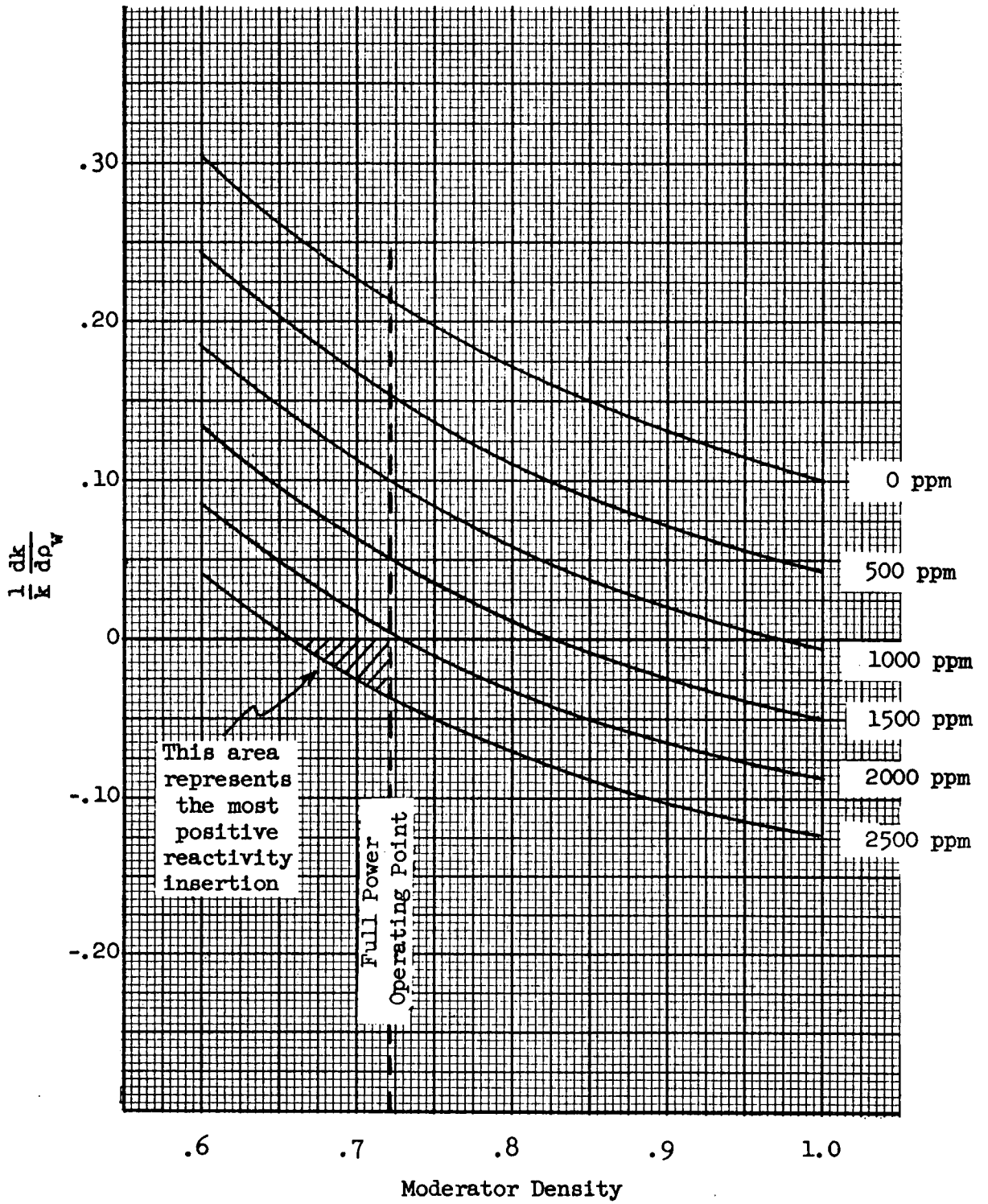


Figure 2.1-8

Spectral Coefficient versus  
Moderator Temperature  
2500 ppm Boron

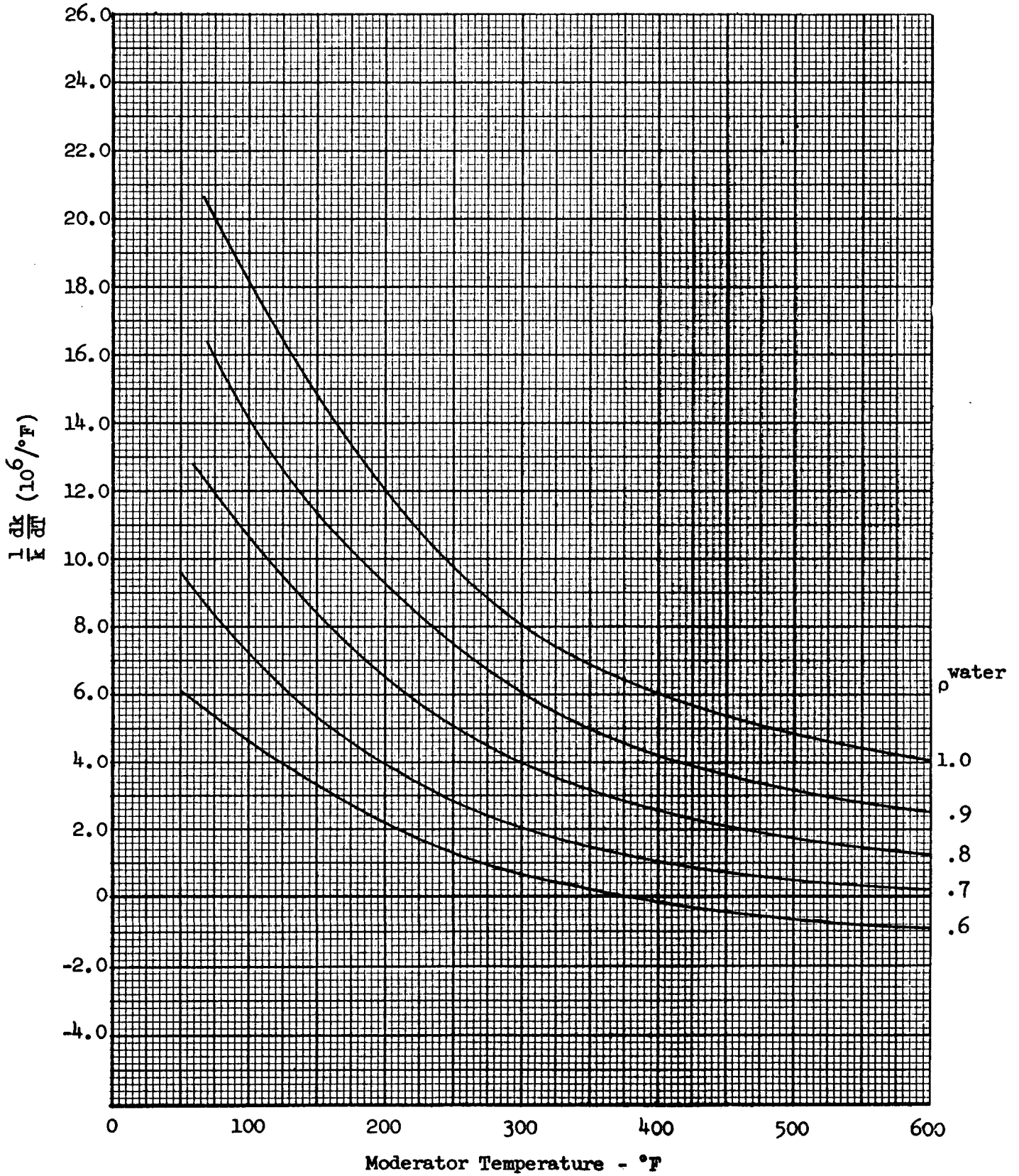


Figure 2.1-9

Spectral Coefficient versus  
Moderator Temperature  
1500 ppm Boron

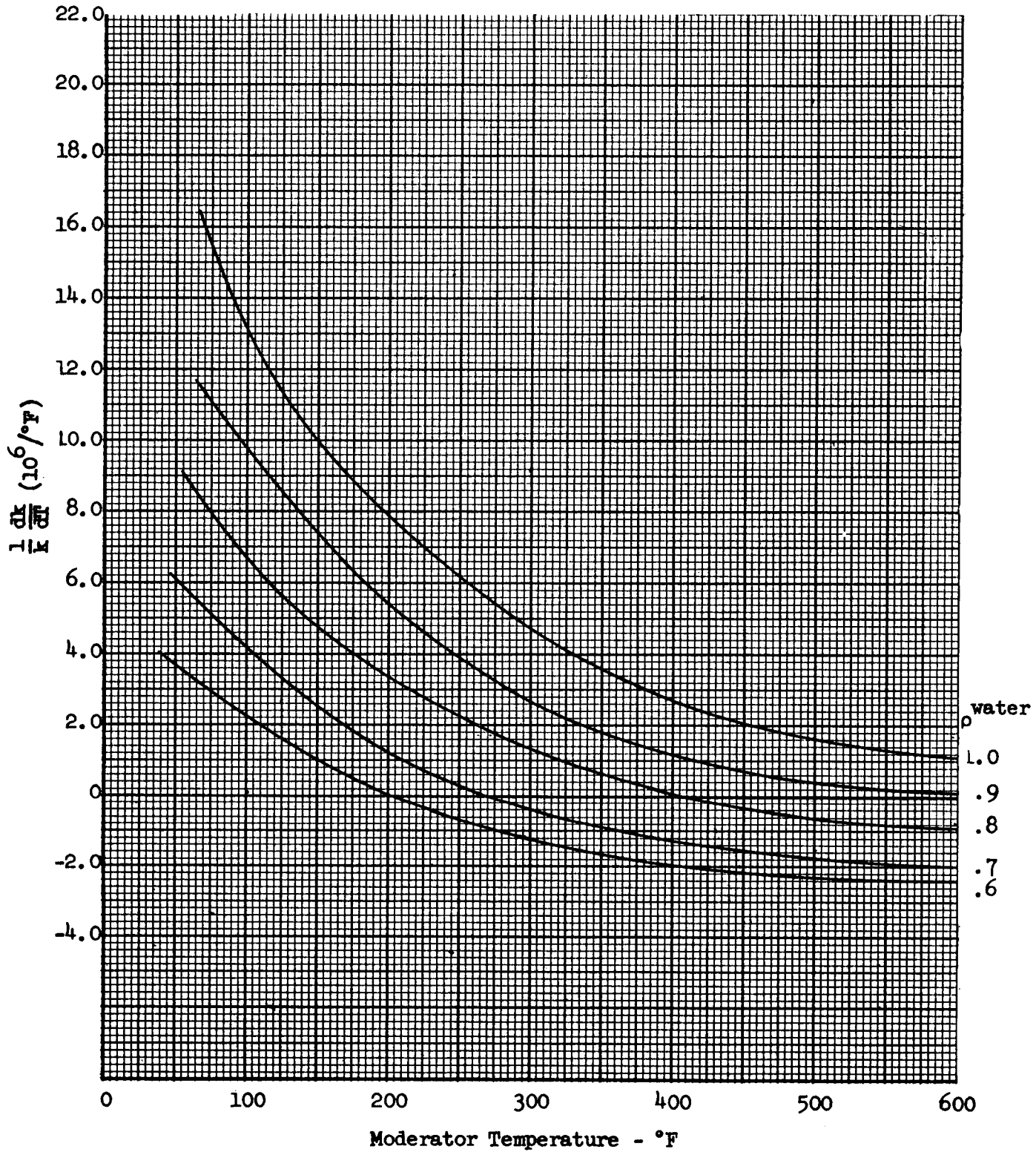


Figure 2.1-10

Spectral Coefficient versus  
Moderator Temperature  
No Boron

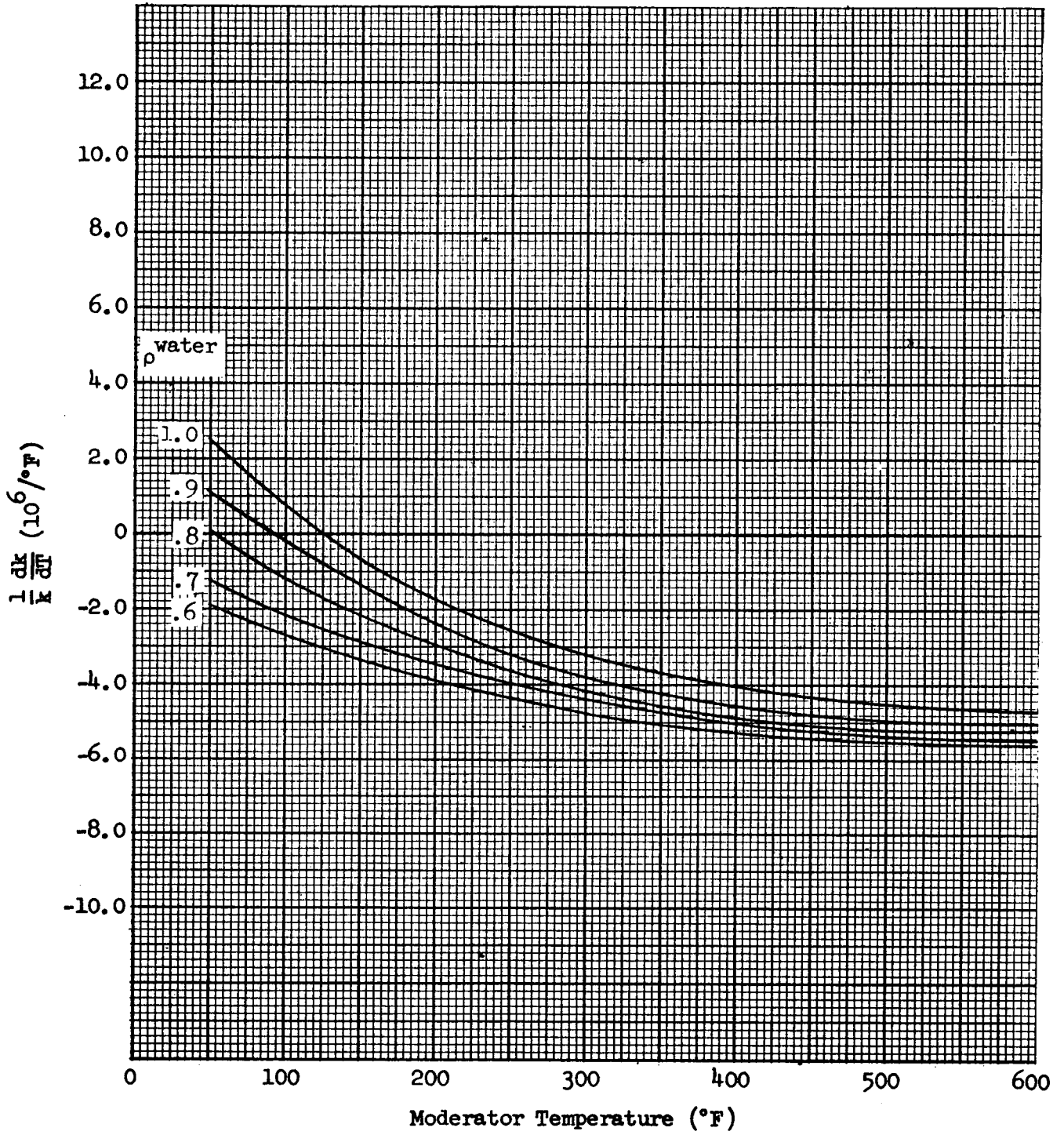
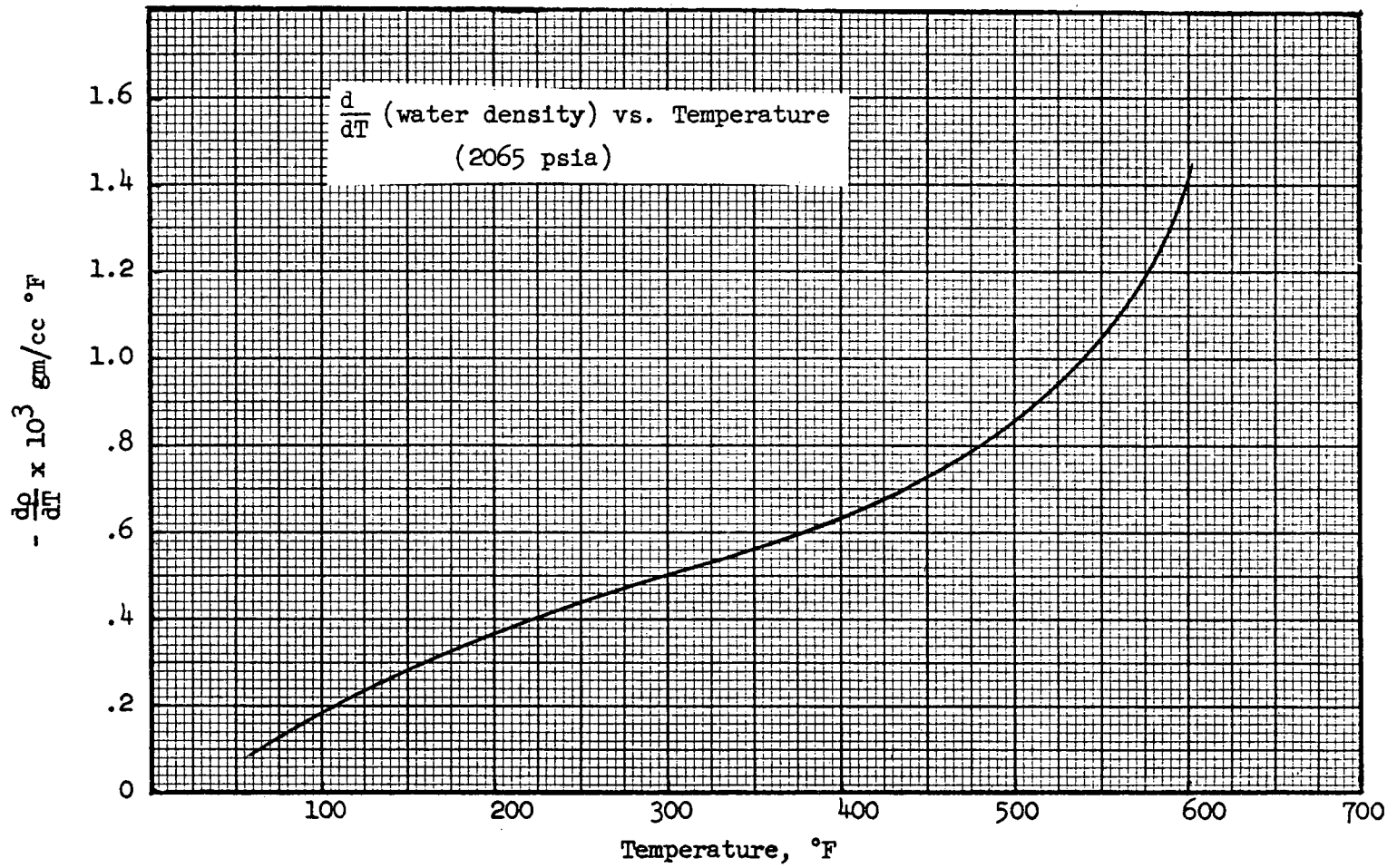


Figure 2.1-11



## 2.2 EFFECT OF NON-UNIFORM MODERATOR TEMPERATURES ON PWR CORES

The situation with non-uniform distribution of moderator temperature must be examined to determine the adverse effect, if any, on power distribution and reactivity variation. In the case with negative coefficients, the non-uniform effects enhance the negative reactivity variation and result in a more uniform distribution of power. Therefore, the non-uniform moderation effects are usually ignored when coefficients are negative. The question to be answered, therefore, is whether the non-uniform effects increase the potential positive reactivity insertion with a positive moderator coefficient and whether the power distribution is generally less uniform and to what degree these effects exist.

### 2.2.1 One Dimensional Analysis

The initial step in answering this question was to examine the effect of temperature variation in the X-Y plane by means of a homogenized calculation in a cylindrical one dimensional analysis. By homogenized it is intended to mean that water holes and water slots are smeared into the assembly region. A boron concentration of 2500 PPM was selected as representative of PWR cores at the beginning of the first cycle. Variations in fuel enrichment and moderator temperature are treated on a region-wise basis. For moderator temperature variation, the core was broken into 9 concentric cylinder regions of roughly equal volume. The temperature was varied from region to region; but, within each region, it was uniform.

The base calculation was for a uniform temperature across the core (at 578°F). Then, the temperature of each region was varied arbitrarily to find the maximum possible increase in reactivity. It was assumed that the saturation temperature could be reached

and that boiling void could be introduced. From Figure 2.1-6 it can be seen that an isothermal increase of approximately 0.1% in reactivity could be expected (area under 2500 PPM curve) and this maximum insertion would occur at about 620°F.

The temperature (or void) in each region was varied arbitrarily until any change in any single region would reduce the core reactivity. Table 2.2-1 presents the resulting distribution in the nine regions and the maximum insertion of slightly under 0.25% in reactivity. This distribution in temperature is not consistent with that which would be obtained as a consequence of the power distribution. Here it was assumed that no region could have a temperature below 578°F. If this could happen, the maximum insertion could be increased to about 0.3% with the temperature in the outer regions reduced to roughly 510°F. This, however, is not a realistic condition. Calculations have been performed to demonstrate the effect of changing the boron concentration. Figure 2.2-1 illustrates the sensitivity of this insertion to boron concentration. It is clear that the results change slowly with concentration.

The individual steps in the previous calculations were employed to develop a set of "regionwise" temperature coefficients. This coefficient is defined as the change in core reactivity per degree Fahrenheit change in temperature per per cent of core volume in which the temperature change is introduced. A factor of 100 times these values can be compared with the isothermal value to gain an idea of the significance of a local variation in temperature. The isothermal value along with "regionwise" values are given in Table 2.2-2. Care should be taken to avoid considering the "regionwise" coefficient as a local coefficient in any rigorous sense because these are not the values (for example) which would be used in a coupled core calculation.

TABLE 2.2-1  
 TEMPERATURE DISTRIBUTION FOR MAXIMUM REACTIVITY INSERTION  
 2500 PPM BORON  
 MAXIMUM REACTIVITY INSERTION - 0.246%

Region	1	2	3	4	5	6	7	8	9
Temperature	640(0)*	640(0)*	640(0)*	620	615	605	578	578	578

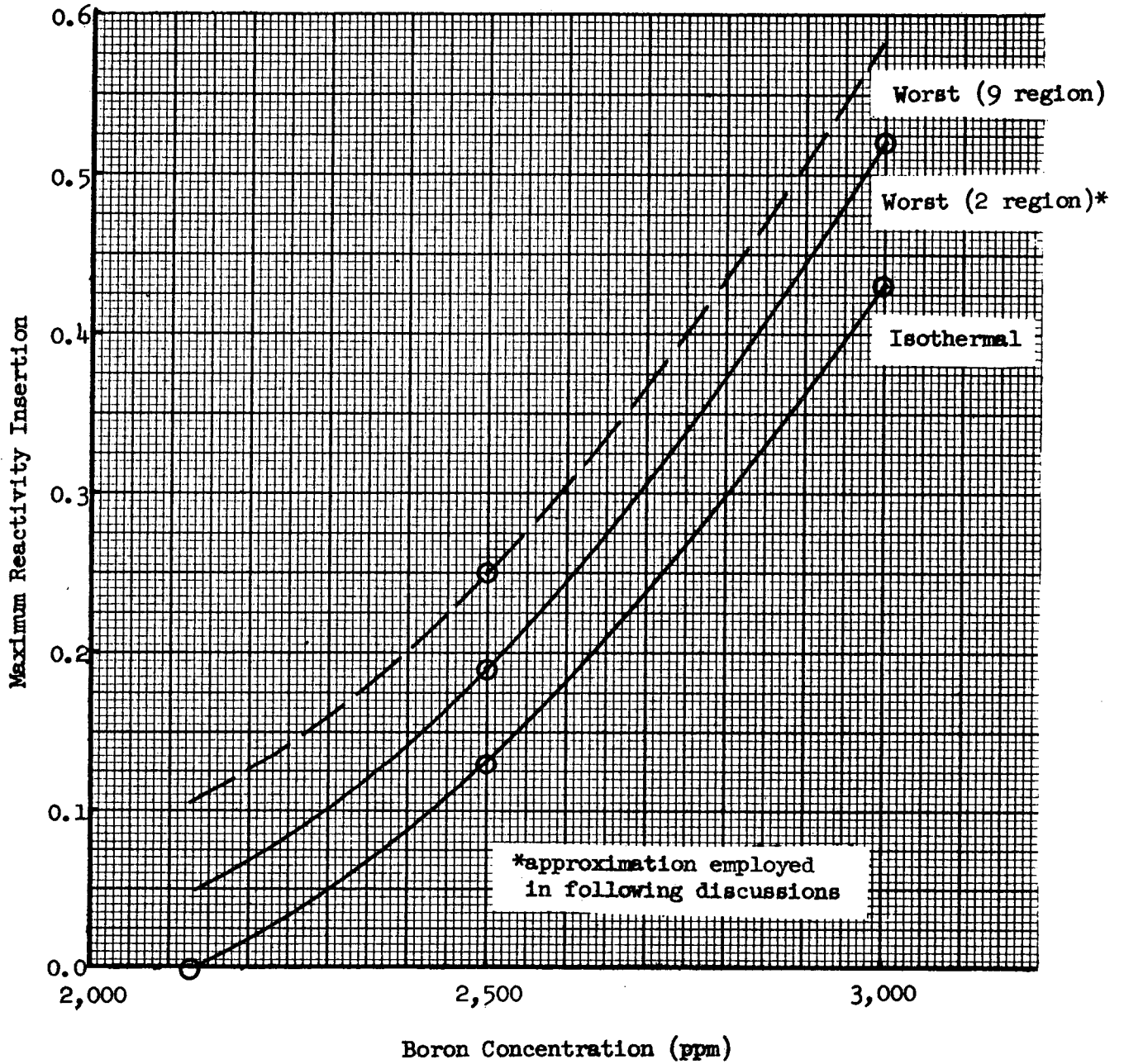
\*Numbers in parenthesis represent per cent quality.

TABLE 2.2-2  
 REGION TEMPERATURE COEFFICIENT ( $10^{-6}/F$ )

<u>Region</u>	<u>Enrich</u>	<u>Vol. Fraction</u>	<u>589°F</u>	<u>612.5°F</u>	<u>632.5°F</u>
1	3.15	.03751	1.22	1.08	.84
2	3.15	.11253	1.22	1.07	.65
3	3.15	.18754	1.17	.99	.68
4	3.40	.09795	.54	.26	.21
5	3.40	.11041	.38	.12	-.41
6	3.40	.12286	.18	-.12	-.34
7	3.85	.10302	-.37	-.54	-1.10
8	3.85	.11040	-.44	-.55	-.99
9	3.85	.11778	-.37	-.49	-.56
Isothermal coefficient ( $10^{-4}/F$ )			+0.35	+0.15	-0.20

Figure 2.2-1

MAXIMUM REACTIVITY INSERTION  
VERSUS  
BORON CONCENTRATION



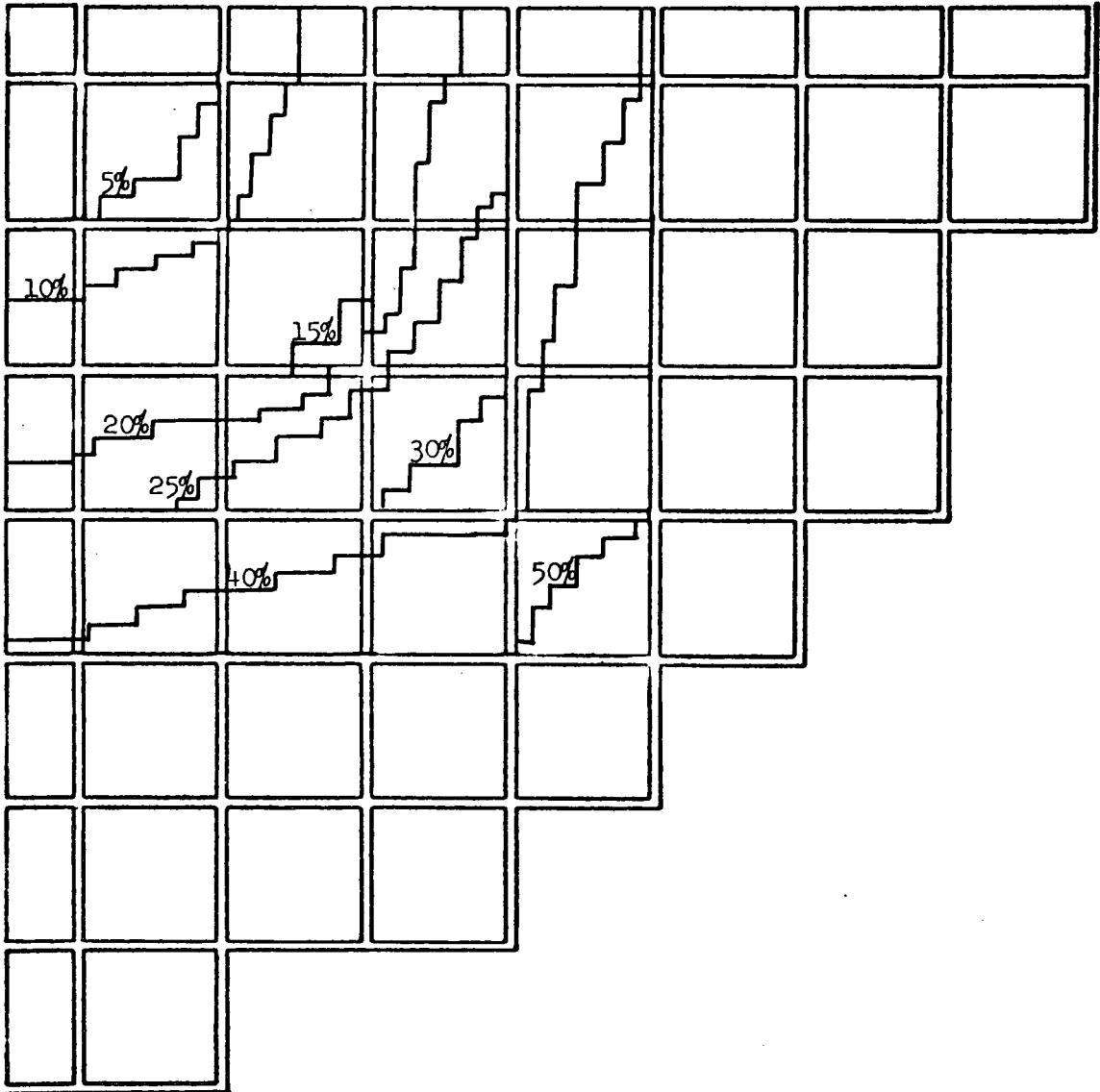
### 2.2.2 Two Dimensional Analysis

It is known that a homogenized one dimensional analysis is not sufficient to determine effects on power distribution which are sensitive to fine structure variations that result from water hole and water slot flux peaking. The objective of the work described in this section is to develop an understanding of the consequences of chemical shim on the distribution of power under the influence of non-uniform moderator temperature.

An X-Y analysis was performed in two dimensions with the effects of water slots and water holes introduced. Again the boron concentration was taken to be 2500 PPM. The moderator temperature was treated in two regions because of the complexity of additional regions in a discrete X-Y representation. The core fraction assigned to each of the two regions was varied. Figure 2.2-2 illustrates the boundaries studied in quarter core geometry for a typical PWR core. Although the water holes created on withdrawal of the Rod Cluster Control (RCC) are not shown in this figure, they are in the calculation. On the basis of the results of the cylindrical calculations the central region was raised to 640°F (approximately saturation condition) while the outer region remained at 578°F. Figure 2.2-3 illustrates the variations in neutron multiplication as a function of core fraction raised to 640°F. With this fraction equal to zero (entire core at 578°F) the neutron multiplication is 0.9991.

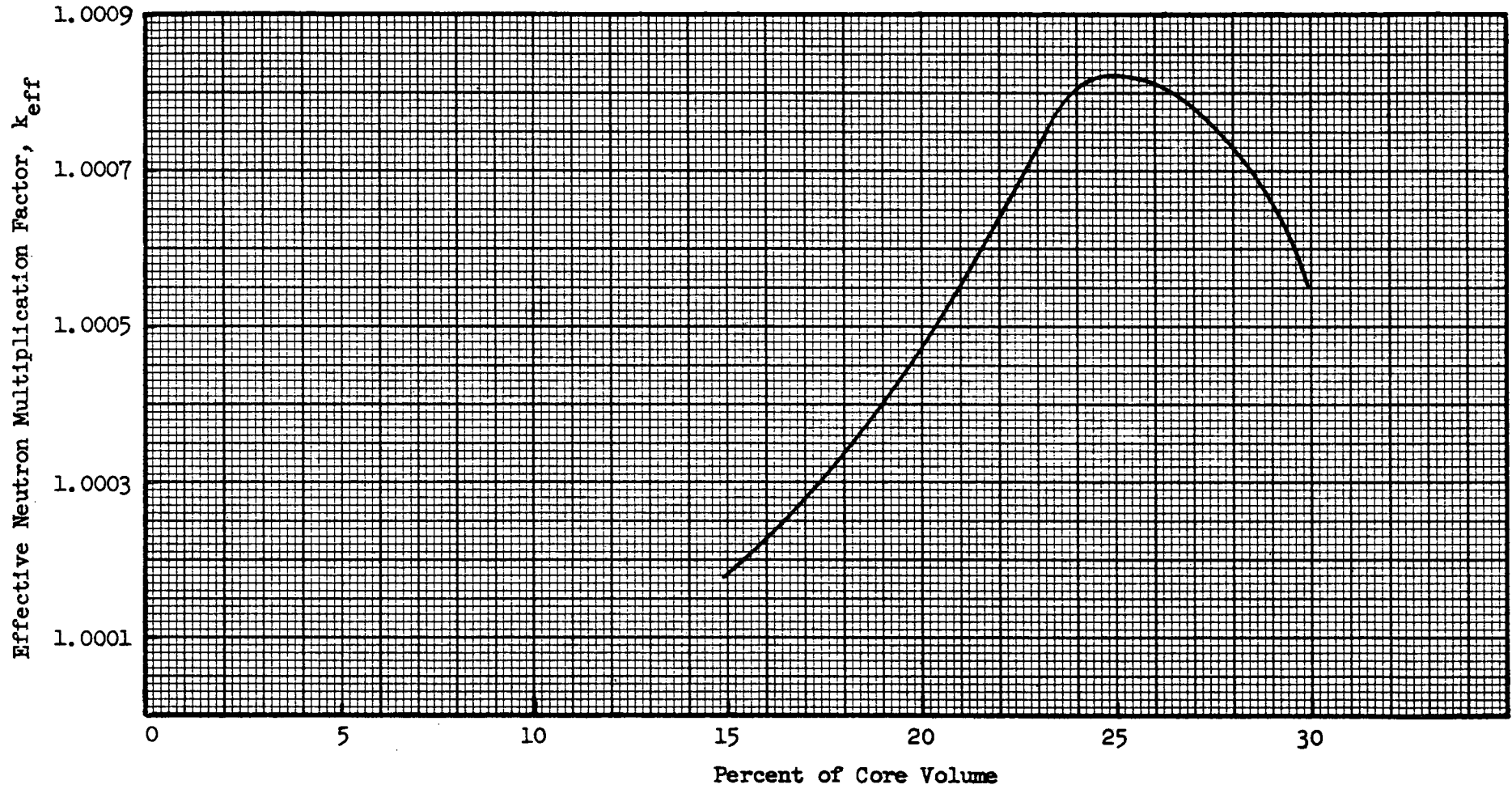
The maximum potential insertion on the basis of this analysis is 0.17% and it occurs with 25% of the core raised to 640°F. This result is consistent with a two region analysis in one dimension with homogenized assemblies and indicates that water holes and water slots do not affect the results significantly. The core for a 25% central region was then studied as a function of its

Figure 2.2-2



REGION BOUNDARIES FOR AREA WITH DECREASED WATER DENSITY

Figure 2.2-3



EFFECTIVE NEUTRON MULTIPLICATION FACTOR VS PERCENT OF THE CORE VOLUME WITH A MODERATOR TEMPERATURE OF 640°F

temperature and void content. The results of this study are presented in Figure 2.2-4 where neutron multiplication is plotted against water density so that the effect of boiling void could be shown directly. The point at saturation density is the same as the peak point in Figure 2.2-3. The result is that the maximum insertion is obtained with approximately 7% boiling void and is 0.19% rather than 0.17%. The conclusion is that the two region study is not an unreasonable simplification (yielding 0.19% rather than 0.25%) when it is employed to obtain effects which require X-Y geometry.

As a part of the X-Y study the variation in power distribution was obtained. Figure 2.2-5 presents the variation in local to average power density at the core center line. This is referred to as  $F^{\text{centerline}}$ . Also shown is the maximum to average power density regardless of radial position. The peak is at the centerline when the entire core is at 578°F. It moves out as the volume fraction of the center region is increased up to 20% and at 40% it returns to the center. Figure 2.2-6 shows the positions of the peak. The result that the power drops at the center line as the temperature is increased argues for the fact that "local" multiplication is not increasing. Experimental verification (Section 2.4.4) lends weight to this argument which is based upon analysis. The rather fine scale in Figure 2.2-5 demonstrates the relative insensitivity of the power distribution to non-uniform moderator temperature distributions. Of even greater importance, of course, is the fact that the power does drop at the point of temperature rise.

Figure 2.2-7 is a trace of the power distribution along the line which is the path of the hot channel indicated by X's in Figure 2.2-6. This is for the calculation with 5% of the core raised to 640°F and gives, therefore, more detail in distribution for the 5% point in Figure 2.2-5. The ripples result from the fact that this particular trace passes near a series of RCC water holes.

Figure 2.2-4

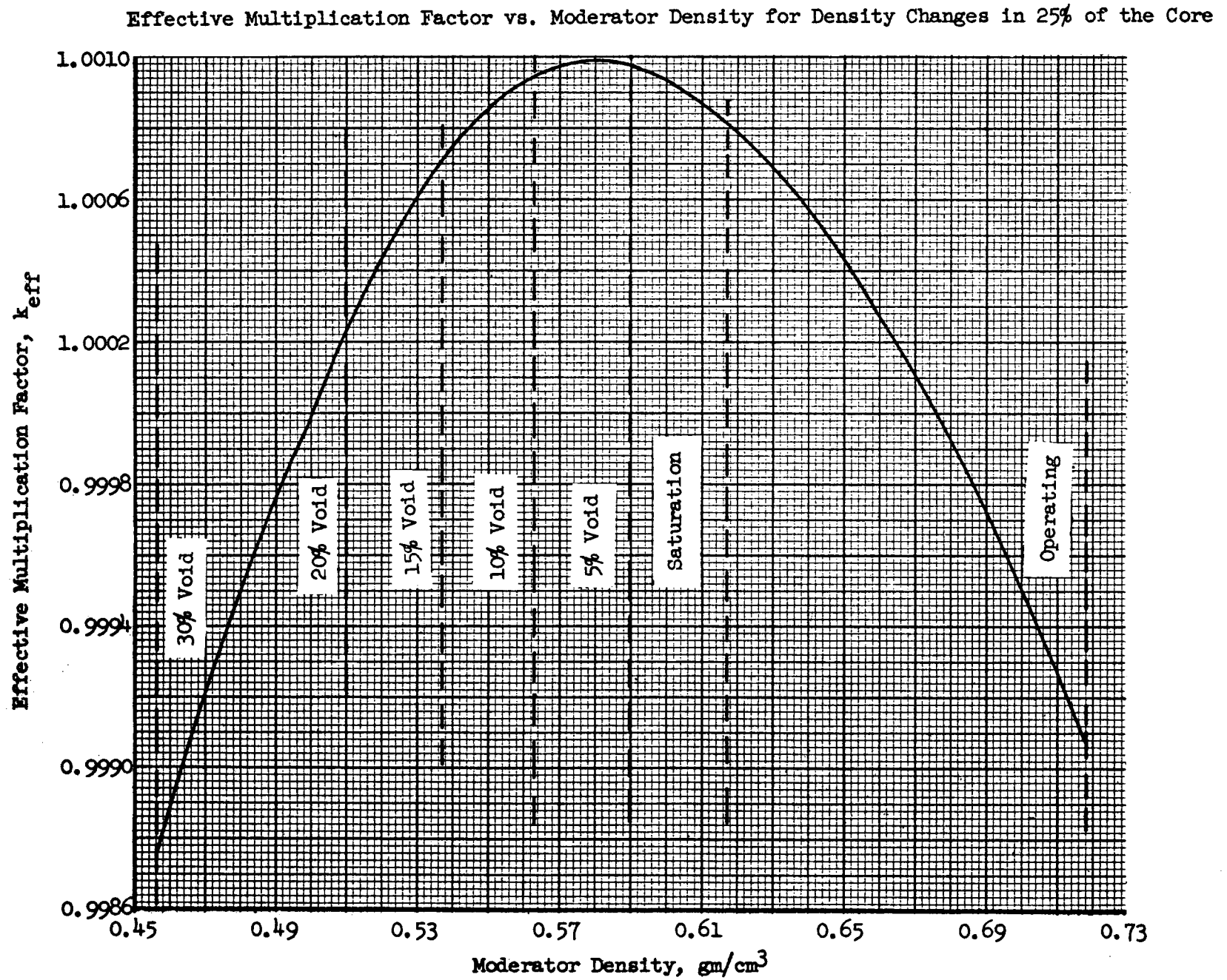
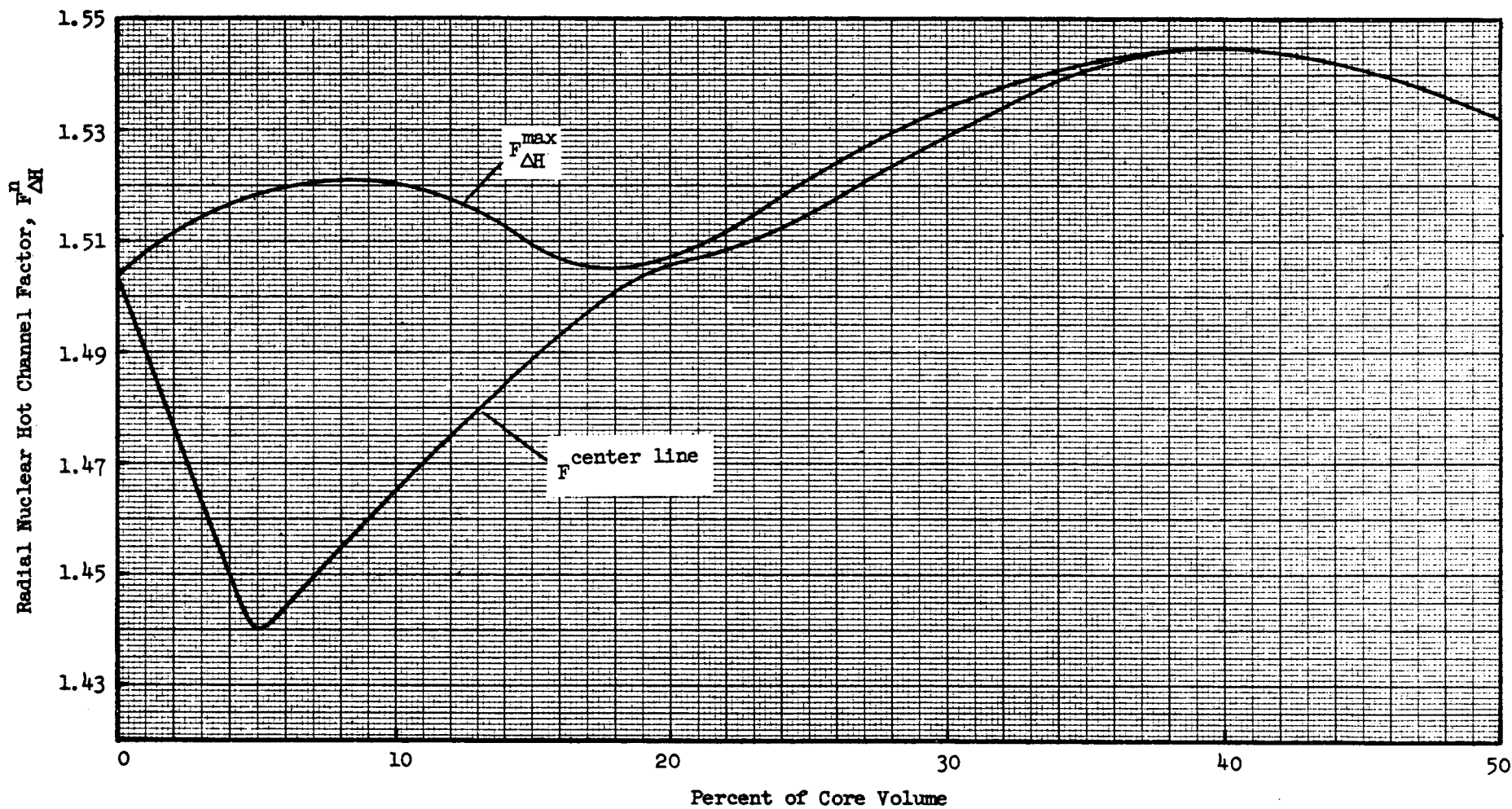
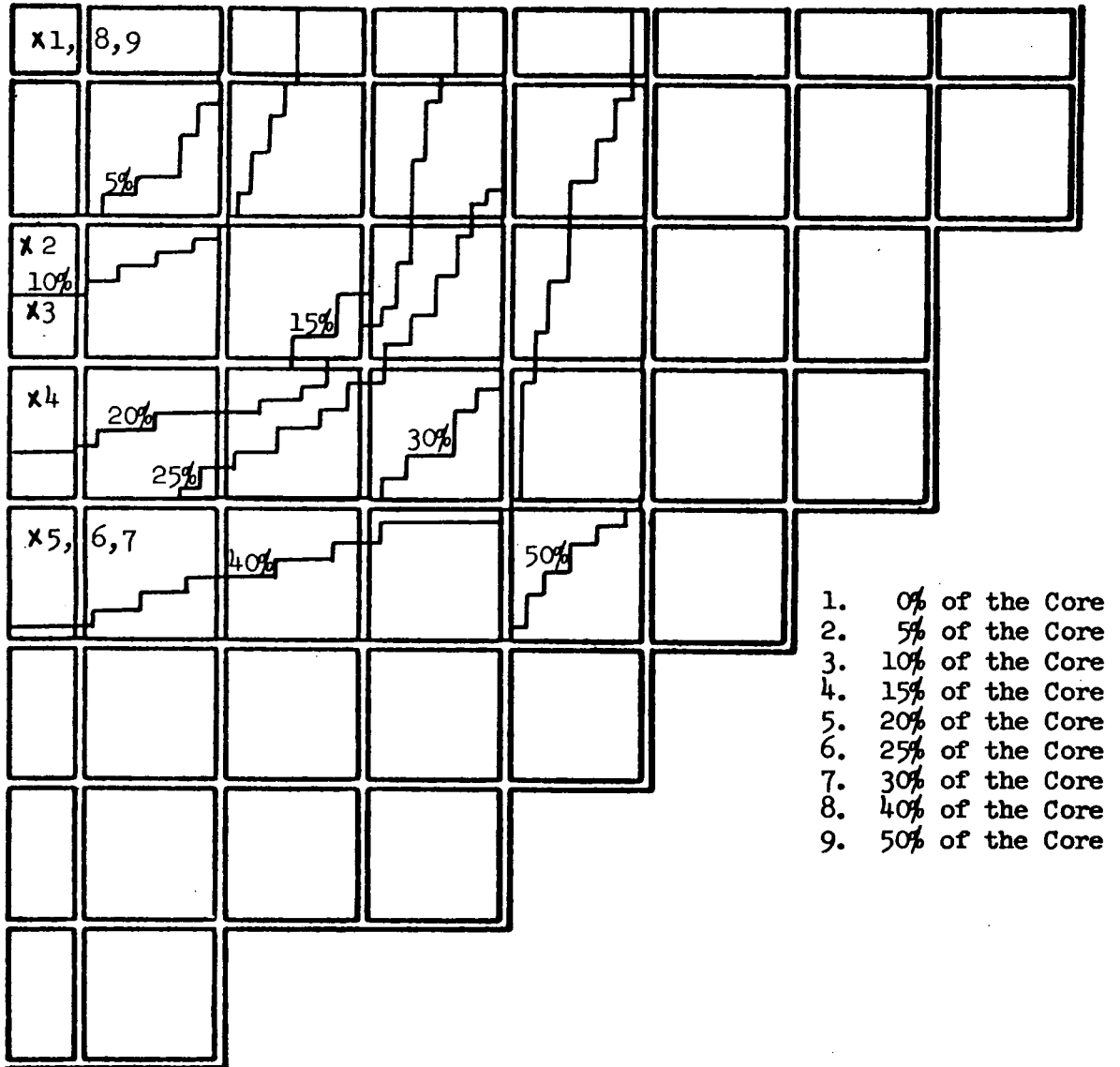


Figure 2.2-5



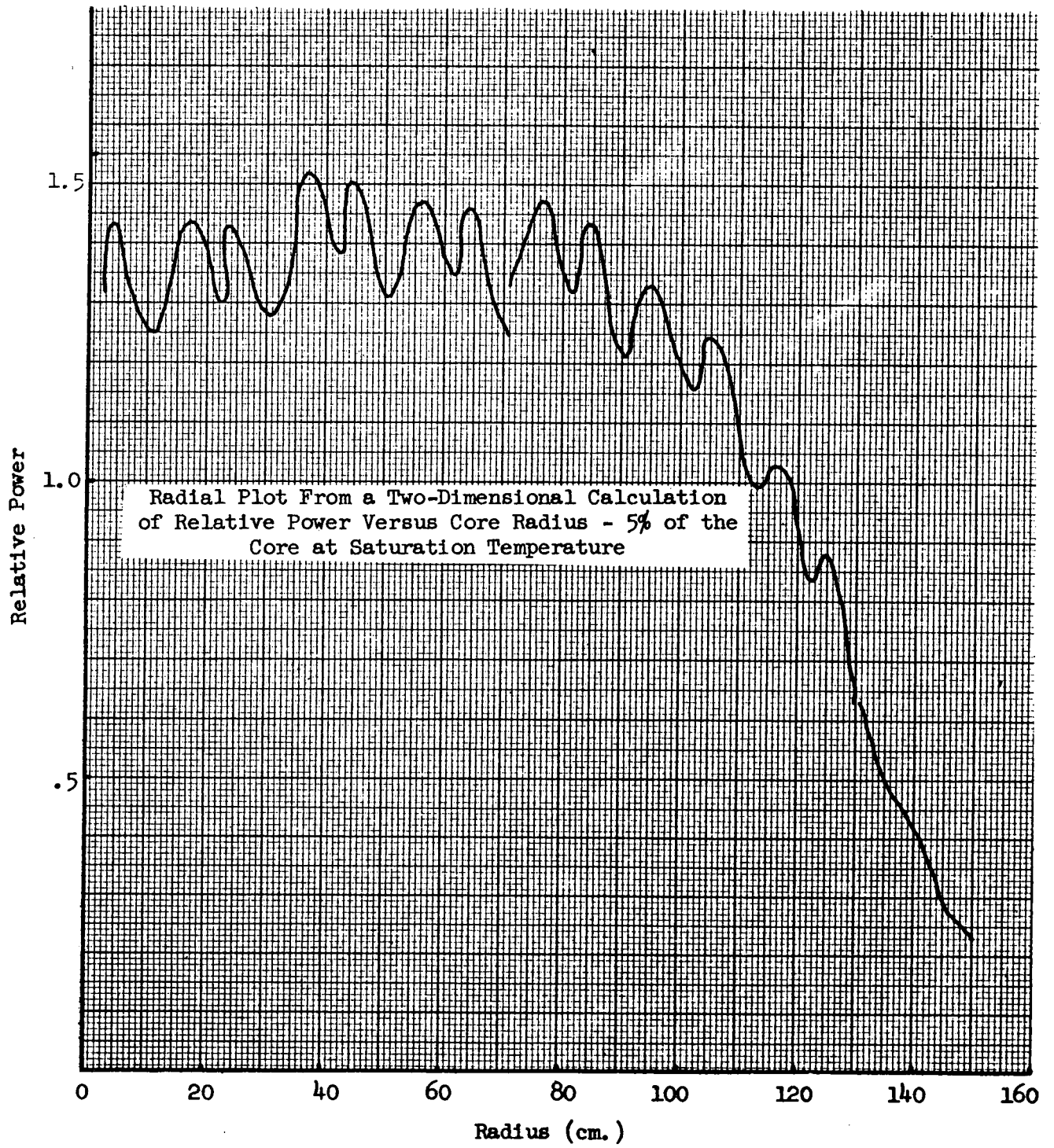
RADIAL NUCLEAR HOT CHANNEL FACTOR VS PERCENT OF THE CORE VOLUME WITH A MODERATOR TEMPERATURE OF 640°F



MOVEMENT OF THE HOT CHANNEL FACTOR WITH INCREASING FRACTIONS OF THE CORE MODERATOR AT SATURATION TEMPERATURE

Figure 2.2-6

Figure 2.2-7



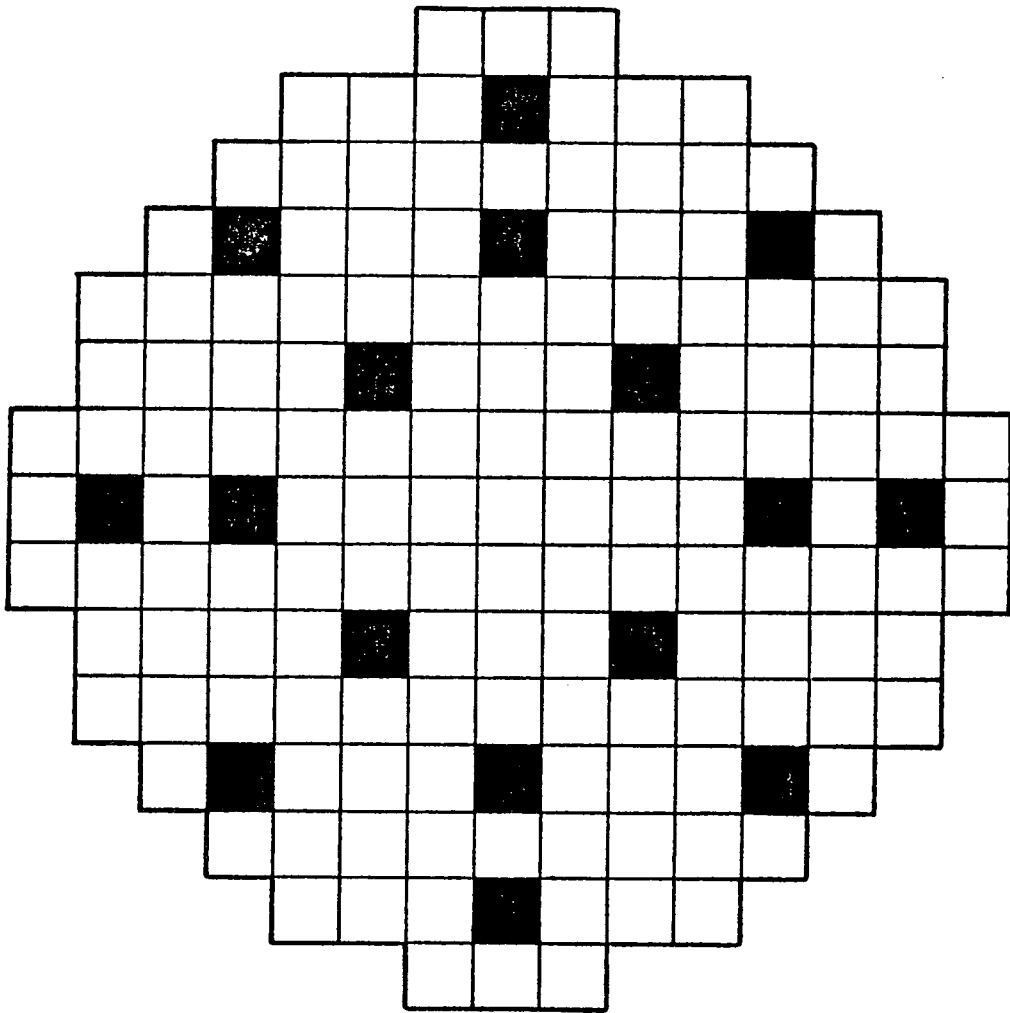
Next, the same type of X-Y analysis was performed for the core with a power control group inserted and the most reactive rod removed. The purpose was to determine if distorted distributions were more seriously affected than normal distributions by non-uniform temperature effects.

The most reactive rod for this power group is that in the center assembly. Figure 2.2-8 shows the rod pattern employed. With the RCC concept, the rods are within rather than between assemblies. Because the rod removed was the center rod, the boundaries for the temperature regions were identical to the previous study as in Figure 2.2-2.

Figure 2.2-9 indicates that the maximum reactivity insertion is for the case with 25% of the core volume raised to saturation and the value is 0.064%. As before, the water density was varied for the 25% case. Figure 2.2-10 indicates a maximum insertion of 0.068% with the center region somewhat below saturation temperature. As might have been expected, the insertion is much smaller for situations which have a distorted power distribution since leakage is more important.

In all the calculations with control rods inserted, the position of the peak did not move from the center, but, the maximum to average power density was reduced as indicated in Figure 2.2-11. Again it is emphasized that the power drops at the point of temperature rise.

Finally, an axial study has been performed (one dimensional calculation) in which the temperature distribution was adjusted in regions to be consistent with the axial power distribution. With this temperature distribution, a moderator temperature coefficient was computed which can be compared with this isothermal calculation.



TYPICAL CONTROL ROD PATTERN WITH STUCK CENTER ROD

Figure 2.2-8

Figure 2.2-9

Effective Neutron Multiplication Factor Versus Percent of the Core Volume With A Moderator Temperature of 640°F - Rod Pattern of Figure 2.2-8

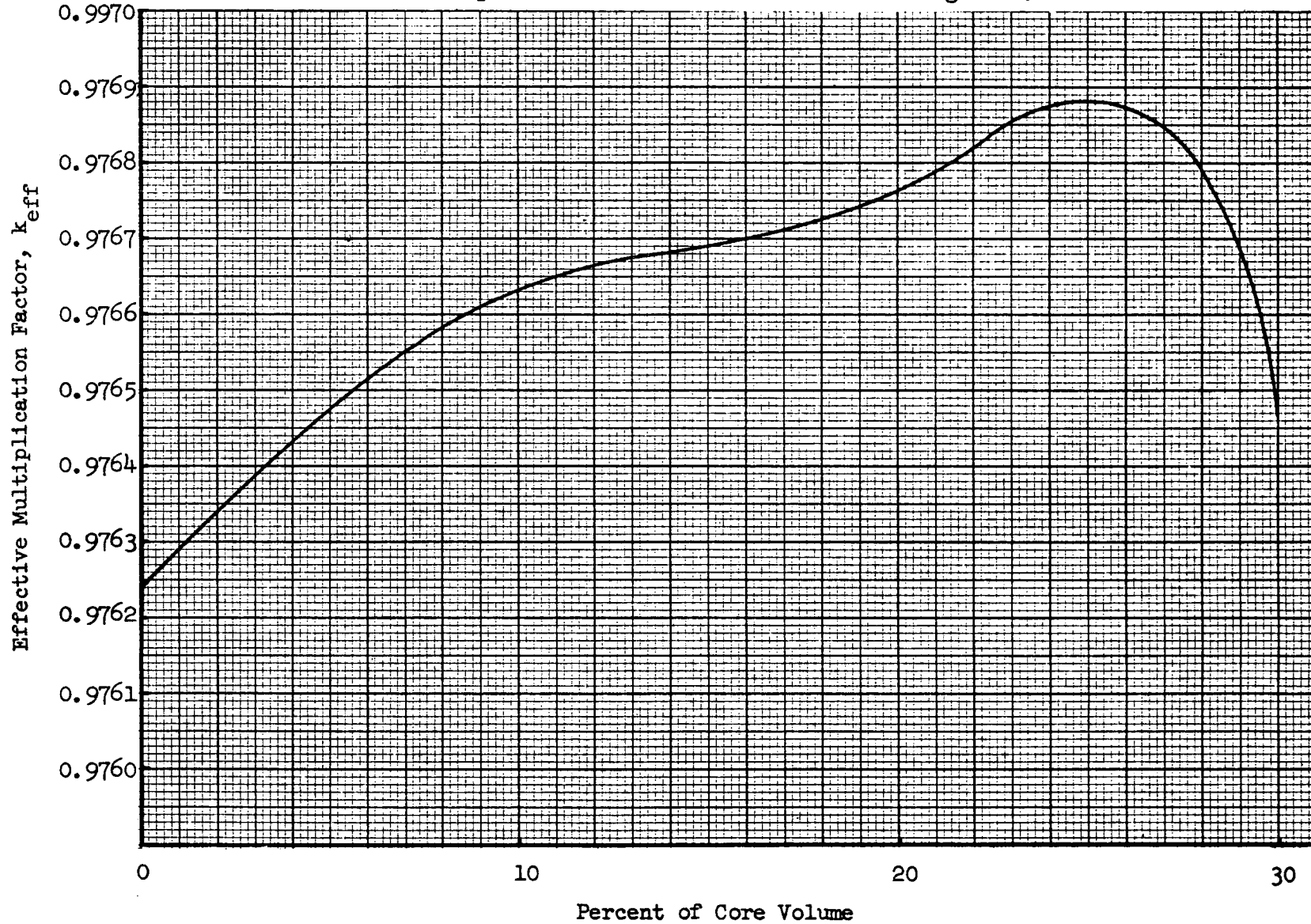


Figure 2.2-10

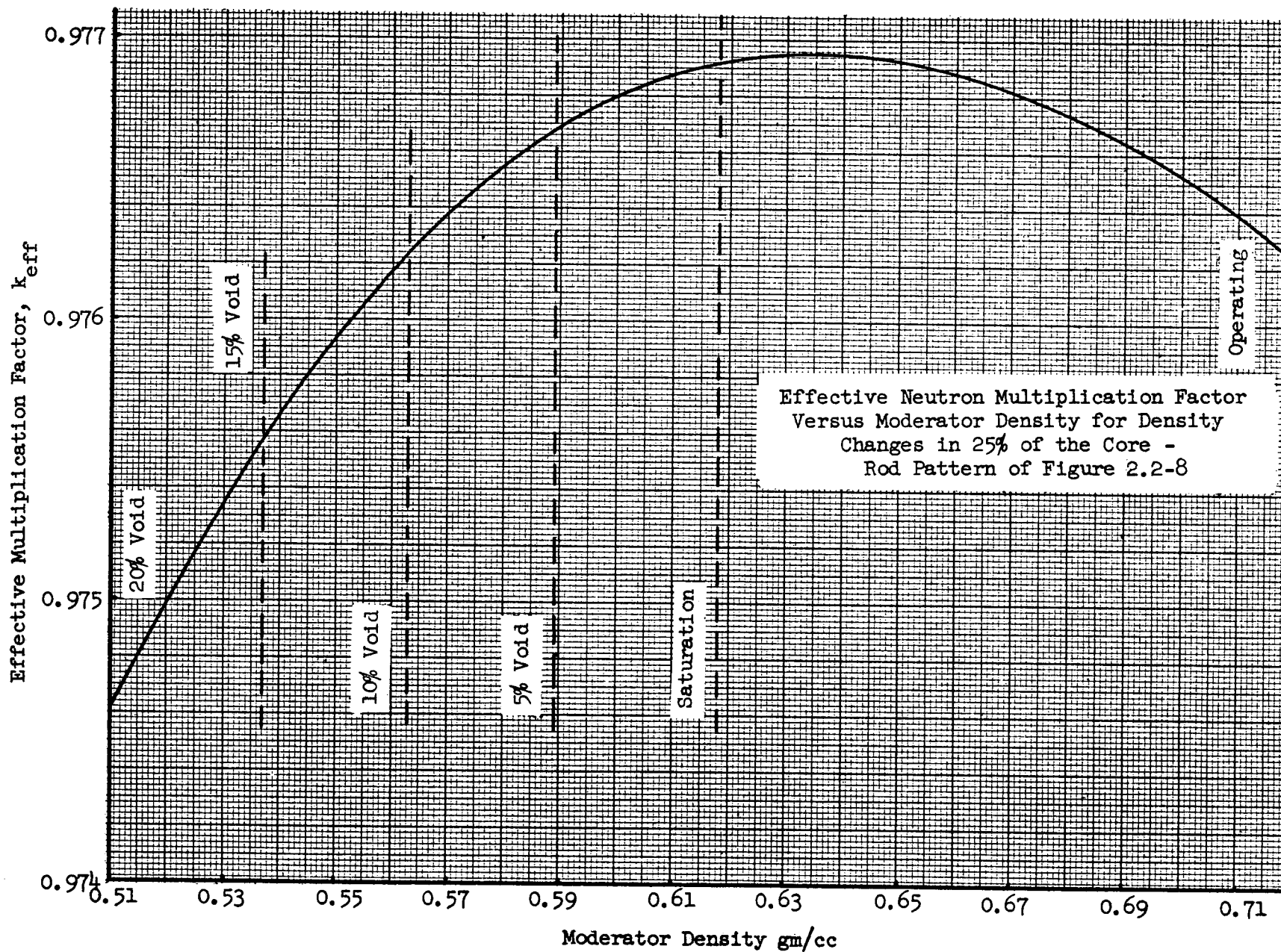
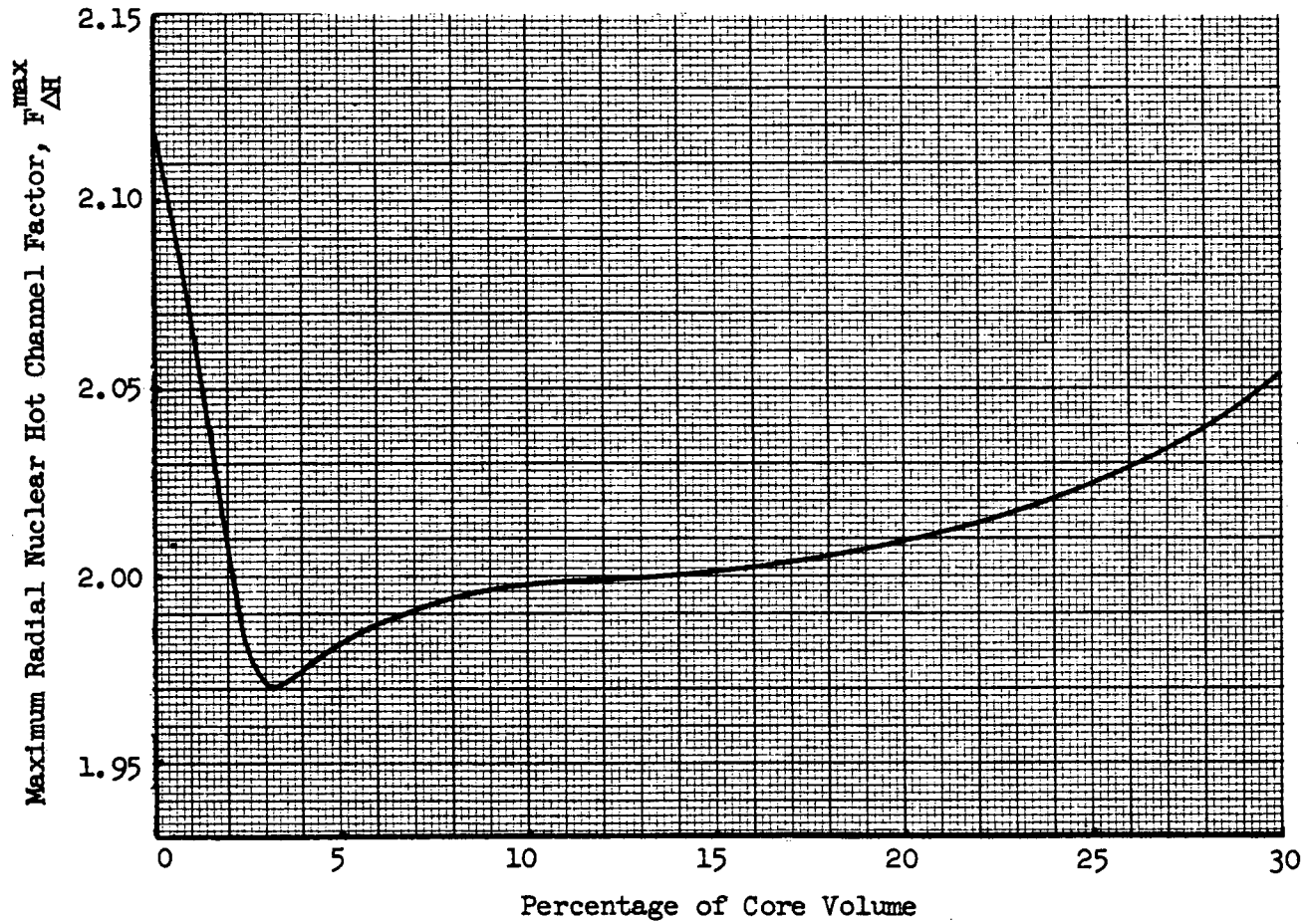


Figure 2.2-11

Maximum Radial Nuclear Hot Channel Factor Versus Percentage of the Core Volume With a Moderator Temperature of 640°F - Rod Pattern of Figure 18



The result is a value of  $+0.36 \times 10^{-4} (\text{°F})^{-1}$  to be compared to the isothermal value of  $+0.42 \times 10^{-4} (\text{°F})^{-1}$ . The axial temperature distribution results in a coefficient which is more negative than the isothermal value.

In conclusion it has been shown that the non-uniform temperature distribution does increase the reactivity insertion although the magnitude remains small. The power distribution does not increase at the point of temperature increase. With maldistribution of power, this reactivity increase is very small. The quantitative conclusions are not changed rapidly as the boron concentration is increased.

### 2.3 SPATIAL STABILITY

The final point to examine in the evaluation of the effect of the positive moderator coefficient on PWR core performance is the question concerning the spatial stability of the power distribution under the influence of the positive moderator coefficient. The manner in which a redistribution in power can add reactivity, including the effect of increased neutron leakage, has been demonstrated in the case of xenon poisoning by many authors. Here it is suggested that a threshold analysis similar to that proposed by Randall and St. John<sup>(2,3)</sup> can lead to an understanding of the factors involved in the potential initiation of spatial instabilities in power distribution because of a positive moderator coefficient.

A one-group neutron diffusion equation is used with one group of delayed neutrons. It is assumed that the reactor is maintained critical at all times.

The diffusion equations are

$$D\nabla^2\varphi + v\Sigma_f(1 - \beta)\varphi - \Sigma_a\varphi + \lambda C = 0 \quad (1)$$

$$\frac{dC}{dt} = \beta v\Sigma_f\varphi - \lambda C \quad (2)$$

Using the one-group relationships,

$$\frac{D}{\Sigma_a} = M^2 \quad (3)$$

$$\frac{v\Sigma_f}{\Sigma_a} = k_\infty \quad (4)$$

the above equations can be rewritten

$$M^2 v^2 \varphi + \left[ (1 - \beta) k_{\infty} - 1 \right] \varphi + \frac{\lambda C}{\Sigma_a} = 0 \quad (5)$$

$$\frac{dC}{dt} = \beta k_{\infty} \Sigma_a \varphi - \lambda C \quad (6)$$

The coolant temperature ( $T_C$ ) and fuel temperature ( $T_F$ ) are both dependent on the flux level. Channels which have high power will have correspondingly high coolant and fuel temperatures. It should be reasonable to express the coolant and fuel temperatures as having linear dependences on the power (flux). We neglect the time constants of the fuel and moderator (assume the temperatures change immediately with the flux). Clearly, this assumption is valid only if the form of the divergence proves to be exponential rather than oscillatory. Only then is the period infinite at the threshold of divergence.

Since these time constants may be comparable to the delayed neutron time constant, we should probably neglect delayed neutrons for consistency; however, the delayed neutron group will be carried along in the equations and the final stability criterion will be shown to be independent of the delayed neutrons.

With these assumptions, we can write

$$T_C = C_1 + C_2 \varphi \quad (7)$$

$$T_F = C_{12} + C_{13} \varphi \quad (8)$$

Some of the parameters in Equations 5 and 6 are dependent on the fuel and coolant temperatures. We assume a linear dependence is an adequate representation. Then

$$k_{\infty} = C_3 + C_4 T_C + C_5 T_F \quad (9)$$

$$\frac{1}{\Sigma_a} = C_6 + C_7 T_C + C_8 T_F \quad (10)$$

$$M^2 = C_9 + C_{10} T_C + C_{11} T_F \quad (11)$$

Note that the product  $k_{\infty} \Sigma_a = v\Sigma_f$  in Equation (6) is (to first order) independent of coolant and fuel temperature and can be taken as constant. The constants  $C_1$  through  $C_{13}$  can be determined by running a series of problems for various coolant and fuel temperatures.

Consider a perturbation in the core. If steady state values are denoted by stars and the perturbations are primed quantities, we have

$$\varphi = \varphi^* + \varphi' \quad (12a)$$

$$C = C^* + C' \quad (12b)$$

$$T_C = T_C^* + T_C' \quad (12c)$$

$$T_F = T_F^* + T_F' \quad (12d)$$

Equations 5, 6, 7 and 8 must be satisfied at steady state conditions. Thus, when we use the relationships 9, 10 and 11,

$$(C_9 + C_{10} T_C^* + C_{11} T_F^*) v^2 \varphi^* + [(1 - \beta)(C_3 + C_4 T_C^* + C_5 T_F^*)]^{-1} \varphi^* + (C_6 + C_7 T_C^* + C_8 T_F^*) \lambda C^* = 0 \quad (13)$$

$$0 = \beta k_{\infty} \Sigma_a \varphi^* - \lambda C^* \quad (14)$$

$$T_C^* = C_1 + C_2 \varphi^* \quad (15)$$

$$T_F^* = C_{12} + C_{13} \varphi^* \quad (16)$$

Equations 5, 6, 7 and 8 must also be satisfied during the perturbation. Thus,

$$\begin{aligned} & (C_9 + C_{10} T_C^* + C_{10} T_C' + C_{11} T_F^* + C_{11} T_F') v^2 (\varphi^* + \varphi') + \\ & \left[ (1 - \beta)(C_3 + C_4 T_C^* + C_4 T_C' + C_5 T_F^* + C_5 T_F') - 1 \right] (\varphi^* + \varphi') + \\ & (C_6 + C_7 T_C^* + C_7 T_C' + C_8 T_F^* + C_8 T_F') \lambda (C^* + C') = 0 \end{aligned} \quad (17)$$

$$\frac{d(C^* + C')}{dt} = \beta k_\infty \Sigma_a (\varphi^* + \varphi') - \lambda (C^* + C') \quad (18)$$

$$T_C^* + T_C' = C_1 + C_2 (\varphi^* + \varphi') \quad (19)$$

$$T_F^* + T_F' = C_{12} + C_{13} (\varphi^* + \varphi') \quad (20)$$

If we subtract the above sets of equations and neglect terms involving the product of the perturbations, we have

$$\begin{aligned} & (C_9 + C_{10} T_C^* + C_{11} T_F^*) v^2 \varphi' + \left[ (1 - \beta)(C_3 + C_4 T_C^* + C_5 T_F^*) - 1 \right] \varphi' + \\ & (C_6 + C_7 T_C^* + C_8 T_F^*) \lambda C' + \left[ C_{10} v^2 \varphi^* + (1 - \beta) C_4 \varphi^* + C_7 \lambda C^* \right] T_C' + \\ & \left[ C_{11} v^2 \varphi^* + (1 - \beta) C_5 \varphi^* + C_8 \lambda C^* \right] T_F' = 0 \end{aligned} \quad (21)$$

$$\frac{dC'}{dt} = \beta k_\infty \Sigma_a \varphi' - \lambda C' \quad (22)$$

$$T_C' = C_2 \varphi' \quad (23)$$

$$T_F' = C_{13} \varphi' \quad (24)$$

The most general solution of this system can be expanded as a sum of particular solutions; the time dependent part is an exponential of the form  $e^{\omega t}$  and the space dependent part is one of the eigenfunctions  $\varphi_n$  of the operator  $(\nabla^2 + B^2)$ . If we consider the particular solutions one by one, the time derivative operator  $d/dt$  may be replaced by  $\omega$  and  $\nabla^2$  may be replaced by  $-B_n^2$ , the  $n^{\text{th}}$  eigenvalue for the buckling.

Making use of 9, 10 and 11, we can rewrite equations 21 and 22 as

$$\begin{aligned}
 & -M^2 B_n^2 \varphi' + (1 - \beta) k_{\infty}^* - 1 \varphi' + \frac{\lambda C'}{\Sigma_a^*} + \\
 & - C_{10} B^{*2} \varphi^* + (1 - \beta) C_4 \varphi^* + C_7 \lambda C^* \left. \right] T_C' + \\
 & - C_{11} B^{*2} + (1 - \beta) C_5 \varphi^* + C_8 \lambda C^* \left. \right] T_F' = 0 \quad (25)
 \end{aligned}$$

$$(\omega + \lambda) C' = \beta k_{\infty}^* \Sigma_a^* \varphi' \quad (26)$$

Equations 23, 24 and 26 are substituted into (25) to eliminate all variables except  $\varphi'$ . After dividing by  $\varphi'$ , we have

$$\begin{aligned}
 & -M^2 B_n^2 + (1 - \beta) k_{\infty}^* - 1 + \frac{\lambda \beta k_{\infty}^*}{\omega + \lambda} + \\
 & C_2 \left[ - C_{10} B^{*2} \varphi^* + (1 - \beta) C_4 \varphi^* + C_7 \lambda C^* \right] + \\
 & C_{13} \left[ - C_{11} B^{*2} \varphi^* + (1 - \beta) C_5 \varphi^* + C_8 \lambda C^* \right] = 0 \quad (27)
 \end{aligned}$$

It is instructive to investigate the last two terms in Equation (27).

$$C_2 \left[ - C_{10} B^{*2} \varphi^* + (1 - \beta) C_4 \varphi^* + C_7 \lambda C^* \right]$$

$$C_2 \varphi^* = T_C^* - C_1 \quad \text{from Equation (7)}$$

$$C_{10} = \frac{\partial(M^2)^*}{\partial T_C} \quad \text{from Equation (11)}$$

$$C_4 = \frac{\partial k_\infty^*}{\partial T_C} \quad \text{from Equation (9)}$$

$$C_7 = \frac{\partial(1/\Sigma_a^*)}{\partial T_C} \quad \text{from Equation (10)}$$

$$\lambda C^* = \beta k_\infty^* \Sigma_a^* \varphi^* \quad \text{from Equation (14)}$$

Making these substitutions, we can rewrite the above term as

$$C_2 \varphi^* \left[ - \frac{\partial(M^2 B^2)^*}{\partial T_C} + (1 - \beta) \frac{\partial k_\infty^*}{\partial T_C} + \beta \frac{\partial k_\infty^*}{\partial T_C} \right]$$

$$\text{or } (T_C^* - C_1) \frac{\partial [k_\infty^* - (M^2 B^2)^*]}{\partial T_C} \equiv \rho_C^* \quad (28)$$

Note that  $T_C^* - C_1$  represents the temperature rise in the coolant and  $\frac{\partial [k_\infty^* - (M^2 B^2)^*]}{\partial T_C}$  is simply the coolant temperature coefficient, so

that the product ( $\rho_C^*$ ) represents the reactivity held by the moderator due to temperature above the hot-zero power value.

Similarly, it can be shown that

$$C_{13} \left[ - C_{11} B^{*2} \varphi^* + (1 - \beta) C_5 \varphi^* + C_8 \lambda C^* \right] = (T_F^* - C_{12})$$

$$\frac{\partial [k_\infty^* - (M^2 B^2)^*]}{\partial T_F} \equiv \rho_F \quad (29)$$

where  $T_F^* - C_{12}$  is the temperature rise in the fuel.

When this is multiplied by the temperature coefficient of reactivity of the fuel, the reactivity associated with the fuel temperature rise above the hot-zero power value is obtained.

Equation (27) can be rewritten as

$$-M^2 B_n^2 + (1 - \beta) k_\infty^* - 1 + \frac{\lambda \beta k_\infty^*}{\omega + \lambda} + \rho_C^* + \rho_F^* = 0 \quad (30)$$

Using the relationship for a critical reactor

$$\frac{k_\infty^*}{1 + (M^2 B_n^2)^*} = 1, \quad (31)$$

we can solve Equation (30) for  $\omega$

$$\omega = -\lambda \left[ 1 + \frac{\beta(1 + M^2 B_n^2)^*}{\rho_C^* + \rho_F^* - \beta(1 + M^2 B_n^2)^* - M^2(B_n^2 - B^2)^*} \right] \quad (32)$$

Since the time dependent part of the solution has the form  $e^{\omega t}$ , negative values of  $\omega$  indicate stability; positive values indicate a small perturbation would diverge from the steady state value. Note that this form of the divergence is exponential as assumed earlier in this derivation. It must be recognized that the value of  $\omega$  will be accurate only so long as  $1/\omega$  is large relative to fuel and moderator heat transfer time constants.

Upon rearrangement

$$\omega = -\lambda \left[ \frac{\rho_C^* + \rho_F^* - M^2 (B_n^2 - B^2)^*}{\rho_C^* + \rho_F^* - M^2 (B_n^2 - B^2)^* - \beta(1 + M^2 B_n^2)^*} \right] \quad (33)$$

If we demand  $\omega < 0$ , we conclude

$$\rho_C^* + \rho_F^* < M^{*2} (B_n^2 - B^2)^* \quad \text{for stability} \quad (34)$$

This stability criterion is quite analogous to that developed by Randall and St. John for xenon oscillations<sup>(2,3)</sup>. Although the present derivation does not include the mathematical refinement of the Randall and St. John derivation, the same principles are employed and the same approximations are made. There it was shown that cores are stable to xenon oscillations when

$$\alpha_{xe} f(\varphi) + \alpha_T \varphi < M^2 (B_n^2 - B^2) \quad (35)$$

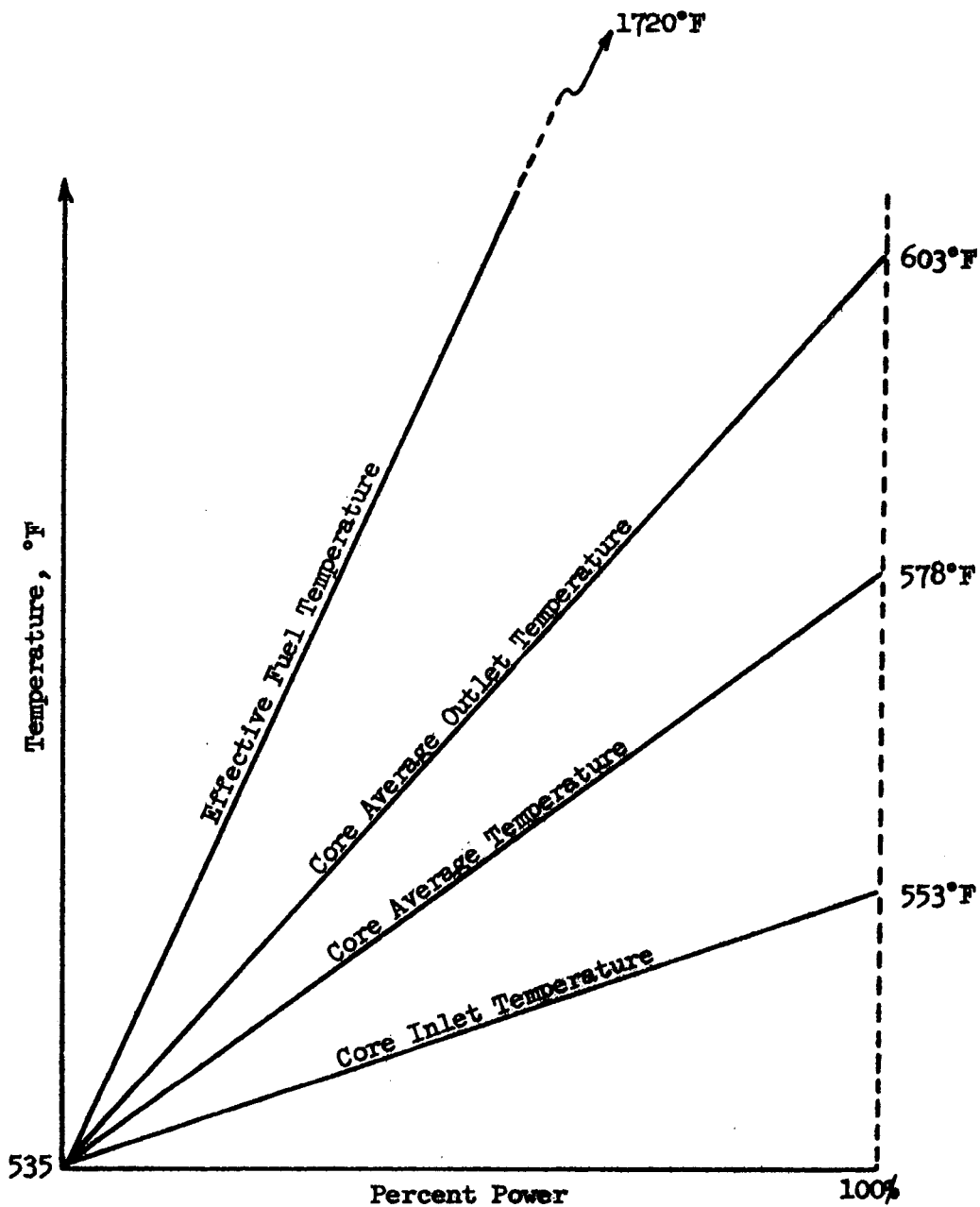
The first term is the effective reactivity held in xenon; the second term is the reactivity held in the power defect; the right side is the difference in leakage between the high flux modes and the fundamental mode. In comparing (34) and (35), it is seen that the xenon driving force is simply replaced by the moderator driving force.

Extensive work at WAPD on xenon oscillations<sup>(4)</sup> has shown that the Randall and St. John stability criterion agrees well with detailed diffusion-depletion calculations. Since many of the same assumptions have been made in the derivation of (34) as in Randall and St. John's equation, we expect (34) to provide good results.

The conclusion of this analysis is that if the sum of the installed reactivity (positive) in the moderator above a constant inlet temperature plus the installed reactivity in fuel temperature (negative) above the constant inlet temperature is algebraically less than the required reactivity change to excite the first harmonic in-power distribution, there will be no power redistribution and spatial stability will exist.

Consider, first, the temperature variations with power level. Figure 2.3-1 illustrates the variation of temperature with power level for a typical PWR core. This is an expansion on the data given in Figure 2.1-2. From equation (28), (29), and (34), a breakdown of the reactivity balance can be established which represents the threshold of instability as in Table 2.3-1. Here the functional form is indicated along with two sets of numbers one of which is the nominal condition obtained by applying numbers as calculated for a typical PWR core. The other set is obtained by assuming a clearly conservative value for each individual component. Consider each term:

1.  $\frac{\partial k_{\infty}}{\partial T_C}$  - The value for the average enrichment ( $+0.83 \times 10^{-4}$ ) is employed in the nominal calculation and the value for the lowest region enrichment is employed in the conservative calculation ( $+1.0 \times 10^{-4}$ ).
  
2.  $B^2 \frac{\partial M^2}{\partial T_C}$  - The nominal value ( $0.38 \times 10^{-4}$ ) is obtained from an assumed isothermal temperature change with the geometric buckling. The conservative value is taken as zero since the weighting for non-uniform temperature distribution is very important in determining leakage.
  
3.  $(T_C^* - T_{in})$  - The reactivity held by coolant should be that above a constant  $T_{in}$  and would suggest 1/2 of the average temperature rise (578-553) as a reasonable value. The nominal value is found in this manner. The conservative value (603-535) includes the increase in  $T_{in}$  with power which is employed in the PWR, plus the total average temperature rise. The total average temperature rise (rather than half of its value) is used because the non-uniform distribution of temperature is important and it is not clear what weighting should be employed in this model. A weighted mean surely is no higher than the average outlet (603) and is probably much lower.



TEMPERATURE VERSUS PERCENT POWER

Figure 2.3-1

Component	$\left(\frac{\partial k_{\infty}}{\partial T_C} - B^2 \frac{\partial M^2}{\partial T_C}\right)(T_C^* - T_{in})$	$\frac{\partial k_{\infty}}{\partial T_F} (T_F^* - T_{in})$	$M^{*2} (B_n^2 - B^2)^*$		Margin to Divergence	
			<u>Azimuthal</u>	<u>Axial</u>	<u>Azimuthal</u>	<u>Axial</u>
Nominal						
a) Factors	$(+0.83 \times 10^{-4} \quad -0.38 \times 10^{-4})(578-553)$	$-1.3 \times 10^{-5}(1720-553)$	$54 \times 4 \times 10^{-4}$	$54 \times 2.9 \times 10^{-4}$	--	--
b) Reactivity	+0.12%	-1.52%	2.16%	1.57%	3.56%	2.97%
Conservative						
a) Factors	$(+1.0 \times 10^{-4} - 0)(603 - 535)$	$(-1.0 \times 10^{-5})(1720-900)$	--	--	--	--
b) Reactivity	+0.68%	-0.82%	0.72%	0.52%	0.87%	0.66%

$$\text{Margin to Divergence} = M^{*2} (B_n^2 - B^2)^* - \rho_C^* - \rho_F^*$$

4.  $\left(\frac{\partial k_{\infty}}{\partial T_F}\right)$  - The nominal value ( $-1.3 \times 10^{-5}$ ) is the average over the operating range as would be suggested by the linear model used in the derivation whereas the conservative value ( $-1.0 \times 10^{-5}$ ) is the minimum value over the operating range (this minimum is the full power point).
  
5.  $(T_F^* - T_{in})$  - The nominal value (1720-553) is the calculated value whereas the conservative value (1720-900) is based upon the slope at the full power point which is about 30% lower than the average slope used in the nominal calculation.
  
6.  $M^2(B_n^2 - B^2)^*$  - This is presented for azimuthal and axial distribution. The radial modes are far more stable. The nominal number employed is the change resulting from fundamental to first overtone solutions of the wave equation. Work by Randall and St. John<sup>(2,3)</sup> as well as work at Westinghouse<sup>(4)</sup> suggest these values may be high by a factor of 3 for flattened power distribution. The conservative value is, therefore, a factor of 3 below the nominal value.

To gain a physical judgment concerning the significance of the margin, the margins in reactivity can be converted into margins in boron concentration by the relation:

$$\Delta C_B = \frac{\Delta \rho \text{ margin}}{\frac{\partial \alpha_m}{\partial C_B} (T_C^* - T_{in})}$$

$\alpha_m$  = Moderator Coefficient  
of Reactivity

For this purpose  $\partial \alpha_m / \partial C_B$  is obtained from the isothermal calculations which yield approximately  $1.2 \times 10^{-7}$  (ppm, °F)<sup>-1</sup>.  $T_C^* - T_{in}$  will be taken, conservatively, as 603-535=68°F. Table 2.3-2 summarizes the results.

TABLE 2.3-2

MARGINS

	<u>REACTIVITY (%)</u>		<u>BORON CONCENTRATION (ppm)</u>	
	<u>Azimuthal</u>	<u>Axial</u>	<u>Azimuthal</u>	<u>Axial</u>
Nominal	3.56	2.97	4360	3640
Conservative	0.87	0.66	1060	810

It is concluded that no spatial stability problem can arise until much higher boron concentrations are considered. As in the case of xenon instabilities, the power coefficient provides sufficient damping to preclude spatial instabilities.

## 2.4 BASIS FOR CONFIDENCE IN ANALYSIS

The calculational scheme has been tested on a wide range of experimental lattices. A summary of the results and discussion of the agreement with measured values is given.

### 2.4.1 Reactivity Analysis

Data from 55 oxide and 61 metal lattice critical and exponential experiments have been evaluated<sup>(5a, 5b)</sup>. The results of these studies are summarized in Table 2.4-1. The values of neutron multiplication are computed using experimentally measured material bucklings, and should equal unity. Table 2.4-1 demonstrates that much of the scatter can be attributed to variations in results from one experimental laboratory to another, whereas references 5a and 5b demonstrate that errors do not develop with variations of the significant parameters concerned with extrapolations of experimental results. Extrapolation from experiments to operating cores is not likely to result in a large error, likewise, extrapolation from one operating core to another should not lead to any significant error as the calculational accuracy is independent of variations in hydrogen to uranium ratio, uranium enrichment, pellet diameter and buckling.

It can be seen from Table 2.4-1 that if only WAPD experimental results are considered, the computational method predicts  $k$  to a standard deviation of 0.36 per cent.

This may be a better estimate of the accuracy of the method because of the more detailed information available to the authors of the method. Much of the additional scatter in the standard deviation for the other cases may be attributed to uncertainty in the experimental configuration. For example, the dimensions and results of many of the cases have been published in several different reports; and in many instances, the quoted values are not the same.

TABLE 2.4-1

RESULTS OF CALCULATIONS AS A FUNCTION OF  
LABORATORY PROVIDING EXPERIMENTAL DATA

<u>LABORATORY</u>	<u>TYPE OF EXPERIMENT</u>	<u>NO. OF EXPERIMENTS</u>	<u>CALCULATED k ± α</u>
Westinghouse Atomic Power Division (WAPD)	Critical	16	0.9968 ± 0.0036
Bettis Atomic Power Laboratory	Critical	14	0.9940 ± 0.0022
Brookhaven National Laboratory	Exponential	35	0.9964 ± 0.0051
Hanford Atomic Products Operation	Exponential	20	0.9953 ± 0.0105
Babcock and Wilcox	Critical	26	0.9885 ± 0.0094

2.4.2 Depletion Analysis

Data from the Yankee spent core analysis have been compared with calculated data using the design techniques. The results are summarized in Figures 2.4-1, 2.4-2 and 2.4-3. Satisfactory prediction of depletion of plutonium production has a direct bearing on the core reactivity characteristics as a function of lifetime. The figures show the comparison between calculations (solid lines) and measured concentrations of the various isotopes. Although some small deviations can be observed between analysis and experiment, they are not considered to be serious.

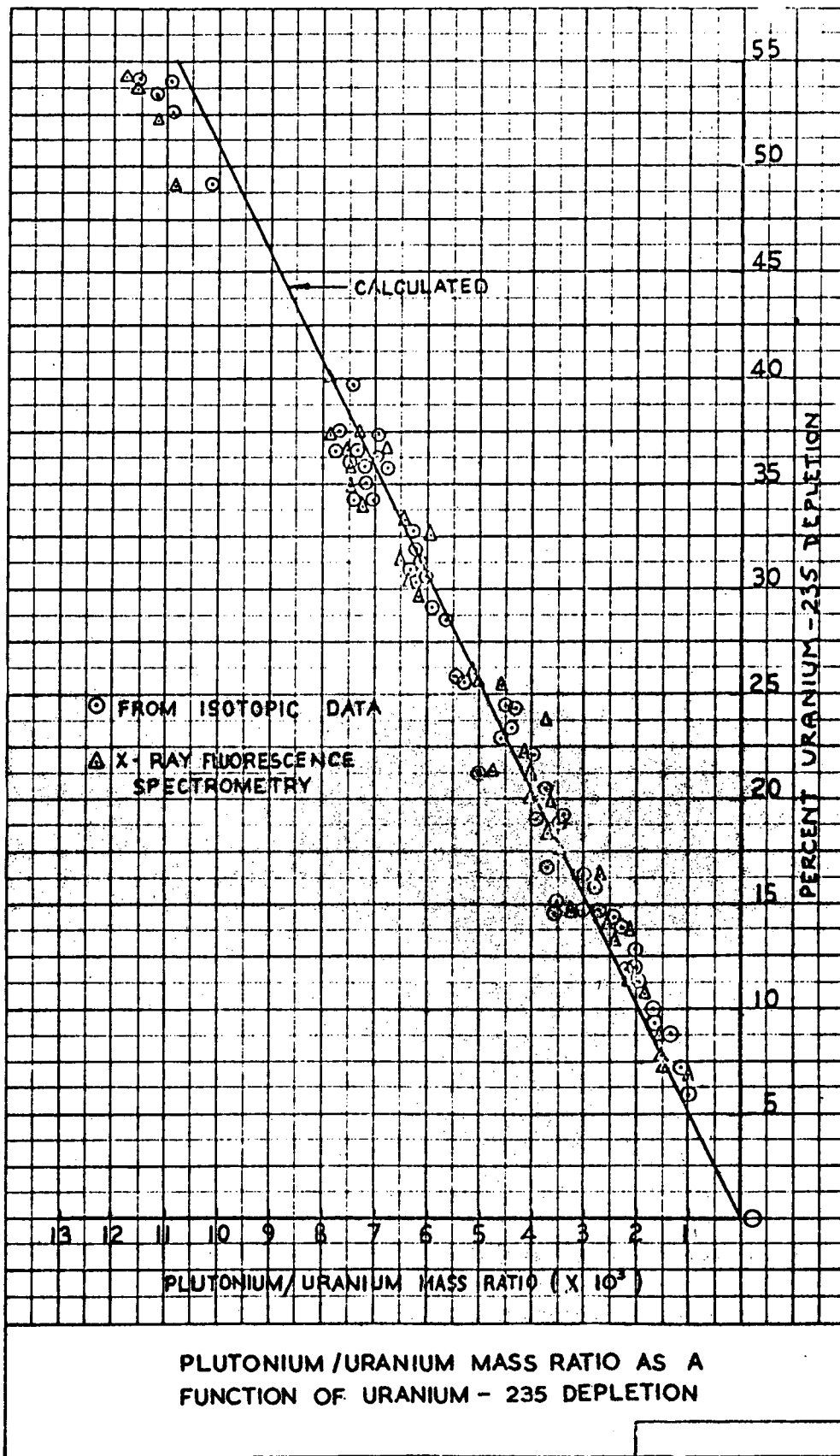


Figure 2.4-1

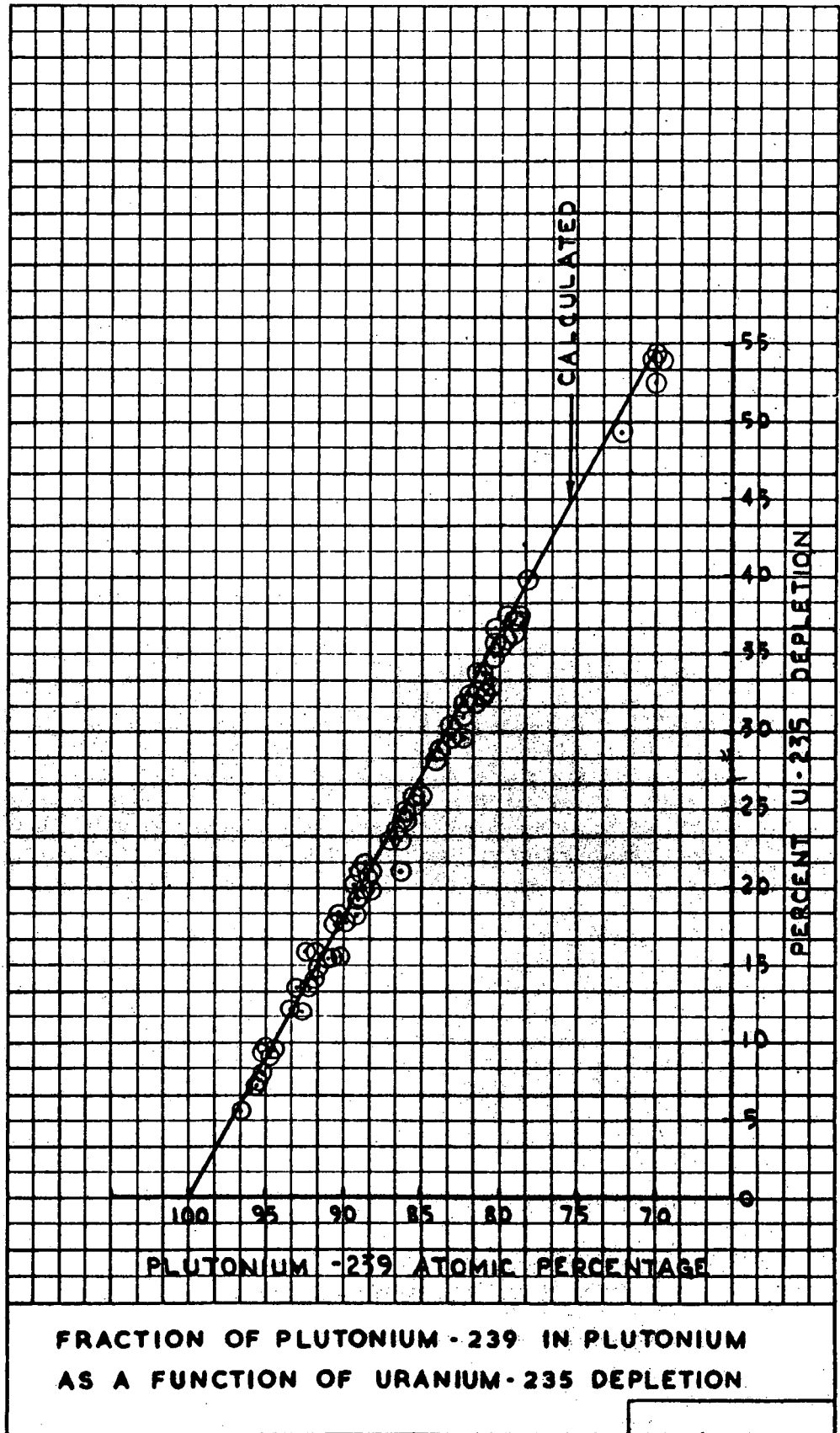


Figure 2.4-2

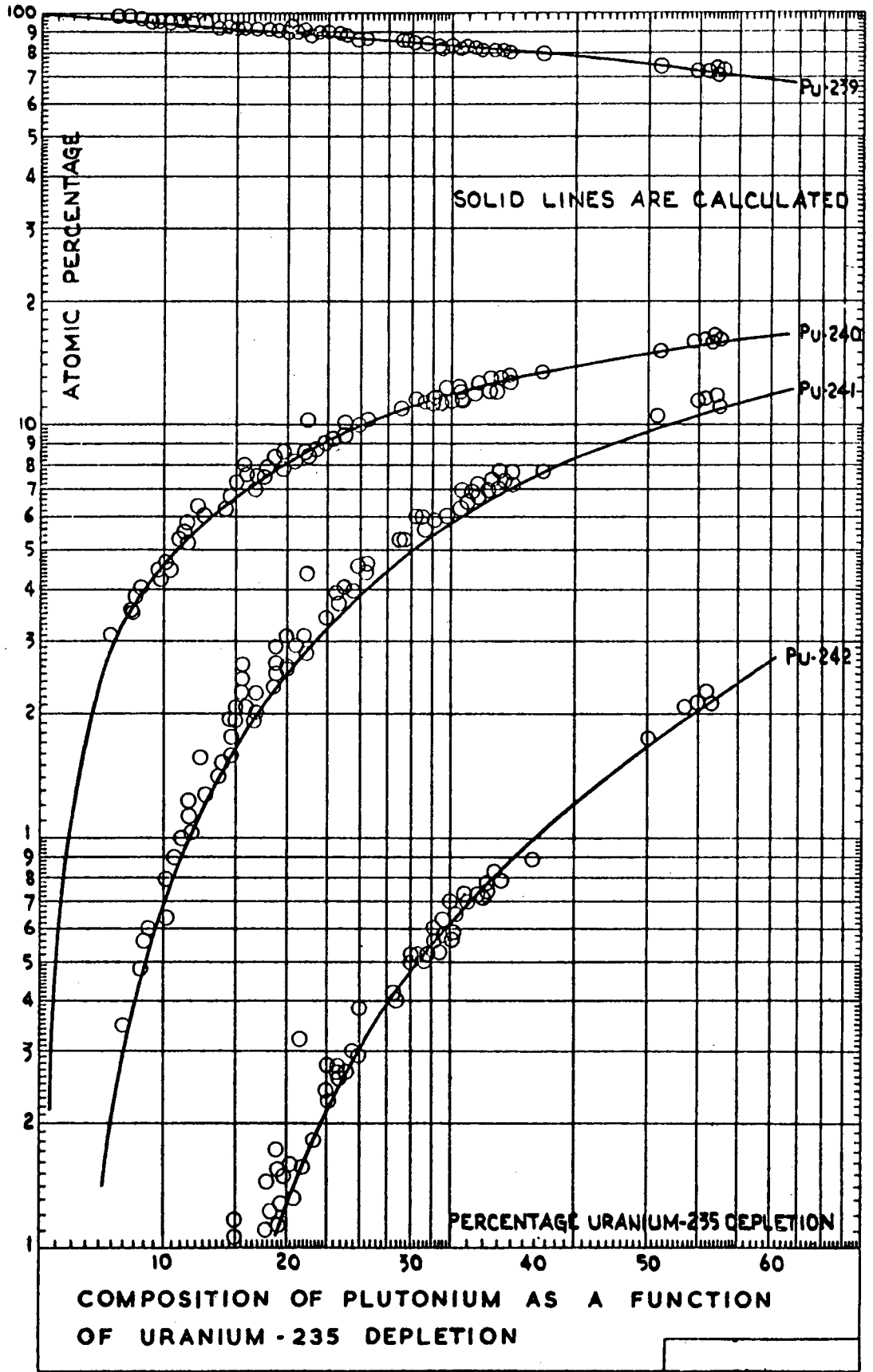


Figure 2.4-3

### 2.4.3 Moderator Coefficient Analysis

Inasmuch as the safe operation of any plant is closely associated with the ability to predict the transient behavior of that plant, correlation of analysis with experiment will be presented to show that the moderator temperature coefficient is quite predictable. Measurements were made during the startup and operation of the SELMI core to obtain data for a core operated entirely by chemical shim. During the startup, the core was heated from room to operating temperature at a constant boron concentration of 1600 ppm. Figure 2.4-4 shows the results of the isothermal moderator coefficient measurements taken during this core heatup, and also the comparable calculated values. The agreement between calculation and experiment is good over the entire temperature range.

In order to measure the moderator coefficient at various boron concentrations, control rods were traded for boron during the hot, no power startup tests. This procedure permitted isothermal moderator coefficient measurements to be made over a range of boron concentrations from 1300 to 1800 ppm. An axial one-dimensional calculation was performed with an homogenized bank of poison used to represent the moving control rods. The results of analysis and measurement are shown in Figure 2.4-5. The calculations were performed to reproduce the actual configurations employed in the measurements. First, the control group was inserted as boron was removed. When the control group was fully inserted, further boron removal was compensated by insertion of all rods (control plus shutdown rods) in a bank. Two dimensional (X-Y) analyses were also performed for all the rods in and all rods out end points, and the results are given in Figure 2.4-5. It can be seen that the one-dimensional calculations in which rods are represented by an homogenized poison predicts the measured data very well. Note the dashed curve in Figure 14 which is the variation of coefficient with boron concentration without the effect of rods. This illustrates the negative effect of rods on the coefficient.

Figure 2.4-4

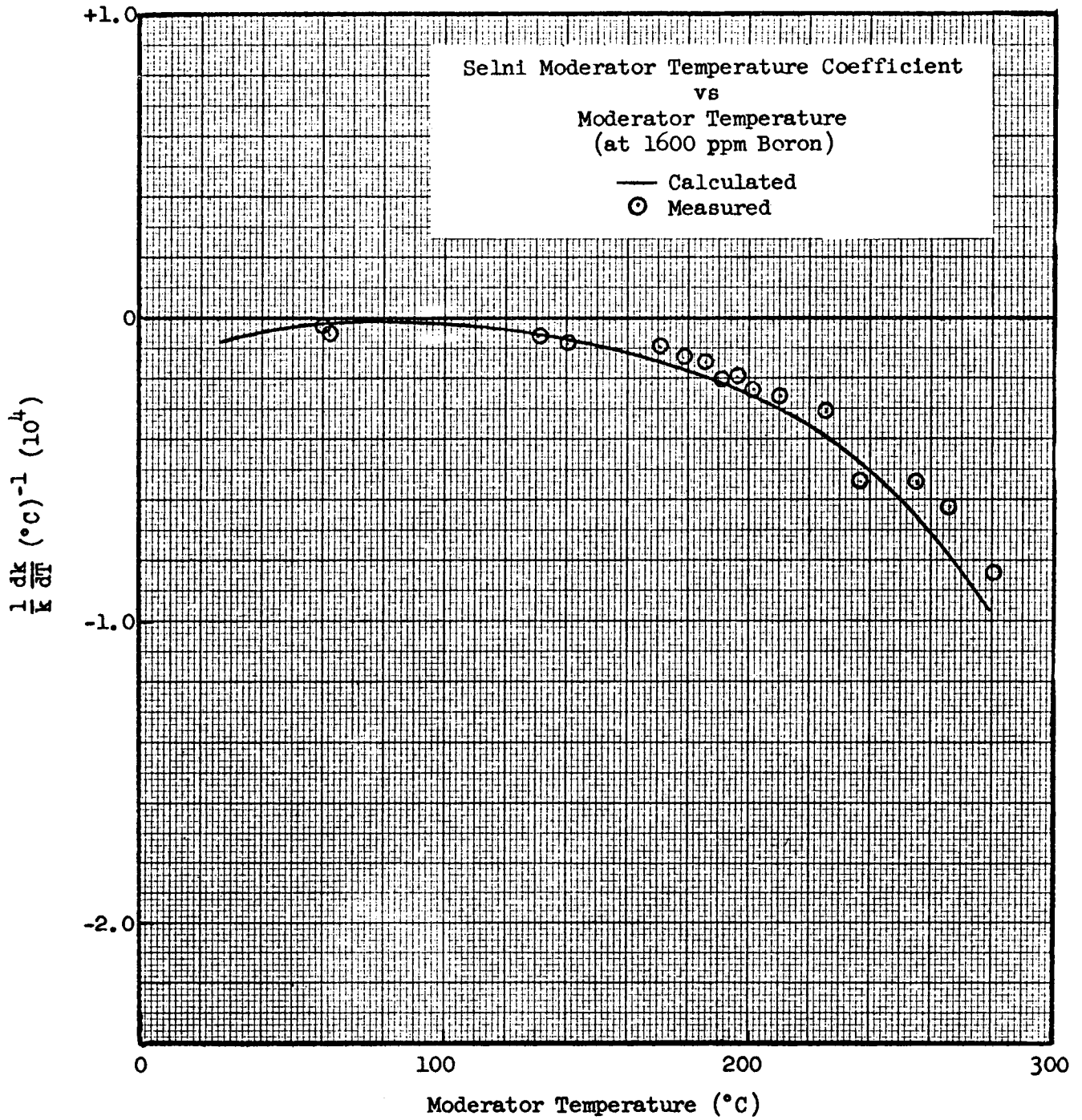
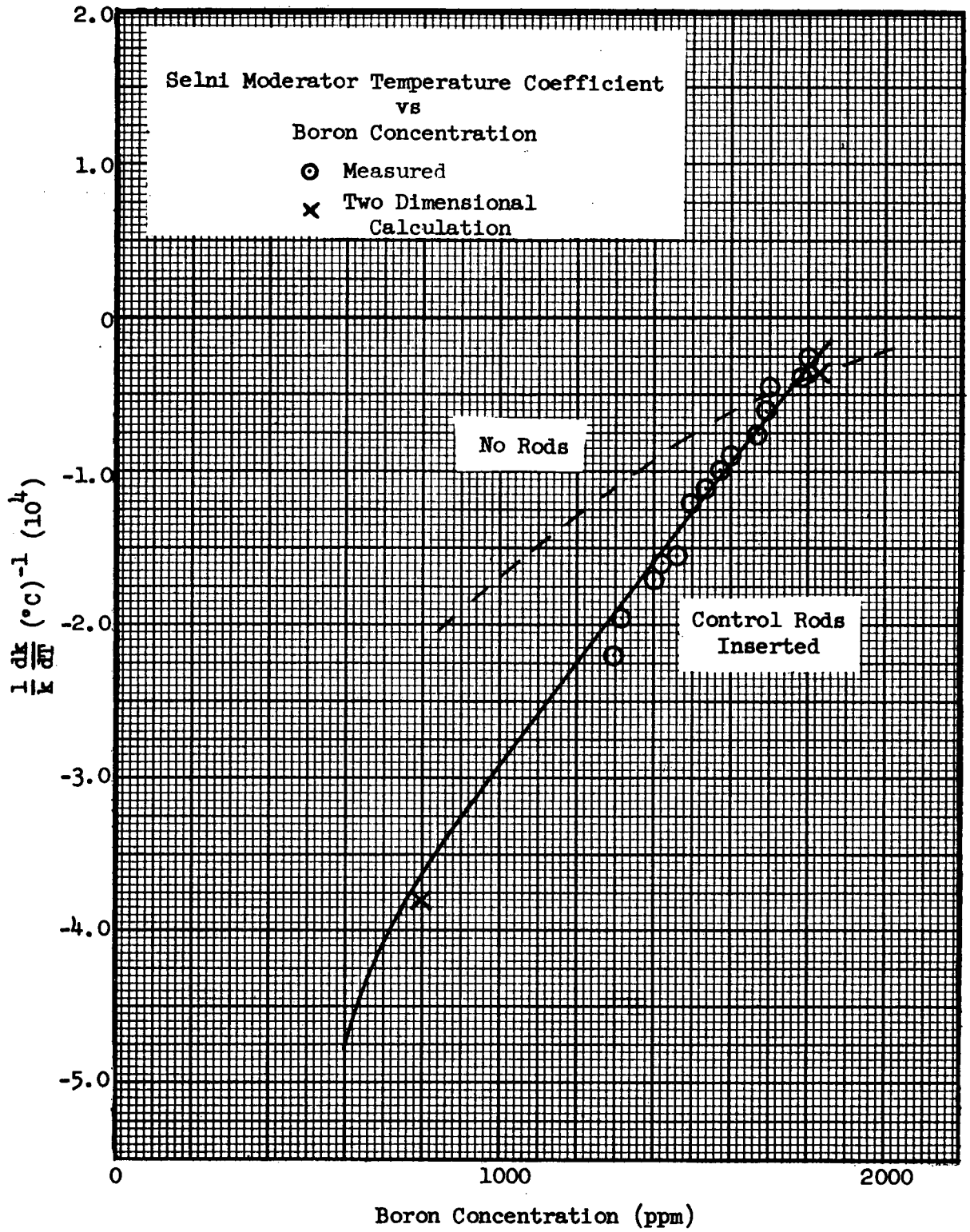


Figure 2.4-5

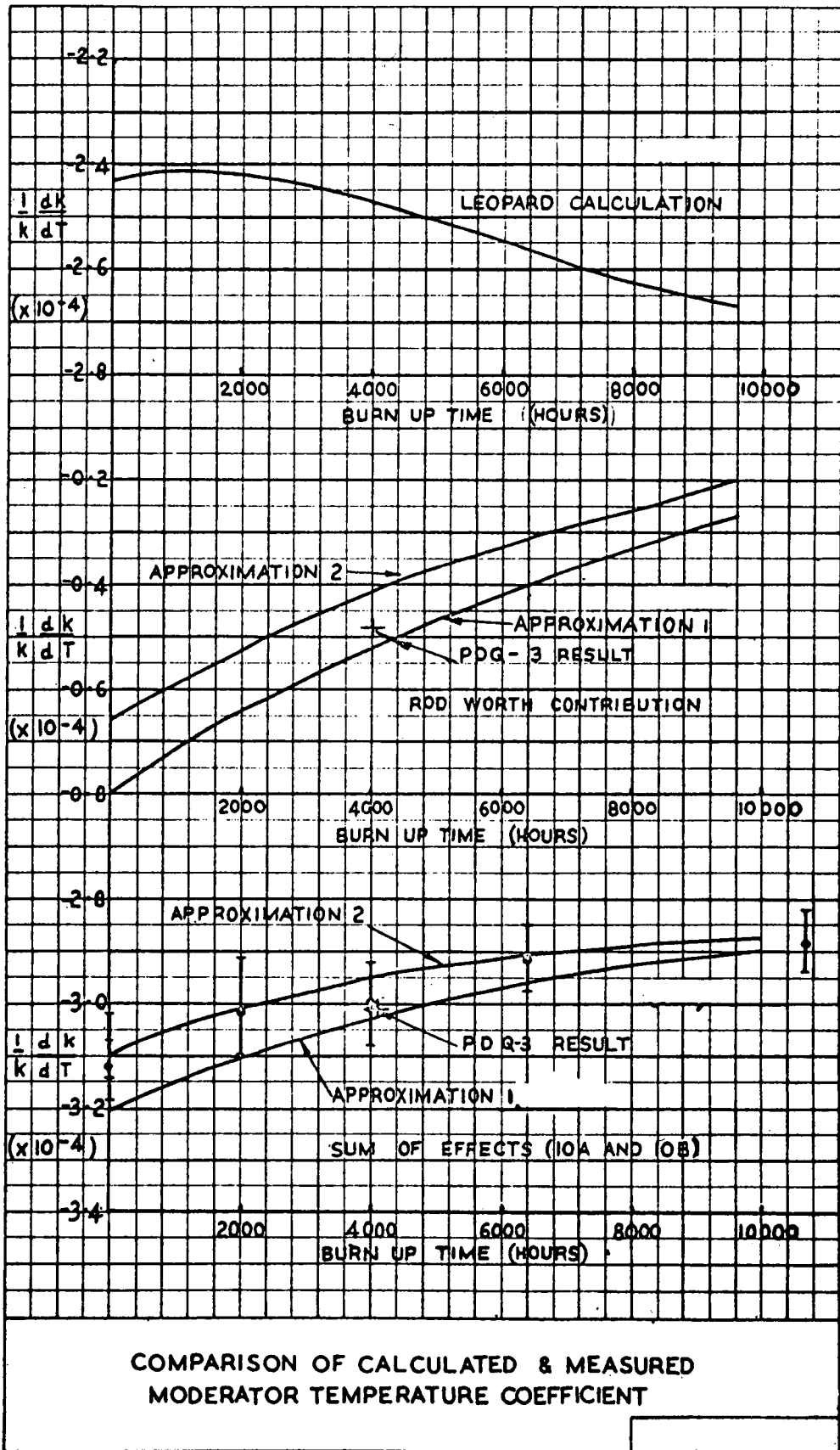


The effect of burnup on the moderator coefficient has been measured in the core follow program which was performed on Yankee Core I<sup>6)</sup> Yankee Core I was controlled by cruciform blade rods, and so it was necessary to separate the effect of control rods from the effect of burnup on the coefficient. Figure 2.4-6 illustrates these components and the agreement between analysis and measurement. The effect of rods was evaluated by treating the rods as an equivalent absorption area (approximation 1 in Figure 2.4-6) with a correlation for the effects of resonance absorption (approximation 2 in Figure 2.4-6). A complete two-dimensional analysis (PDQ point) is shown for one case. It can be seen that the analysis lies within the experimental uncertainty and that the burnup effect on the uncontrolled moderator coefficient results in a more negative coefficient with increasing burnup as indicated by the top curve in Figure 2.4-6.

#### 2.4.4

##### Local Void Analysis

To be sure that non-uniform distribution analysis is accurate, a series of local void experiments have been performed. Local void experiments were performed for two different core configurations. The first series of experiments was carried out in a 47 x 47 square core of 2.7% enriched fuel with a W/U of 2.9, with no boron. The second series was performed using a 53 x 53 square core of 3.7% enriched fuel with a W/U of 2.9, and with 1046 ppm boron in the water. In both cores voids were simulated by empty 0.1875 inch O.D., 0.022 inch wall aluminum tubes inserted between fuel rods. The moderator in the voided region consisted of 11.52% aluminum, 16.29% void and 72.19% water. Experiments have been performed which demonstrate that aluminum is a valid mock-up for void in PWR cores. This was done by a comparison of voided aluminum tubes and solid aluminum rods. Data were taken for the following cases:



COMPARISON OF CALCULATED & MEASURED  
MODERATOR TEMPERATURE COEFFICIENT

Figure 2.4-6

1. No void tubes
2. Four void tubes (2x2) located around the central fuel rod
3. Sixteen void tubes (4x4) at core center
4. 196 void tubes (14x14) at core center

The calculated power distribution is compared with the experimental power scans in Figures 2.4-7 and 2.4-8 for the unborated and borated cores for the four cases examined. The aluminum was represented directly in the calculation and not considered as void. The agreement between experiment and calculation is good except at the transition point between voided and non-voided regions. Here the calculations tend to overestimate the peak.

The reactivity effects of the void tubes were calculated assuming a constant axial reflector savings. Calculation and experiment for each case examined are compared in Table 2.4-2. Calculations overestimate the reactivity effect of the voids by approximately 10%, which is considered good agreement in view of the small magnitude of the effects being studied. The difference is of the same order as the precision of the measurement. Perhaps the agreement could be improved by a better treatment of the axial reflector. In fact, the power distribution comparison is probably a more valid and more precise test of reactivity variation than the gross reactivity measurements.

Although it was not possible to add sufficient boron to result in an overall positive reactivity change, due to experimental limitations, sufficient boron was employed to provide an adequate test of the ability to predict the effect of boron. The positive increment due to boron can be found by the differences between unborated and borated core results in Table 2.4-2. Table 2.4-3 presents these results.

The comparison is considered to be quite satisfactory.

Figure 2.4-7

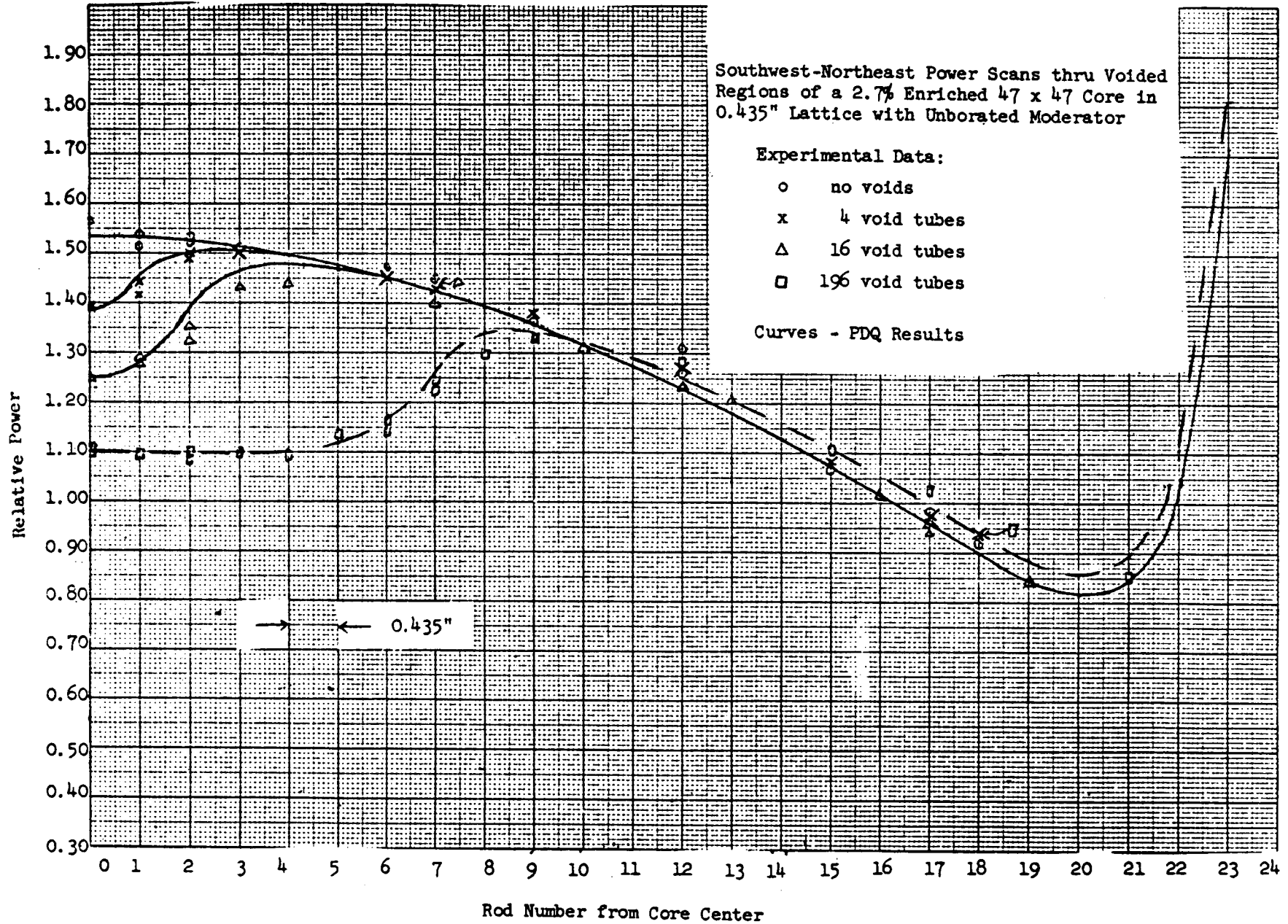


Figure 2.4-8

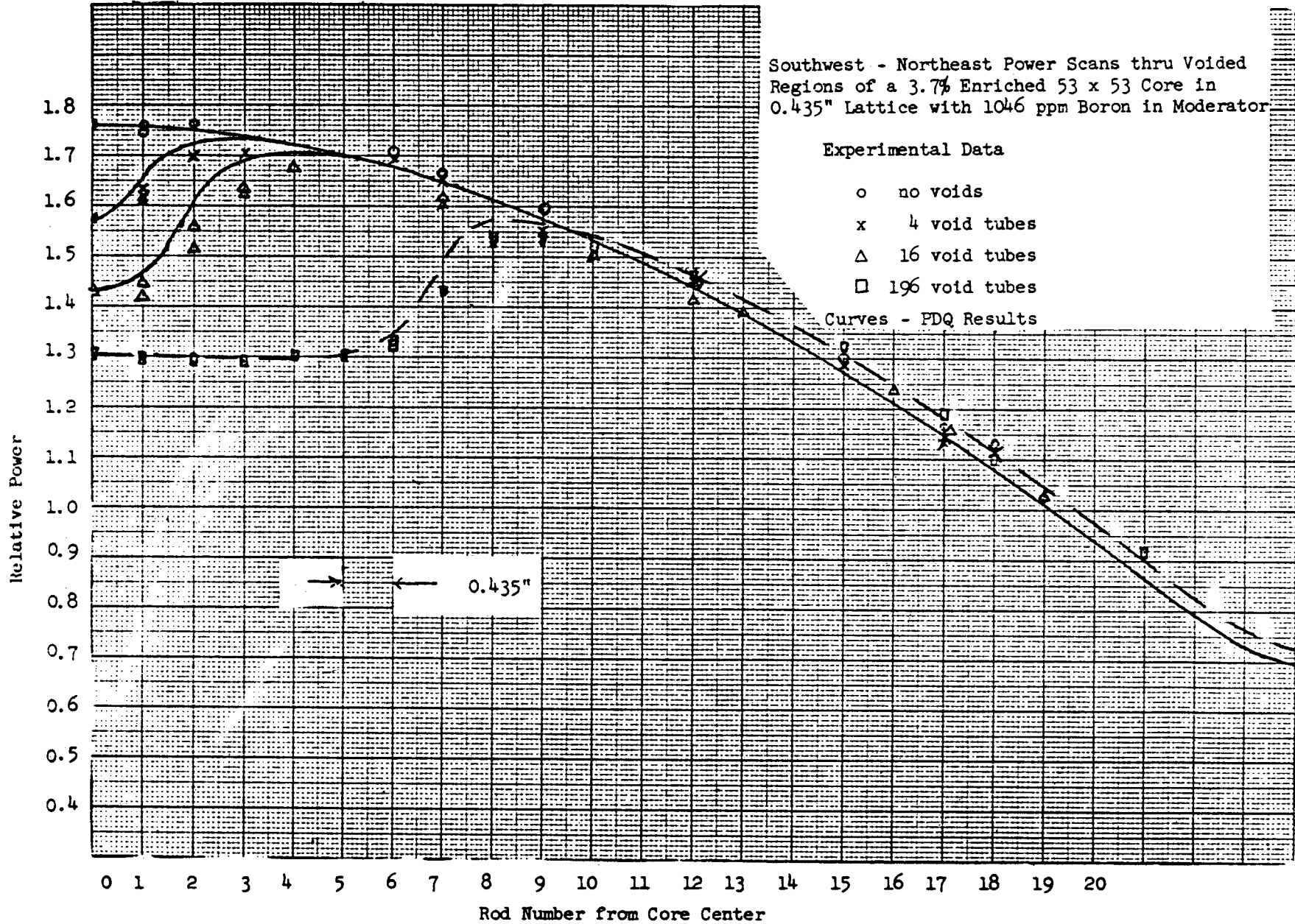


TABLE 2.4-2

CALCULATED AND MEASURED REACTIVITY EFFECTS OF VOID TUBES

	<u>No. of Tubes</u>	<u>Reactivity Change % <math>\Delta k/k</math></u>	
		<u>Measured</u>	<u>Calculated</u>
Unborated Core	0		
	4	-0.03	-0.034
	16	-0.11	-0.125
	196	-1.33	-1.416
Borated Core	0		
	4	-0.017	-0.020
	16	-0.076	-0.085
	196	-0.850	-0.942

TABLE 2.4-3

CALCULATED AND MEASURED BORON REACTIVITY  
EFFECT ON LOCAL VOIDED CHANNELS

<u>No. of Tubes</u>	<u>Reactivity Effect of Boron (% <math>\Delta k/k</math>)</u>	
	<u>Measured</u>	<u>Calculated</u>
4	+ 0.013	+ 0.010
16	+ 0.034	+ 0.040
196	+ 0.48	+ 0.48

2.4.5

Doppler and Power Coefficient Analysis

As the fuel pellet temperature increases with power, the resonance absorption in U-238 increases due to Doppler broadening of the resonances. In order to predict the reduction in reactivity caused by this effect, it is necessary to know the temperature of the fuel as a function of power level, the distribution of power within the core, as well as the radial distribution of temperature within the individual fuel rods. However, uncertainties arise during operation at power which make it difficult to predict the temperature of the fuel pellet. For example, pellets do not remain intact (i.e. uncracked) and in a concentric relationship with the clad, as has been observed from the Yankee spent fuel analysis<sup>(7)</sup>. In addition, the composition of the gas in the gap is a combination of residual gas as fabricated and diffused fission product gases. This generally results in an uncertainty in the temperature drop across the gap as a function of power level and burnup.

To reduce these uncertainties, a semi-empirical model has been developed for calculating the effective fuel temperature ( $T_{eff}$ ) based on fitting the measured power coefficients of the Yankee, Saxton, BR-3 and SELNI reactor cores. The measured power coefficient  $1/k \delta k / \delta P$  can be written

$$\frac{1}{k} \frac{\delta k}{\delta P} = \frac{1}{k} \frac{\delta k}{\delta T_{eff}} \cdot \frac{\delta T_{eff}}{\delta P}$$

The first term in the product on the right side of the equation is the Doppler coefficient which can be computed without knowing the heat transfer behavior of the fuel pellet or the relationship of  $T_{eff}$  and power. The second term on the right side can then be related to the measured values of power coefficients. In this manner an empirical

expression for the effective fuel temperature is obtained which makes it possible to relate  $T_{\text{eff}}$  to power, and thus calculated the power coefficient.

The method of analysis described in the preceding paragraph assumes accuracy of prediction of the Doppler coefficient as a function of the effective fuel temperature. This assumption presumes that the behavior of the U-238 resonance integral with a change in the fuel temperature is well known. Data is presented here to support this assumption. A correlation has been developed for the U-238 resonance integral which is known as the metal-oxide correlation<sup>(5a, 5b)</sup>. This correlation has been found to agree with Hellstrand's uranium metal<sup>(8)</sup> and uranium dioxide<sup>(9)</sup> correlations for isolated rods. The correlation is also consistent with Hellstrand's temperature correlations<sup>(10)</sup>. Thus, a single combined correlation replaces the four Hellstrand correlations. The combined metal-oxide correlation is

$$R.I.^{28} = 2.16X + 1.48 + (0.0279X - 0.0537) T_{\text{eff}}^{1/2}$$

where  $T_{\text{eff}}$  is in degrees Kelvin and

$$X = \frac{\Sigma_{\text{so}}}{N_{\text{O}}^{28}} P_{\text{O}} + \frac{D}{L_{\text{O}} N_{\text{O}}^{28}}^{1/2}$$

$\Sigma_{\text{so}}$  = scattering cross section of the fuel (10.7 barns for uranium and 3.8 barns for oxygen)

$N_{\text{O}}^{28}$  = U-238 number density in the fuel region

$L_{\text{O}}$  = mean chord length in the fuel

$D$  = shielding factor (calculated by Sauer's method)

$P_{\text{O}}$  =  $1 - P_c$

This form of the resonance integral is not strictly rigorous, but its validity is demonstrated in Figure 2.4-9 where it is compared with Hellstrand's results for various temperatures. References 5a and 5b demonstrate that this correlation agrees well with Monte Carlo calculations.

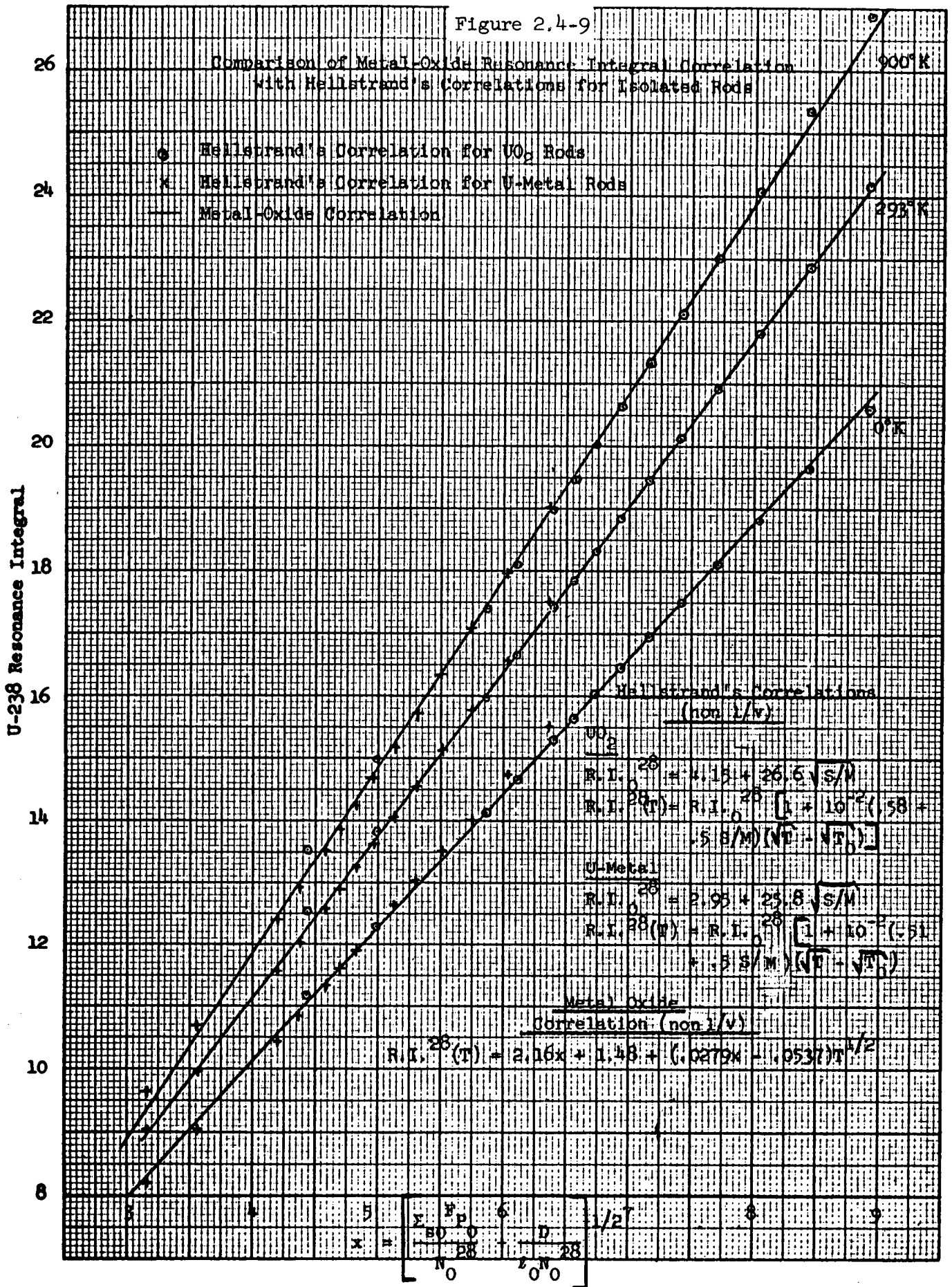
An extensive evaluation of power coefficient measurements has been made for the Yankee, Saxton, BR-3 and SELNI cores. The results of these measurements are given in Figure 2.4-10 which shows the change in the effective fuel temperature per kw/ft as a function of core average kw/ft. From these data an empirical equation for  $T_{eff}$  has been developed which will predict  $T_{eff}$  as a function of power level<sup>(11)</sup>. This equation for  $T_{eff}$  is given below.

$$T_{eff} (P/P_o) = 0.55 \Delta T_{fuel} + \alpha(\bar{q}'' ) \delta \bar{q}'' + 1.571 P/P_o \Delta T_{o(clad + film)} + T_{coolant}$$

where

$P/P_o$	= fraction of full power
$\Delta T_{fuel}$	= difference between maximum and surface fuel pellet temperature (function of power)
$\alpha(\bar{q}'')$	= empirical parameter dependent upon average heat flux
$\delta$	= ratio of the cold diametral gap to the inner diameter of the clad
$\Delta T_{o(clad + film)}$	= temperature drop across clad and film (function of power)
$T_{coolant}$	= average temperature of the coolant (function of power)

The empirically determined  $\alpha(\bar{q}'')$  is given in Figure 2.4-11 as a function of pellet surface heat flux. The difference in the effective temperature obtained from the experimental data of Figure 2.4-10 and from the correlation employing Figure 2.4-11 is shown in Figure 2.4-12 as a function of surface heat flux. It can be seen that even though



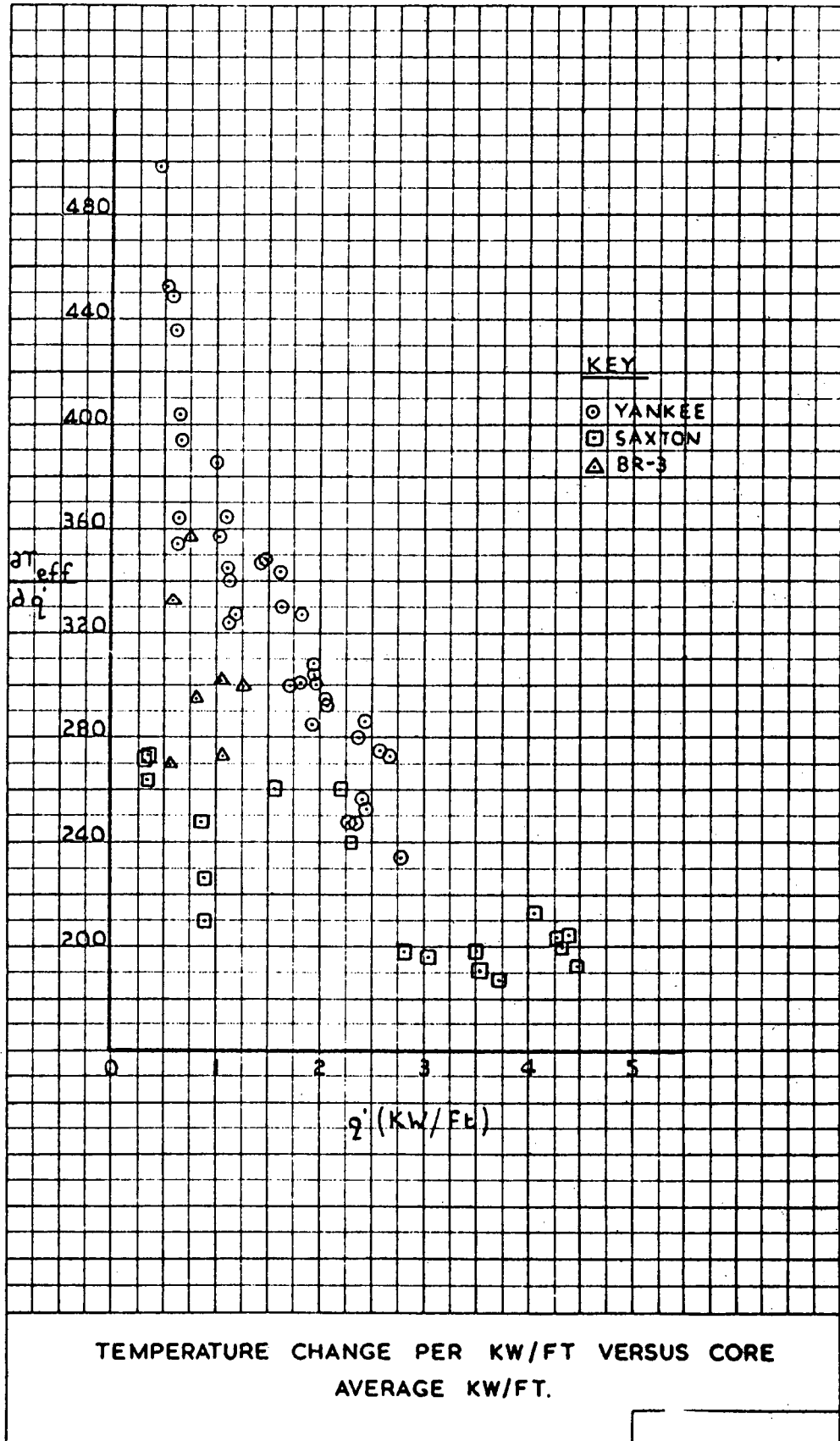


Figure 2.4-10

Figure 2.4-11

$\alpha$  Versus Pellet Surface Heat Flux

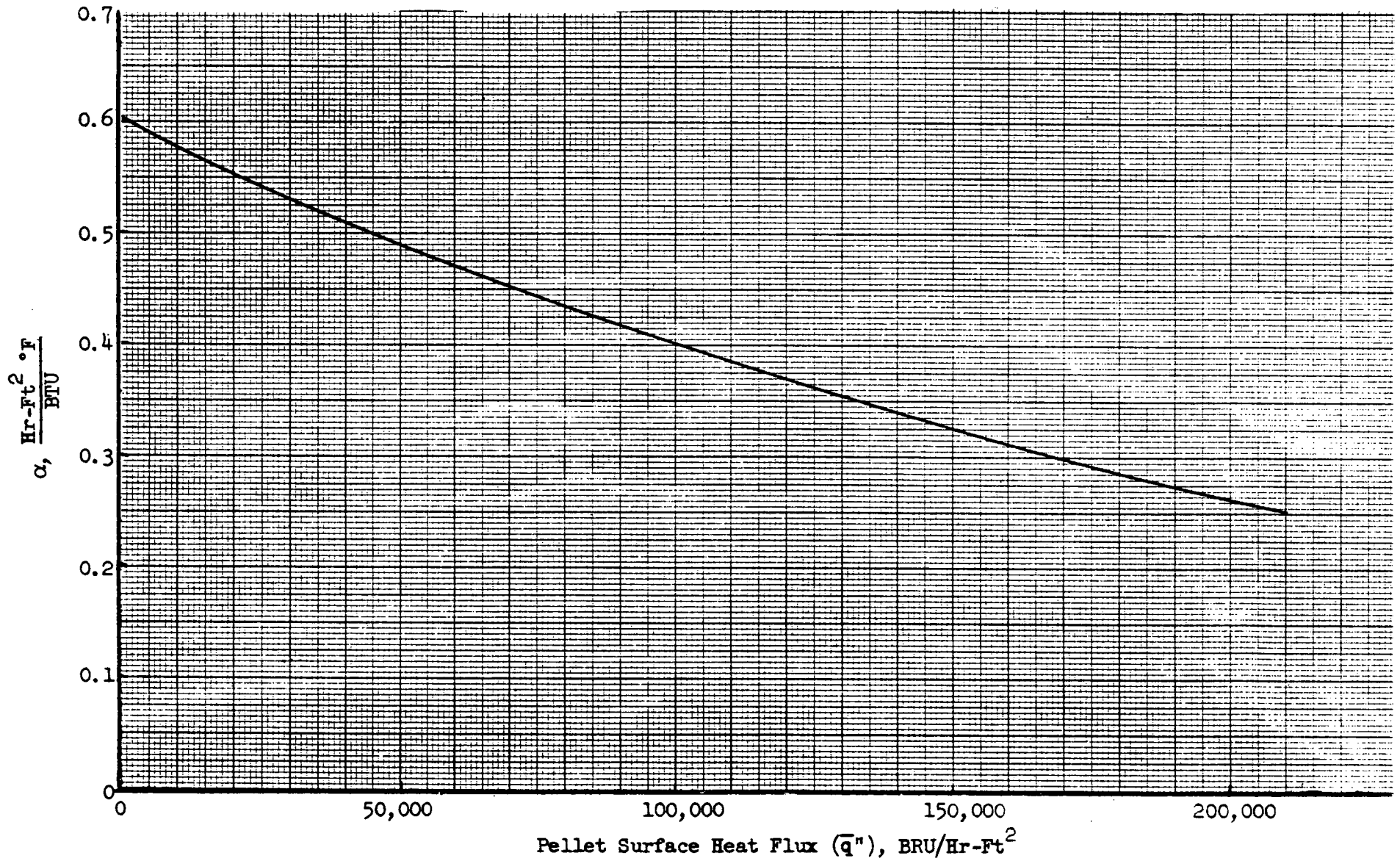
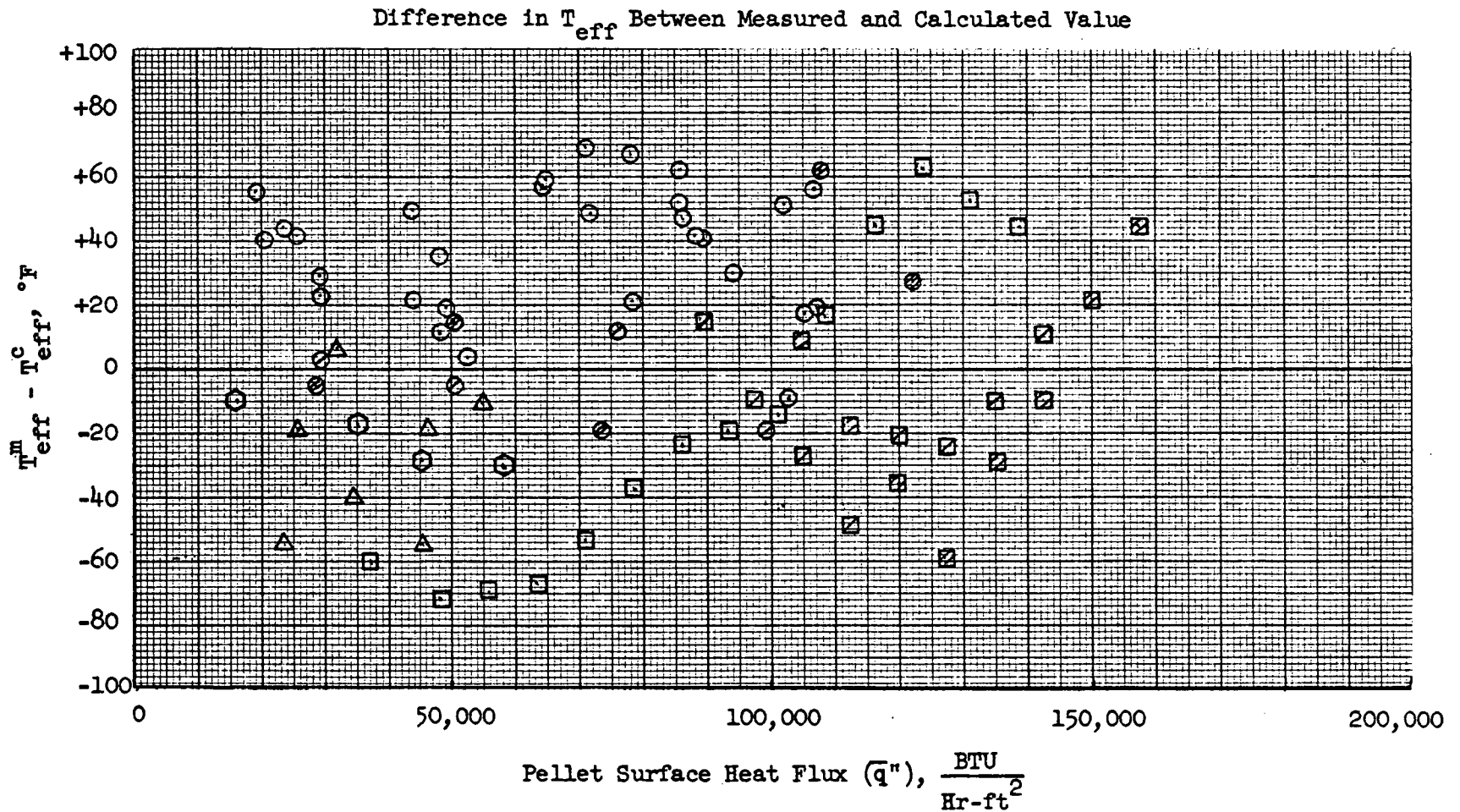


Figure 2.4-12

- ⊙ - Yankee Core No. 1
- ⊗ - Yankee Core No. 2
- ⊚ - Yankee Core No. 3
- - Saxton with Crud, With Boron
- ▣ - Saxton no crud, No Boron
- ▤ - Saxton no crud, With Boron
- △ - BR-3
- ⊖ - SELNI



there is some scatter in the experimental data (Figure 2.4-10), all the experimental points fall into a small band when the  $T_{eff}$  correlation is used. The most scattered experimental data points deviate from the predicted value (solid line) by no more than  $\pm 80^{\circ}\text{F}$ .

It is concluded that the  $T_{eff}$  correlation can predict  $T_{eff}$  at any power level to within  $\pm 80^{\circ}\text{F}$ , which constitutes less than  $\pm 5\%$  of the effective fuel temperature at full power for typical PWR cores.

3.0 CONTROL AND PROTECTION ASPECTS

3.1 ROUTINE TRANSIENTS

3.1.1 Automatic Control

The primary function of the reactor control system, in response to turbine load changes, is to change the reactor power level rapidly to coincide with the turbine load with a minimum of transient disturbances in the plant. i.e. temperature and pressure variations. With a small moderator feedback, the bulk of this control action is performed by the control rods. The automatic control system for a chemical shim plant has been modified with various compensation signals to improve this performance, e.g. derivative signals, pressurizer pressure feedback, and derivative of nuclear flux as a feedback signal. The control system is designed to perform over the whole range of moderator coefficients associated with boron concentration reductions during each core cycle.

Analog studies have been performed to illustrate the relative insensitivity of transient response to changes in moderator temperature coefficient from a value which is slightly negative to a value more positive than expected in any power reactors utilizing chemical shim control. The following transients were studied:

1. Ten per cent step increase in load from low power,
2. Ten per cent step decrease in load from full power, and
3. Ten per cent step increase in load to full power.

Load Increase from Low Power

An analog study was made to illustrate the response to a step increase in governor valve area leading to a 10% load increase in steady state. The variation in steam flow (i.e. turbine load) is a result of the steam pressure variation changing the flow through an assumed constant governor valve area. Two values of moderator temperature coefficient were used,  $-0.5 \times 10^{-4}$  and  $+1.0 \times 10^{-4}$   $\delta k/F$ .

The incremental rod worth used here is a relatively low value leading to higher transient peaks. Figures 3.1-1 and 3.1-2 compare transient responses of the significant reactor variables for the positive and negative values of the moderator temperature coefficient. It is seen that there is no significant difference between the curves for the negative and positive moderator coefficient except the positive coefficient shows a slightly less damped (more oscillatory) behavior. The low power operation transients, as shown here, exhibit a somewhat sluggish response to control rod motion because of the inherent neutron kinetics characteristics.

#### Load Decrease from Full Power

Analog studies were performed to illustrate the transient response for a 10% step load reduction from full power with the minimum incremental control rod worth thus yielding the maximum transient peaks. As in the previous load increase, two values of moderator temperature coefficient were used,  $-0.5 \times 10^{-4}$  and  $+1.0 \times 10^{-4}$   $\delta k/F$ . Figures 3.1-3 and 3.1-4 compare transient responses of significant reactor variables for the positive and negative values of the moderator temperature coefficient. The difference between the cases with the positive and negative coefficient is more apparent but does not present any difficulties. The transient with the positive coefficient is more underdamped as expected. It should be noted that these two transients are obtained with the same controller set points, e.g. derivative gains, proportional gains, etc. to yield a true comparison. The set points used are preferable for operation with a negative coefficient. Flexibility in adjustments of controller set points is provided which can improve the damping for the positive coefficient if desired, but this is not necessary.

A second set of analog studies was performed with higher incremental rod worth,  $4.0 \times 10^{-4}$   $\delta k/\text{inch}$ . The results are shown in Figures 3.1-5 and 3.1-6. The higher incremental rod worth results in a lower peak average temperature as compared to the results of the study with minimum incremental rod worth. The transient with the positive coefficient is also more oscillatory. There is however no significant difference in the overall transient between the cases with positive and negative moderator temperature coefficients.

$$\alpha_f = -0.5 \times 10^{-5} \delta k / ^\circ F$$

$$(\delta k / \text{in}) \text{ Control Group} = 1.2 \times 10^{-4}$$

$$\textcircled{1} \alpha_w = 0$$

$$\textcircled{2} \alpha_w = +1 \times 10^{-4} \delta k / ^\circ F$$

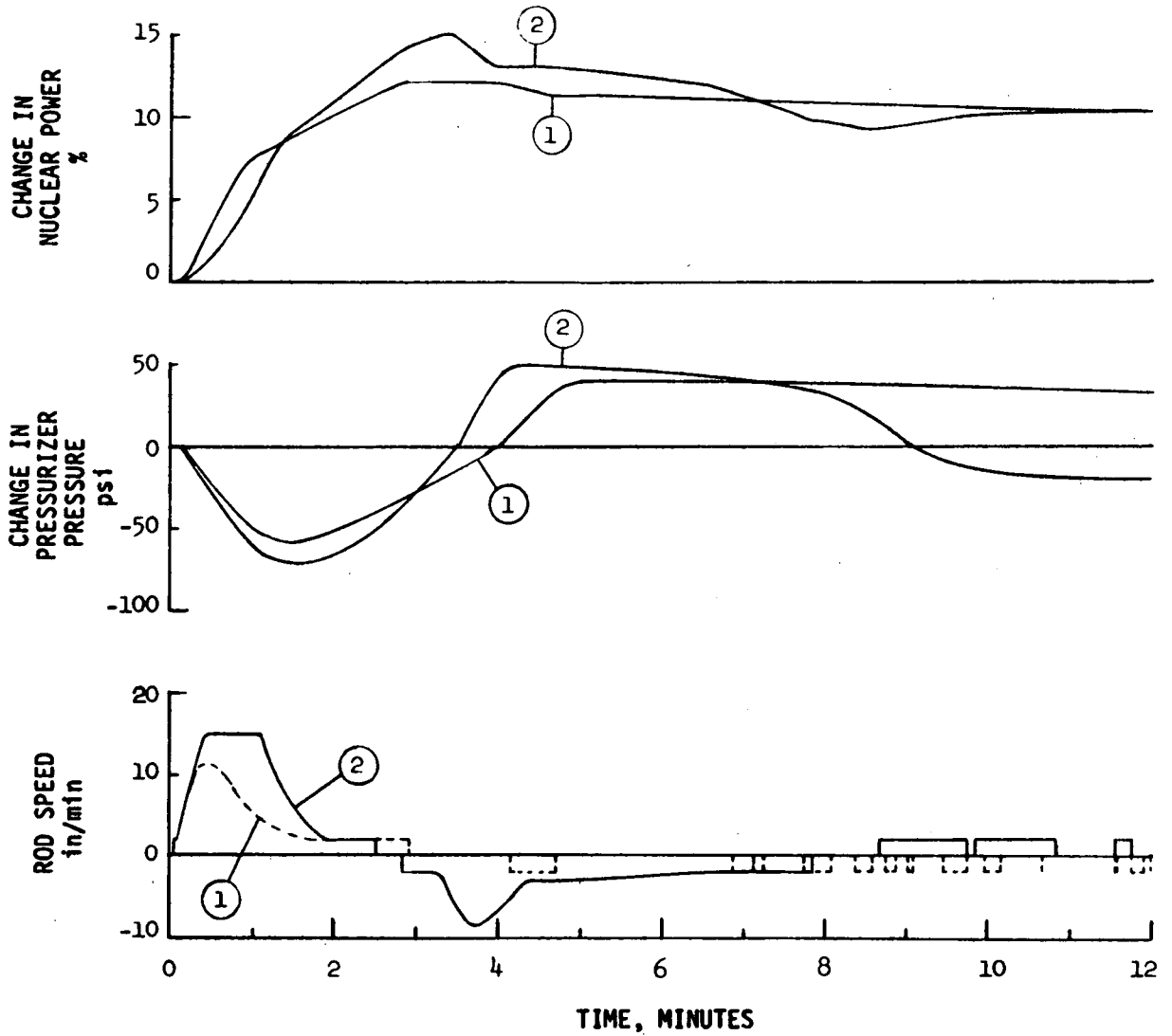


FIGURE 3.1-1

TRANSIENT RESPONSES FOR A 10% STEP LOAD INCREASE  
FROM 20% POWER - NUCLEAR POWER, PRESSURIZER PRESSURE, ROD SPEED

$$\alpha_f = -0.5 \times 10^{-5} \delta k / ^\circ F$$

$$(\delta k / \text{in}) \text{ Control Group} = 1.2 \times 10^{-4}$$

$$\textcircled{1} \alpha_w = 0$$

$$\textcircled{2} \alpha_w = +1 \times 10^{-4} \delta k / ^\circ F$$

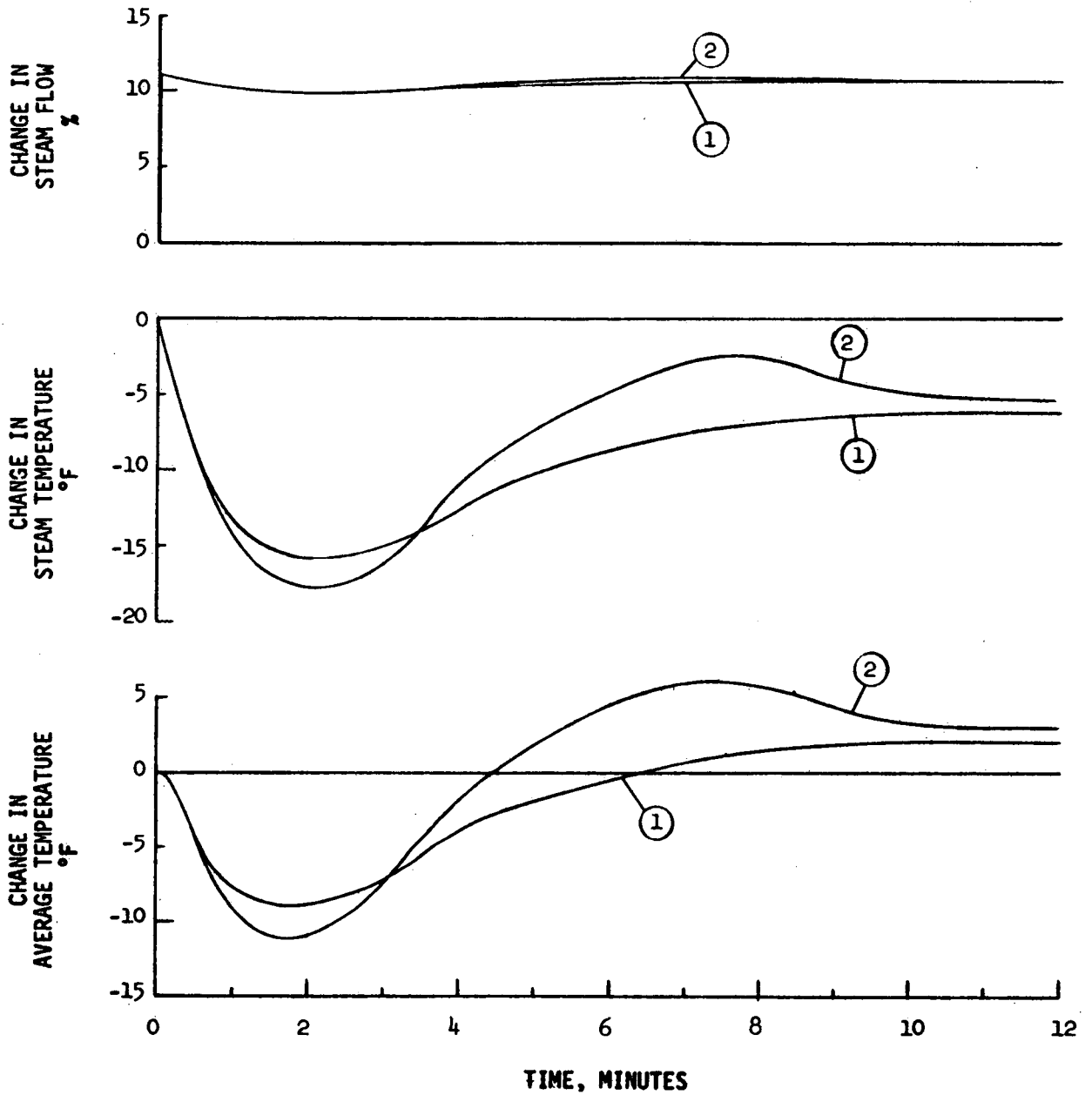


FIGURE 3.1-2

TRANSIENT RESPONSES FOR A 10% STEP LOAD INCREASE  
FROM 20% POWER - STEAM FLOW, STEAM TEMPERATURE, AVERAGE TEMPERATURE

$$\alpha_f = -0.5 \times 10^{-5} \delta k / ^\circ F$$

$$(\delta k / \text{in}) \text{ Control Group} = 1.2 \times 10^{-4}$$

$$\textcircled{1} \alpha_w = 0$$

$$\textcircled{2} \alpha_w = +1 \times 10^{-4} \delta k / ^\circ F$$

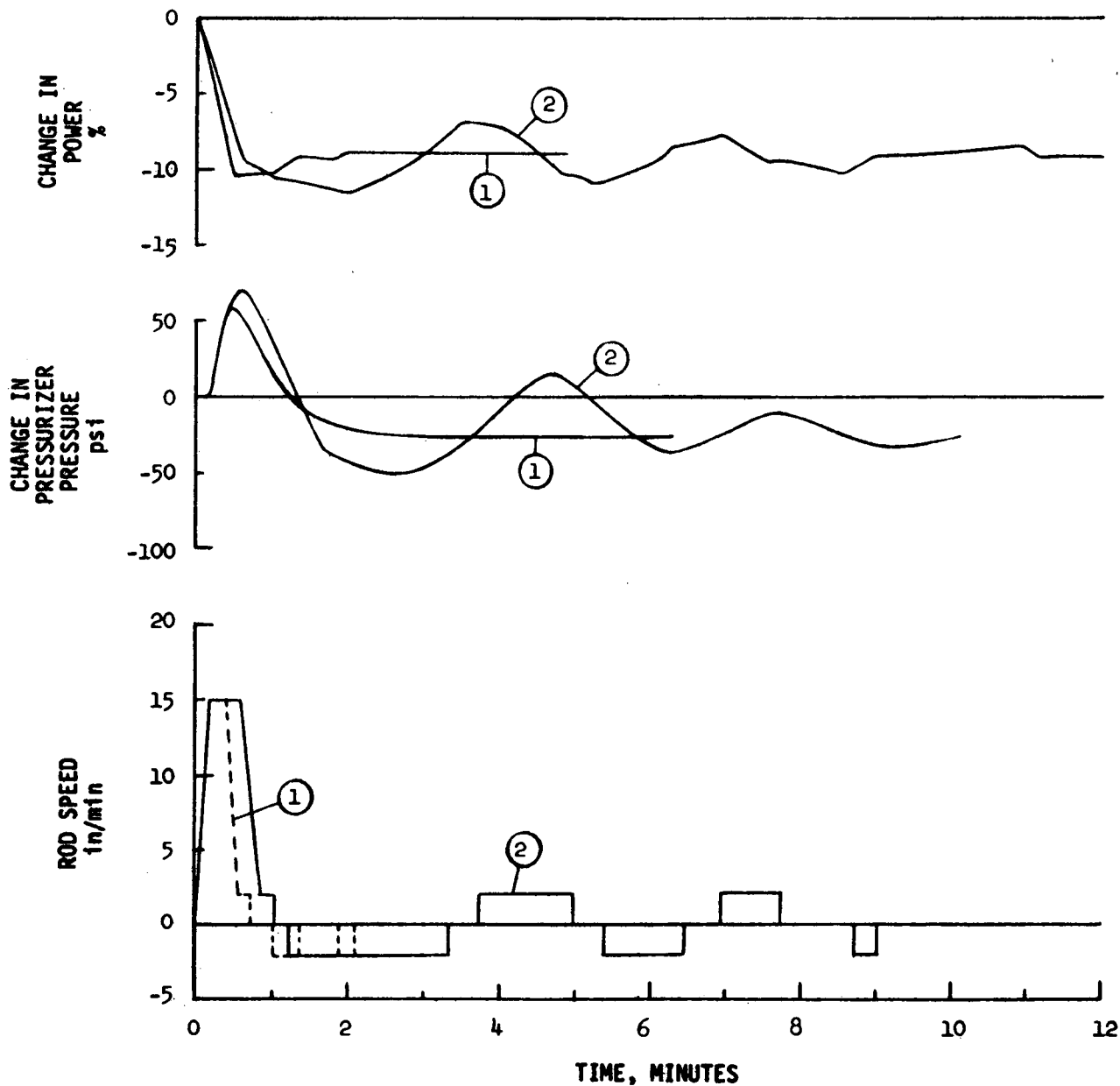


FIGURE 3.1-3

TRANSIENT RESPONSES FOR A 10% LOAD DECREASE FROM FULL POWER -  
POWER, PRESSURIZER PRESSURE, ROD SPEED

$$\alpha_f = -0.5 \times 10^{-5} \text{ } \delta k / ^\circ F$$

$$(\delta k / \text{in}) \text{ Control Group} = 1.2 \times 10^{-4}$$

$$\textcircled{1} \alpha_w = 0$$

$$\textcircled{2} \alpha_w = +1 \times 10^{-4} \text{ } \delta k / ^\circ F$$

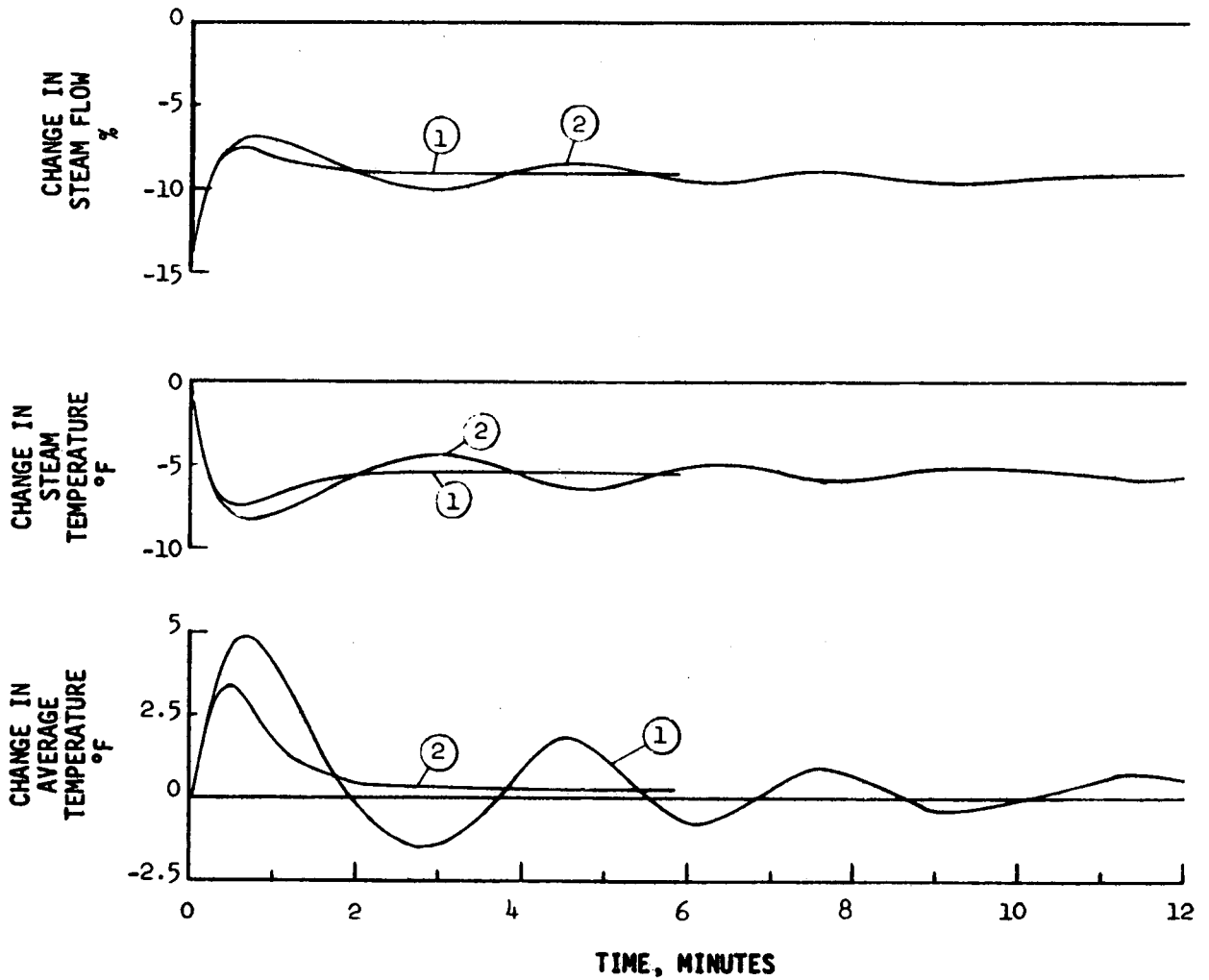


FIGURE 3.1-4

TRANSIENT RESPONSES FOR A 10% LOAD DECREASE FROM FULL POWER -  
STEAM FLOW, STEAM TEMPERATURE, AVERAGE TEMPERATURE

$$\alpha_f = -0.5 \times 10^{-5} \text{ } \delta k / ^\circ F$$

$$(\delta k / \text{in}) \text{ Control Group} = 4 \times 10^{-4}$$

$$\textcircled{1} \alpha_w = 0$$

$$\textcircled{2} \alpha_w = +1 \times 10^{-4} \text{ } \delta k / ^\circ F$$

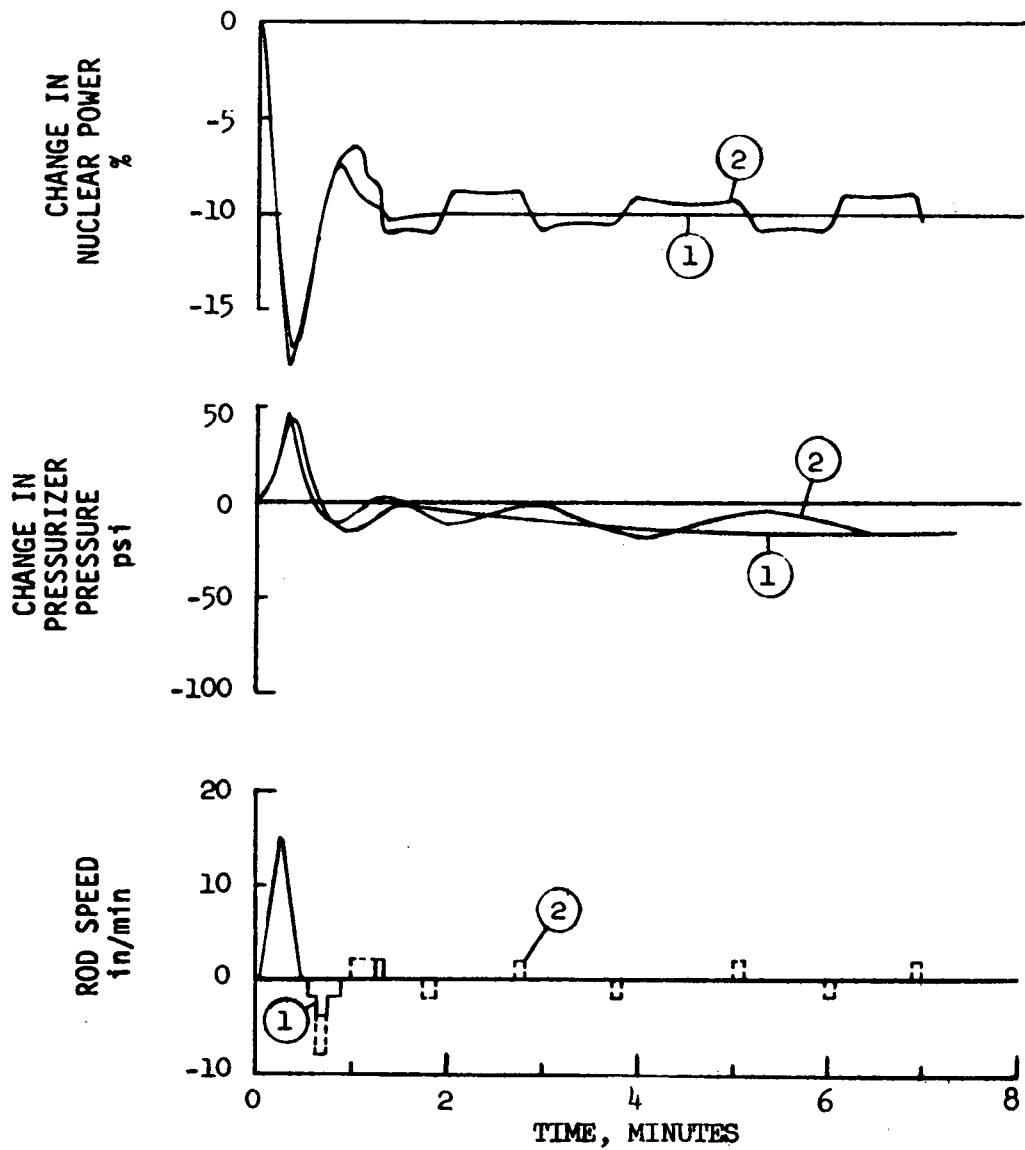


FIGURE 3.1-5

TRANSIENT RESPONSES FOR A 10% LOAD DECREASE  
FROM FULL POWER - NUCLEAR POWER, PRESSURIZER  
PRESSURE, ROD SPEED

$$\alpha_f = -0.5 \times 10^{-5} \delta k / ^\circ F$$

$$(\delta k / \text{in}) \text{ Control Group} = 4 \times 10^{-4}$$

$$\textcircled{1} \alpha_w = 0$$

$$\textcircled{2} \alpha_w = +1 \times 10^{-4} \delta k / ^\circ F$$

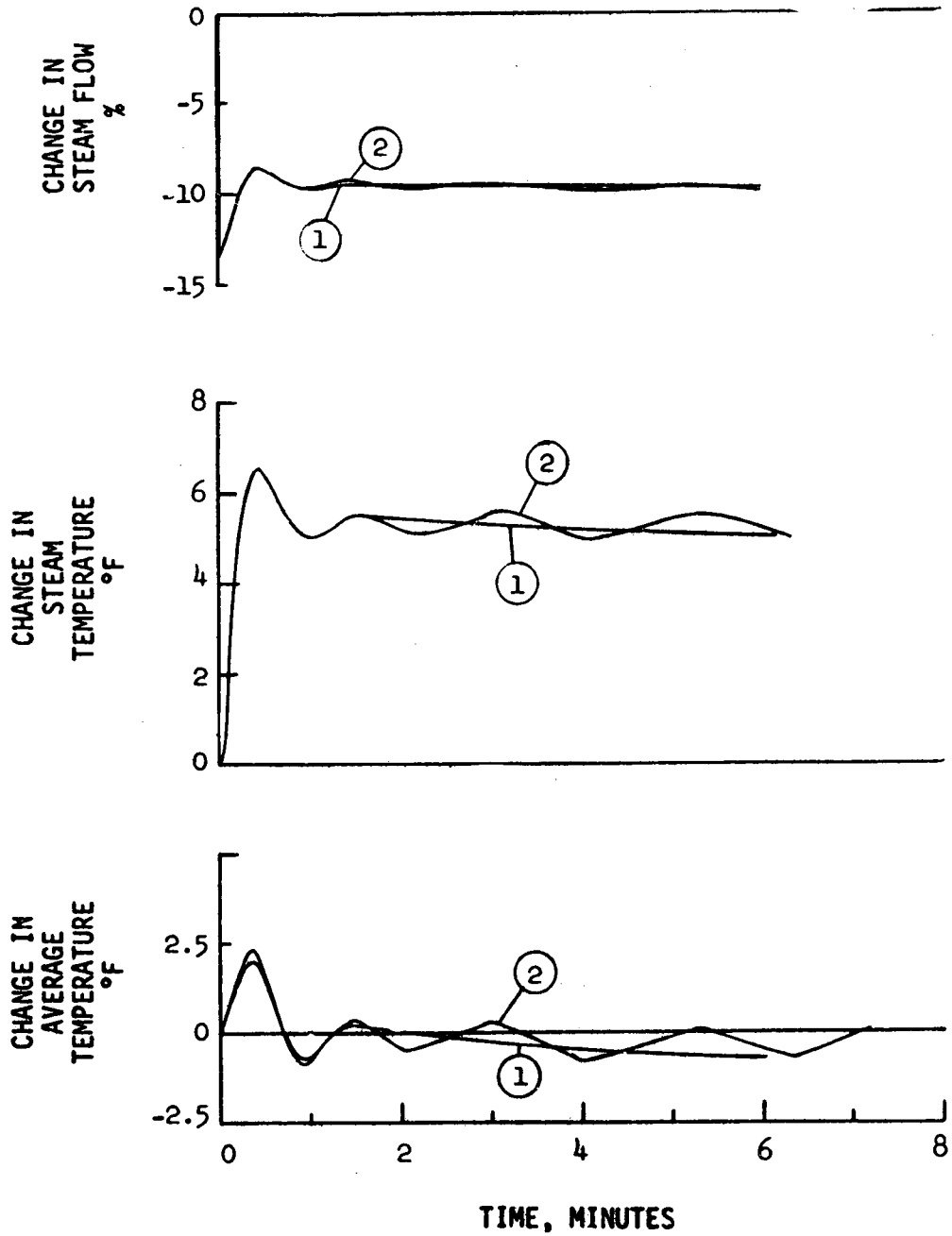


FIGURE 3.1-6

TRANSIENT RESPONSES FOR A 10% LOAD DECREASE  
FROM FULL POWER - STEAM FLOW, STEAM TEMPERATURE,  
AVERAGE TEMPERATURE

### Load Increase to Full Power

A set of analog studies was performed to illustrate the transient behavior following a 10% step load increase to full load. The same moderator temperature coefficients as were used in the previous cases studied were used,  $-0.5 \times 10^{-4}$  and  $+1.0 \times 10^{-4}$   $\delta k/F$ . The high value of incremental rod worth was used.

The results of these studies are shown in Figures 3.1-7 and 3.1-8. The responses are essentially the reverse of the load decrease with the exception of pressurizer pressure where flashing of water to steam occurs initially. Again the response for the positive coefficient is underdamped but without any significant effects. As stated earlier, the response with the positive coefficient could be improved with adjustments in the controller parameters.

#### 3.1.2 Manual Control

An analog study was made of plant performance with a positive moderator coefficient under manual control to see what operator reaction is required. Figure 3.1-9 shows the response to a 10% step load decrease from low power operation where the operator was instructed to wait one minute before taking action, assuming a low incremental rod worth. The peak temperature is greater than under automatic control but poses no problem. The equilibrium conditions are achieved with little operator action as shown by the curve indicating control rod motion. Figure 3.1-10 shows the response for same conditions as in Figure 3.1-9 with the exception that a two-minute delay was assumed before operator action. Figure 3.1-11 illustrates a similar transient with higher incremental rod worth and shows no problems with respect to oscillations or excessive operator action to achieve equilibrium conditions.

$$\alpha_f = -0.5 \times 10^{-5} \delta k / ^\circ F$$

$$\textcircled{1} \alpha_w = 0$$

$$(\delta k / \text{in}) \text{ Control Group} = 4 \times 10^{-4}$$

$$\textcircled{2} \alpha_w = +1 \times 10^{-4} \delta k / ^\circ F$$

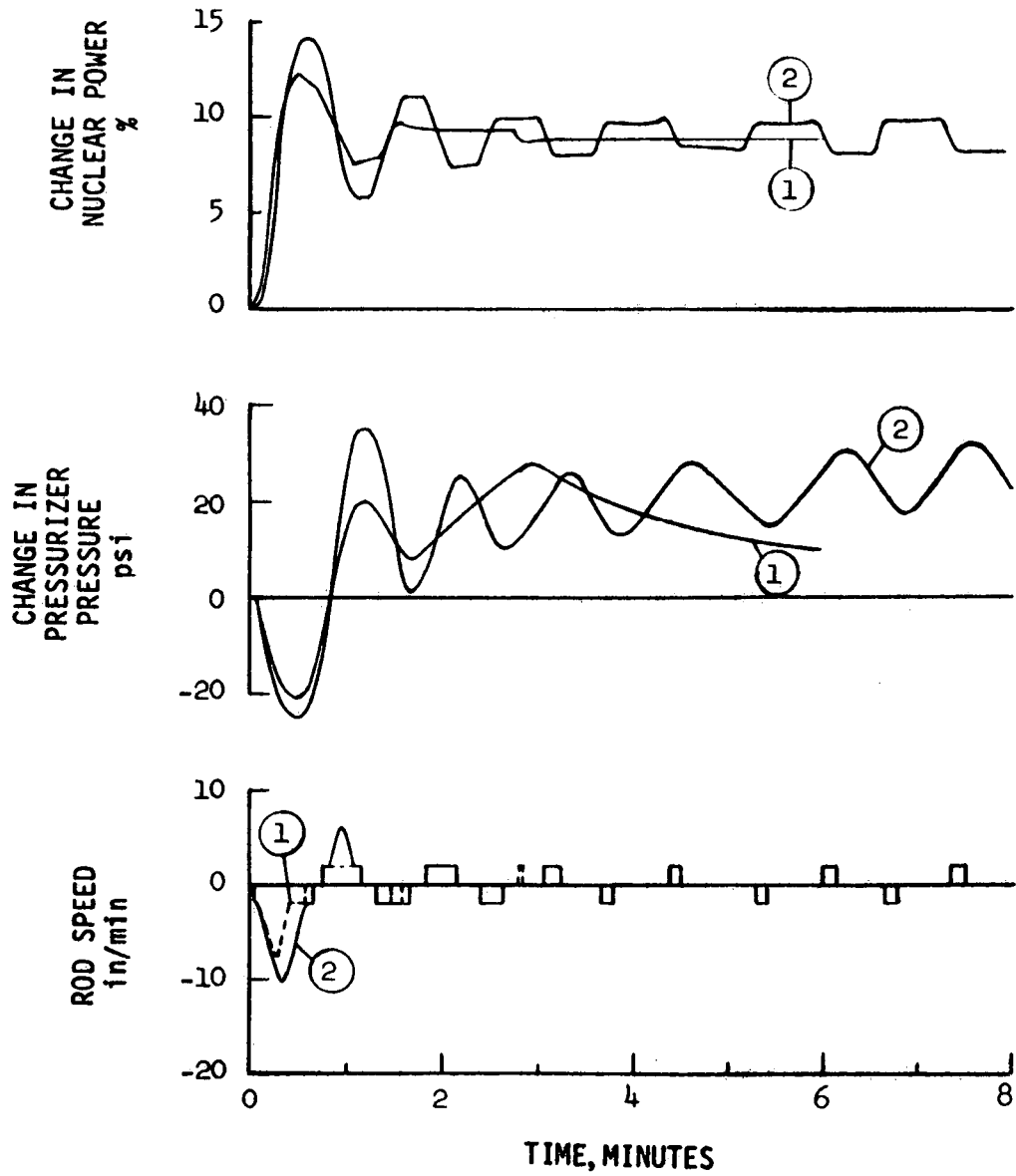


FIGURE 3.1-7

TRANSIENT RESPONSES FOR A 10% STEP LOAD INCREASE FROM 90% POWER -  
NUCLEAR POWER, PRESSURIZER PRESSURE, ROD SPEED.

$$\alpha_f = -0.5 \times 10^{-5} \delta k / ^\circ F$$

$$(\delta k / \text{in}) \text{ Control Group} = 4 \times 10^{-4}$$

$$\textcircled{1} \alpha_w = 0$$

$$\textcircled{2} \alpha_w = +1 \times 10^{-4} \delta k / ^\circ F$$

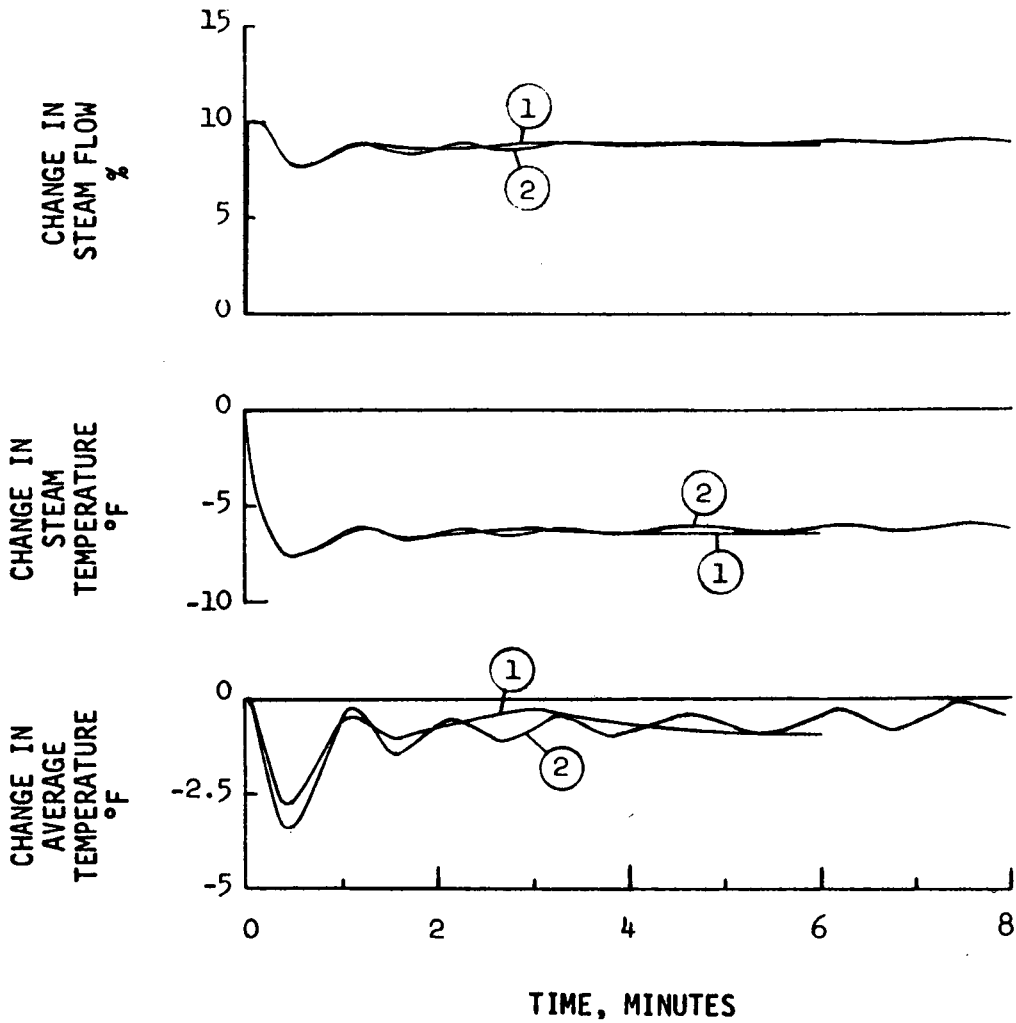


FIGURE 3.1-8

TRANSIENT RESPONSES FOR A 10% STEP LOAD INCREASE FROM 90% POWER -  
STEAM FLOW, STEAM TEMPERATURE, AVERAGE TEMPERATURE

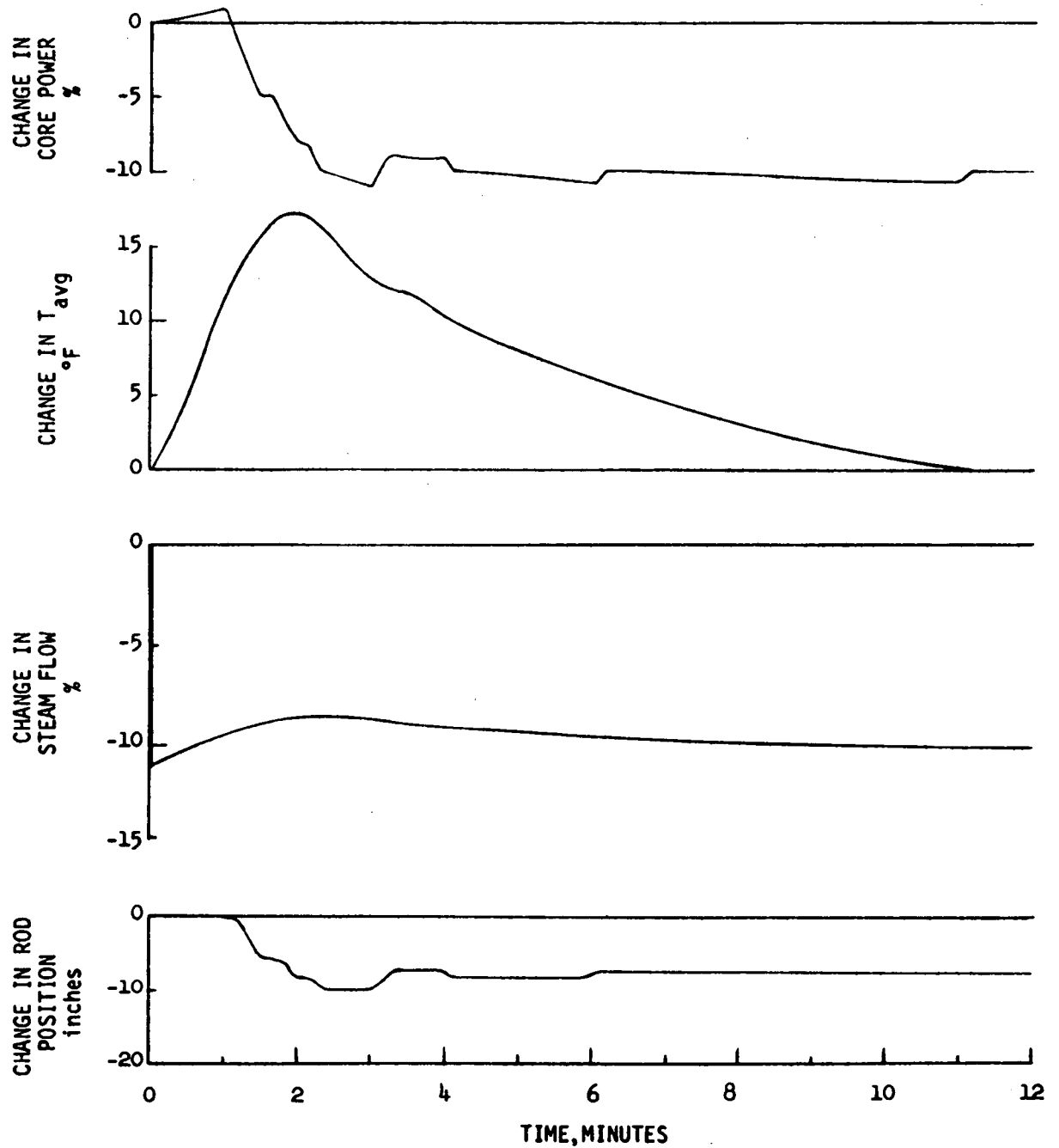


FIGURE 3.1-9

LOW POWER OPERATION, 10% STEP LOAD DECREASE, MANUAL CONTROL  
NO OPERATOR ACTION FOR 1 MINUTE, INCREMENTAL ROD WORTH =  $3 \times 10^{-4}$   $\delta k/in$   
 $\alpha_w = +0.5 \times 10^{-4}$   $\delta k/^\circ F$

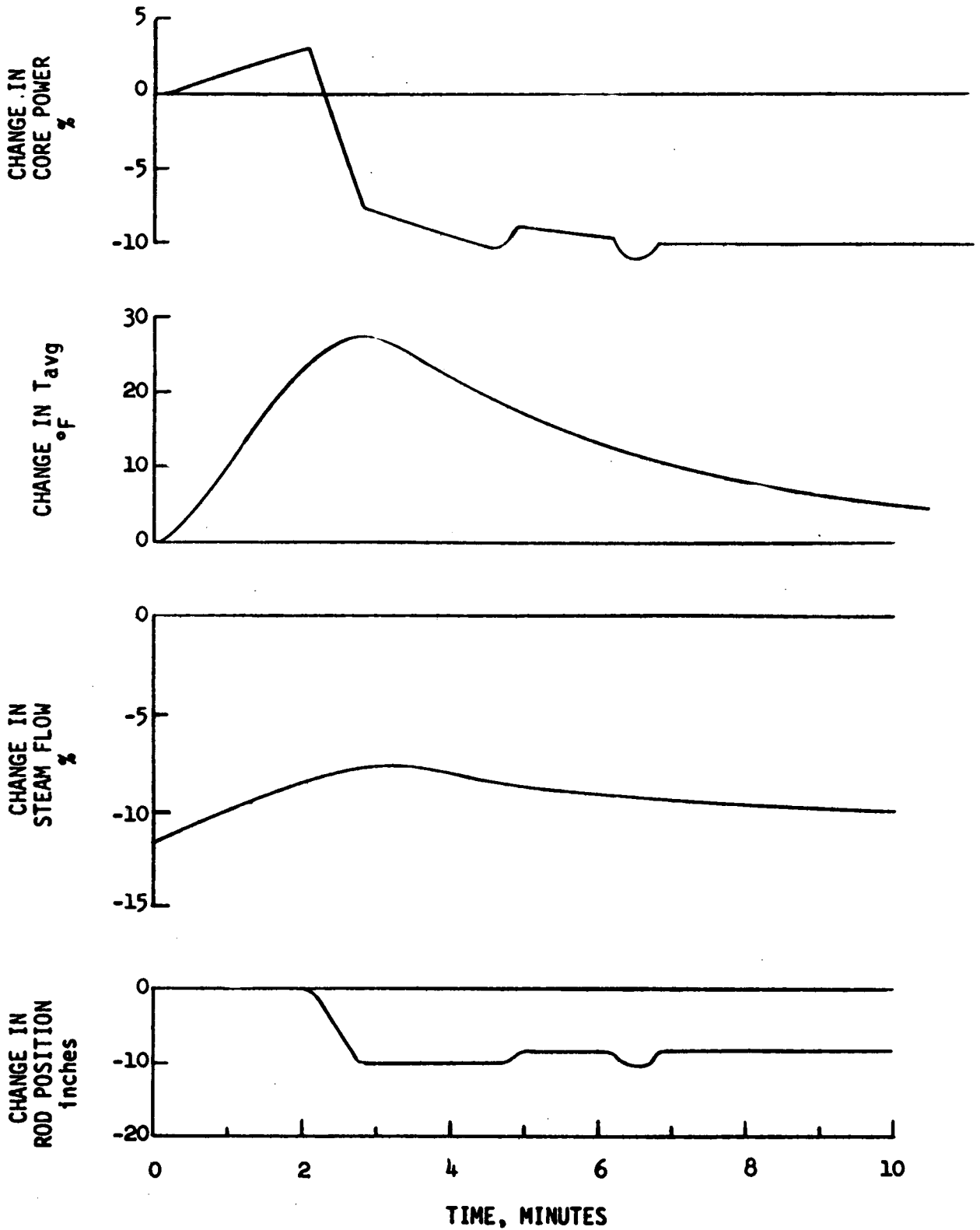


FIGURE 3.1-10

LOW POWER OPERATION, 10% STEP LOAD DECREASE, MANUAL CONTROL  
NO OPERATOR ACTION FOR 2 MINUTES INCREMENTAL ROD WORTH =  $3 \times 10^{-4}$   $\delta k/inch$   
 $\alpha_w = +0.5 \times 10^{-4}$   $\delta k/^\circ F$

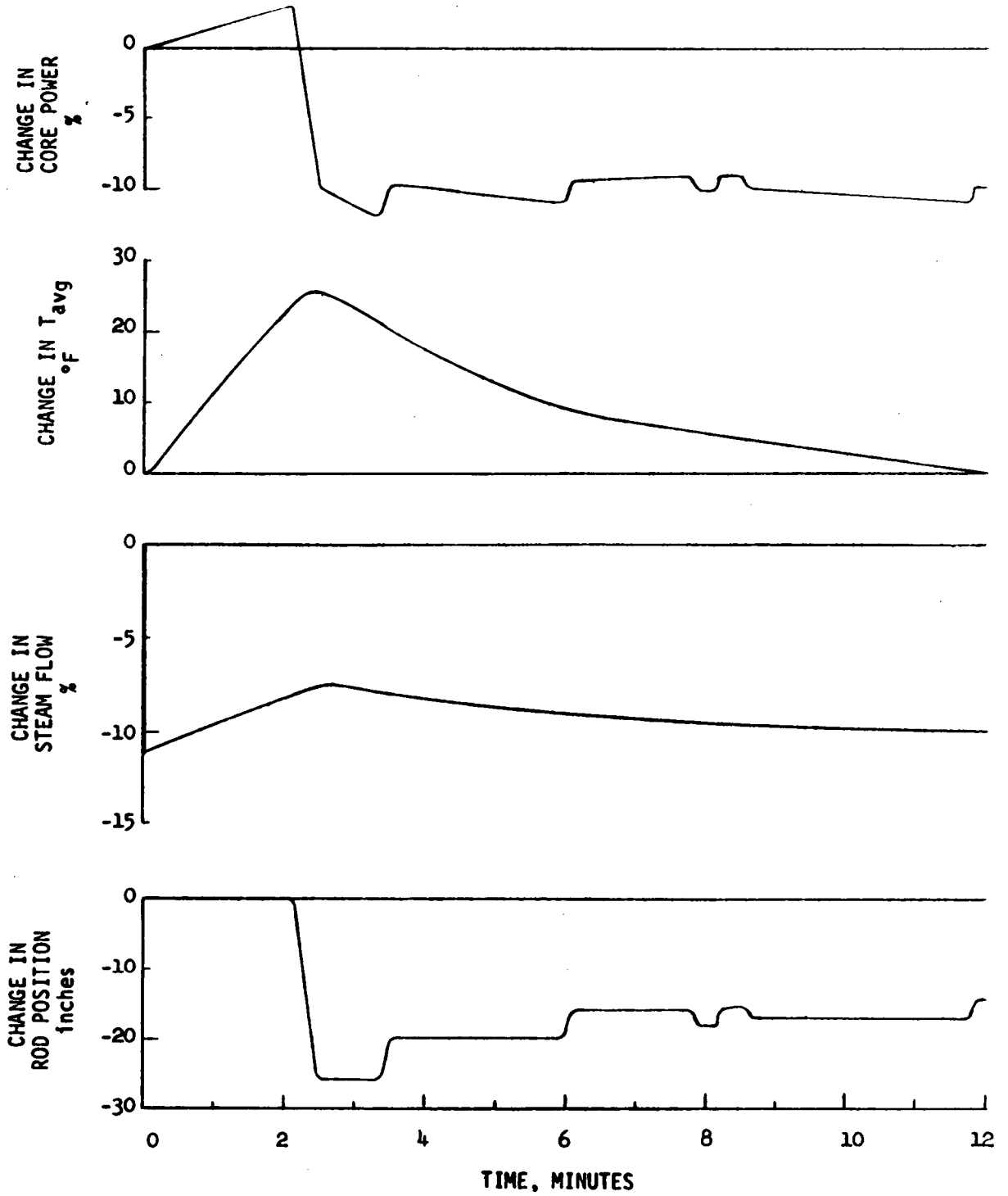


FIGURE 3.1-11

LOW POWER OPERATION, 10% STEP LOAD DECREASE, MANUAL CONTROL  
NO OPERATOR ACTION FOR 2 MIN., INCREMENTAL ROD WORTH =  $6 \times 10^{-4}$   $\delta k/\text{inch}$   
 $\alpha_w = +0.5 \times 10^{-4}$   $\delta k/^\circ F$

## 3.2 ABNORMAL TRANSIENTS

### 3.2.1 Moderator Temperature

Accident conditions have been evaluated which can result in coolant temperature changes leading to positive reactivity addition. There are various means of decreasing the reactor coolant system temperature rapidly, e.g. a secondary steam line break or cold feedwater addition, and these accidents are investigated for end of life conditions, i.e. with the most negative moderator coefficient. There is no realistic means of rapidly increasing reactor coolant temperature, of interest with a positive moderator coefficient, because of the thermal inertia (long time constants) in the fuel and coolant. The response time of the protection system is much faster for incidents such as rod withdrawal. The incident is therefore terminated before any significant coolant temperature increase, with respect to reactivity insertion, can occur.

### 3.2.2 Moderator Pressure

Another means of introducing positive reactivity is to reduce moderator density by reducing system pressure. The rate of depressurization caused by opening a power operated relief valve is less than 10 psi/second, and from full power, a reactor trip is initiated by the low pressure trip before a 200 psi reduction in pressure occurs. The amount of void under these conditions is less than 4% anywhere in the core with an average void of closer to 0.5%. With this amount of void, the reactivity insertion is negligible. Neglecting inherent constraints on temperature distributions, a maximum reactivity insertion of 0.3% can be calculated; that is, by assuming an unrealistic distribution of temperature and void as described in Section 2.2. Even assuming this reactivity to be inserted before the trip, the rate of reactivity insertion is less than the maximum rate normally assumed for a rod withdrawal transients. This transient is therefore well within the capability of the reactor protection system.

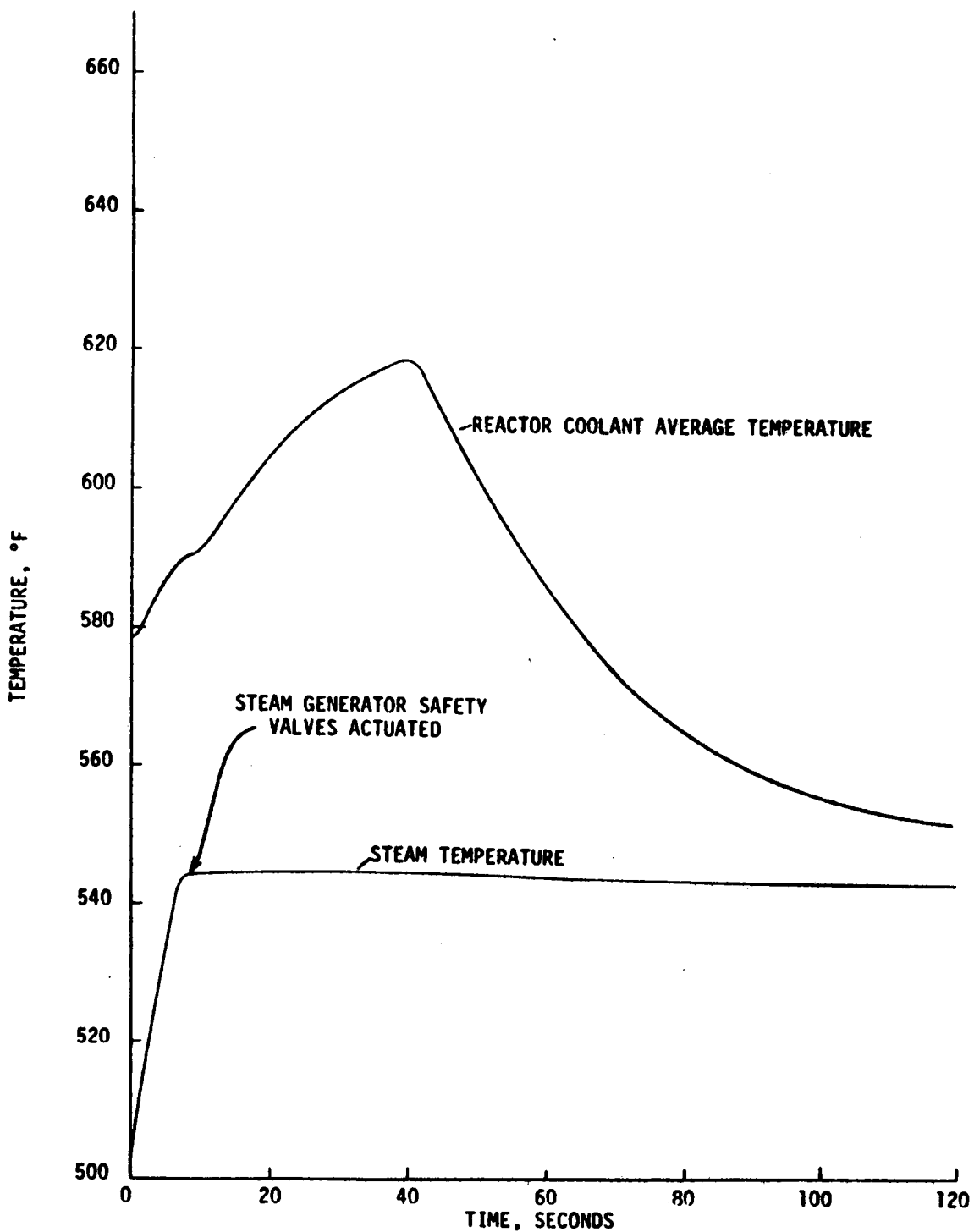
### 3.2.3 Complete Loss of Load

The complete loss of turbine load without an immediate reactor trip will result in an increase in both reactor coolant temperature and pressure. Control rod insertion will normally occur to reduce the core power and limit the temperature and pressure rise. For a complete loss of load from full load, the control rod motion under normal automatic control will not be capable of a rapid enough core power reduction and with a positive moderator coefficient the reactor power will even tend to increase. The transient is then rapidly terminated by a high pressurizer pressure or overpower reactor trip.

Figures 3.2-1 and 3.2-2 illustrate an analog calculation of a loss of load transient from full load. In this case, a positive coefficient of  $+0.5 \times 10^{-4} \delta k/F$  was used because it yields a power increase less than that which would definitely result in an overpower trip and therefore cause the transient to be terminated by the high pressure of high pressurizer level trips which occur later. The point at which a high pressure trip will occur is indicated on the figures. No automatic control rod insertion was assumed and the transient was permitted to continue beyond the high pressure trip point until a high pressurizer water level trip is reached at approximately 34 seconds. Even for these elevated temperature, power and pressure transients the maximum void anywhere in the core is less than 5% and the average void is less than 0.7%. This condition does not approach one whereby a significant void insertion of reactivity occurs and the transient is well within the capability of the rods to shut the core down safely.

### 3.2.4 Hypothetical Ejection of a Control Rod

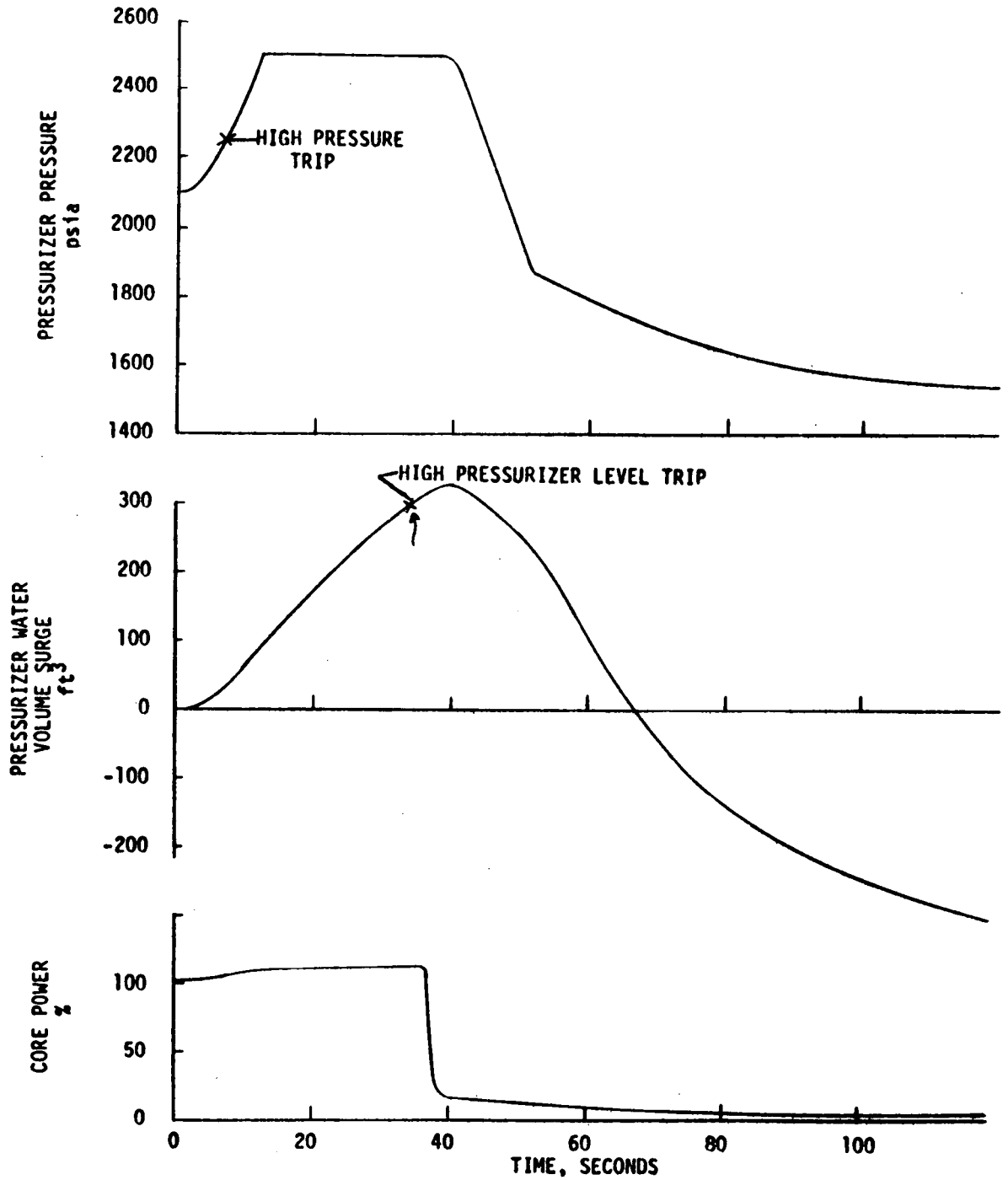
The transient following a hypothetical control rod ejection results in a sudden increase in power leading to a fairly rapid increase in



TRANSIENT RESPONSE TO A COMPLETE LOSS OF LOAD FROM FULL POWER WITHOUT AN IMMEDIATE REACTOR TRIP (TEMPERATURES)

$$\alpha_w = +0.5 \times 10^{-4} \text{ } \delta k / ^\circ\text{F}$$

FIGURE 3.2-1



TRANSIENT RESPONSE TO A COMPLETE LOSS OF LOAD FROM FULL POWER WITHOUT AN IMMEDIATE REACTOR TRIP (PRESSURE, VOLUME SURGE, CORE POWER)

$$\alpha_w = +0.5 \times 10^{-4} \text{ } \delta k / ^\circ F$$

FIGURE 3.2-2

moderator temperature. Even for this condition there is an inherent limit to the total amount of reactivity which can be inserted with a positive moderator coefficient.

In order to obtain an extreme positive moderator reactivity feedback the entire core power increase is assumed to be concentrated in one-fourth of the core. This is consistent with the iterative physics calculations described in Section 2.2 which indicate that this pattern of energy input gives the maximum positive reactivity.

The rod ejection transient results in a distorted power distribution and also is discussed in Section 2.2 a distorted distributed coupled with the non-uniform temperature distribution reduces the total reactivity insertion resulting from positive moderator effects. For the unrodded core (i.e. with uniform power distribution) the maximum moderator density reactivity insertion is 0.19% while for the distorted distribution associated with an ejected rod the maximum insertion is less than 0.1%.

Acceptable results have been obtained with rod ejection calculations even using the moderator feedback curve for the unrodded core shown in Figure 2.2-4. In particular, the positive moderator feedback in conjunction with the postulated ejected rod transient does not significantly affect the ultimate consequences of this accident.

3.3 BASIS FOR CONFIDENCE IN ANALOG STUDIES

The detailed design of the reactor control and protection system and the evaluation of various accident conditions is performed using a detailed analog plant simulation. The analog simulation has been verified with actual plant performance tests for several plants. Reactor response to load changes with and without automatic control was compared to results of analog studies for the Carolina-Virginia Tube Reactor<sup>(12)</sup> and the SELNI plant. The comparison showed that the ability to predict transient response is very good. Figure 3.3-1 presents a typical comparison of the analog computer results and an actual plant transient for the SELNI plant during initial power operation.

COMPARISON OF TRANSIENT BEHAVIOR, PREDICTED VS. ACTUAL FOR THE  
SELNI PLANT RAPID LOAD DECREASE FROM 185 to 140 MWe

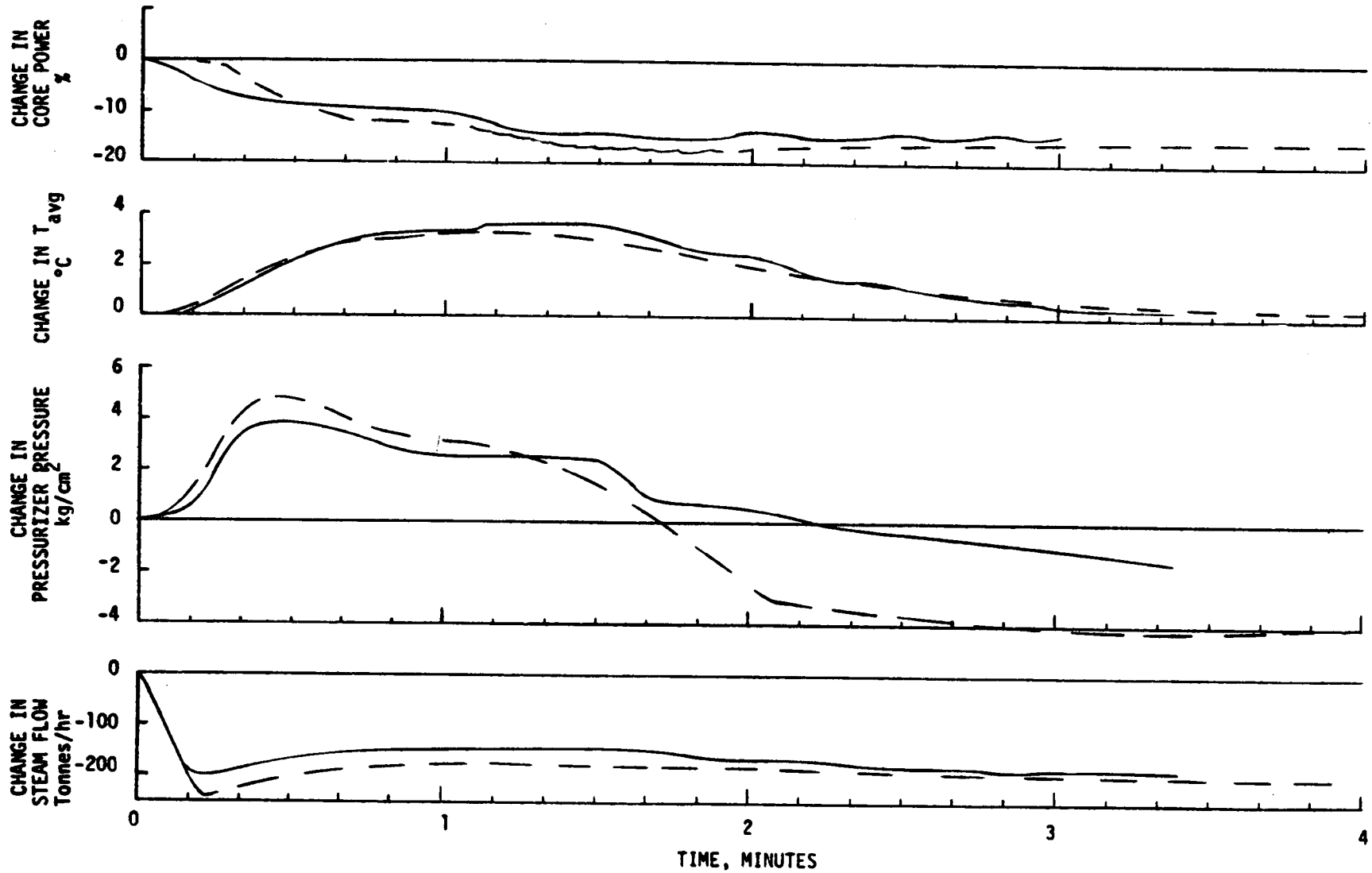


FIGURE 3.3-1

4.0

CONCLUSIONS

The following conclusions were reached regarding the effects of reactivity coefficients on the operation of present generation high burnup reactors with chemical shim:

1. The power coefficient, independent of boron concentration, is the primary prompt terminating mechanism for transients in the PWR Core.
2. Reactivity changes due to moderator effects with positive moderator reactivity coefficients are limited to small values in both rate and magnitude.
3. Power is reduced in the regions of a local temperature increase.
4. Boron concentration must be increased by almost 1000 ppm before concern for spatial stability arises.
5. Operation of a pressurized water reactor at power with a positive moderator coefficient causes no deleterious effects in the controlled response of the plant.
6. The influence of a positive coefficient of reactivity on the various accident conditions considered in the design of a pressurized water reactor is calculable through detailed spatial nuclear and thermal investigation of the core.
7. The consideration of accident situations has shown that the existence of a positive coefficient does not prejudice the well established safety of the pressurized water reactor.

REFERENCES

1. Grund, J. E. , "Experimental Results of Potentially Destructive Reactivity Additions to an Oxide Core," IDO-17028 (1964).
2. Randall, D., and St. John, D. S., "Xenon Spatial Oscillations," *Nucleonics* 16, No. 3, 82 (1958).
3. Randall, D., and St. John, D. S., "Xenon Spatial Oscillations," *Nuclear Science and Engineering* 14, No. 2, 204 (1962).
4. Strawbridge, L. E., Allard, E. C., Bhalla, C. P., "Xenon Induced Core Instabilities," WCAP-3269-48 (1965).
- 5a. Strawbridge, L. E., "Calculations of Lattice Parameters and Criticality for Uniform Water Moderated Lattices," WAPD-3269-25 (1964).
- 5b. Strawbridge, L. E. and Barry, R. F., "Criticality Calculations for Uniform Water Moderated Lattices," *Nuclear Science and Engineering* 23, (58-73) (1965).
6. Poncelet, C. G., "Effects of Fuel Burnup on Reactivity and Reactivity Coefficients in Yankee Core I," WCAP-6076 (1965).
7. "Yankee Core Evaluation Program Quaterly Progress Report for the Period Ending June 30, 1963," WCAP-6055 (1963).
8. Hellstrand, E., and Lundgren, G., "The Resonance Integral for Uranium Metal and Oxide," *Nuclear Science and Engineering* 12, 435 (1962).
9. Hellstrand, E., J. Applied Physics 28, 1493 (1957).
10. Hellstrand, E., Blomberg, P., and Horner, S., "The Temperature Coefficient of the Resonance Integral for Uranium Metal and Oxide," *Nuclear Science and Engineering* 8, 497 (1960).
11. Sha, W. T., "An Experimental Evaluation of the Power Coefficient in Slightly Enriched PWR Cores," WCAP-3269-40 (1965).
12. Loving, J. J., "Reactor Response Analysis by Load Changes With and Without Automatic Control," CVNA 220.